UNIVERSITY OF CALIFORNIA,
IRVINE

Progress Towards the Total Synthesis of Batrachotoxin

And

A Concise Method for the Synthesis of Substituted Pyridines

DISSERTATION

submitted in partial satisfaction of the requirements
for the degree of

DOCTOR OF PHILOSOPHY

in Chemistry

by

Justin Adam Hilf

Dissertation Committee:
Professor Scott D. Rychnovsky, Chair
Professor Christopher D. Vanderwal
Assistant Professor Sergey V. Pronin

2016

DEDICATION

To my Mother, Father, Brother

&

Friends

For your everlasting love and support

TABLE OF CONTENTS

LIST OF FIGURES

LIST OF SCHEMES

LIST OF TABLES

LIST OF ABBREVIATIONS

Å	Angstroms
Ac	Acetyl
Atm	Atmosphere
Bn	Benzyl
Boc	tert-butoxycarbonyl
Bp	Boiling point
Bu	Butyl
BuLi	Butyllithium
°C	Degree Celsius
cat.	Catalytic
CSA	Camphorsulfonic acid
CI	Chemical ionization
CMC	*N*-Cyclohexyl-*N*′-(2-morpholinoethyl)carbodiimide metho-*p*-toluenesulfonate
d	day(s)
DBU	1,8-Diazabicyclo[5.4.0]undec-7-ene
δ	Chemical shift
DIBAL-H	Diisobutylaluminum hydride
DMAP	4-Dimethylaminopyridine
DMF	*N*,*N*-Dimethylformamide
DMP	Dess-Martin periodinane
DMPU	1,3-dimethyl-3,4,5,6-tetrahydro-2(1H)-pyrimidinone
DMSO	dimethyl sulfoxide
dppf	1,1'-bis(diphenylphosphino)ferrocene
d.r.	Diastereomeric ratio
ee	Enantiomeric excess
EI	Electron-impact ionization
e.r.	Enantiomeric ratio
eq.	Equation
equiv.	Equivalents

ESI	Electrospray ionization
Et	Ethyl
GC	Gas chromatography
h	hour(s)
HMPA	*N*,*N*,*N*',*N*',*N*'',*N*''-hexamethylphosphoramide
HRMS	High resolution mass spectrometry
Hz	Hertz
i	iso
IR	Infrared spectrometry
J	Coupling constant
KHMDS	Potassium hexamethyldisilazide
LAH	Lithium aluminium hydride
LiDBB	Lithium di-tert-butylbiphenylide
LDA	Lithium diisopropylamide
LiHMDS	Lithium hexamethyldisilazide
µ	micro
m	milli
M	Molar
m-CPBA	3-Chloroperoxybenzoic acid
min	minute(s)
Me	Methyl
MHz	Megahertz
MS	Mass spectrometer
n	nano
NMR	Nuclear magnetic resonance
nOe	Nuclear Overhauser Effect
Ph	Phenyl
ppm	parts per million
rt	room temperature
sec	second(s)
t	tert

TBAF	tetra-*n*-butylammonium fluoride
TBS	*t*butyldimethylsilyl
TBDPS	*t*butyldiphenylsilyl
TES	triethylsilyl
Tf	trifluoromethanesulfonyl
TFA	trifluoroacetic acid
THF	Tetrahydrofuran
THP	Tetrahydropyran
TIPS	Triisopropylsilyl
TLC	Thin layer chromatography
TMS	Trimethylsilyl
Ts	4-Toluenesulfonyl
TsOH	4-Toluenesulfonic acid

ACKNOWLEDGMENTS

This work benefitted greatly from many individuals. First and foremost, I would like to thank Professor Scott Rychnovsky. Scott graciously accepted me into his group as I returned to UC Irvine at the start of my fourth year and encouraged me to thrive. Over the past three years, I have learned a great deal from him; in how to think and carry myself as a chemist, leader, and most importantly, friend. We have had a number of conversations, both personal and scientific, and they have always been positive and supportive experiences. I greatly appreciate the space and flexibility he has granted all of his group members to grow and learn together.

I would also like to thank Professor Keith Woerpel for giving me the opportunity to work in his laboratory During my first three years of graduate school. Working together has helped me to grow and develop into an independent chemist.

Thanks to Professors Chris Vanderwal and Sergey Pronin for sitting on the committee for this degree. Your time and support is very much appreciated. I would especially like to thank Chris for taking time to discuss science throughout my graduate career, even after I had moved to New York University. I have learned a great deal from you.

All those in the Rychnovsky group and Woeprel group that I have had the pleasure to work and learn with over the years. They are not only my coworkers, but also my good friends. Notably (and in no particular order): Greg Suryn, Sarah Block, and Eric Novitsky (team 4004); Jacob DeForest (team BTX); Michael Holzwarth (team Pyridine), Nick Sizemore, Matt Perry, and Gidget Tay.

During grad school, I have made a number of friends who have made a significant impact on me. Jon and Jessica Paretsky, Avi Khanna, Wes Kramer, Elliot and Karli Fuller, and Alex and Lindsey Wagner have been the best of friends; we have grown tremendously together and I hope we continue to share great memories together. Without you, I would have never made it this far. Wynne Kandur, Peg Green, and Vi Tran were indispensible support during my time in Keith Woerpel's lab and during my transition back to UCI. Matt Beaver was my bay-mate for my first year at UCI. He trained me during my early time in grad school, and has continued to be great mentor and friend.

Justin and Jolie McNulty are two friends from high school that have supported me through the last five years. Their encouragement and support has made a great impact on me and reminded me (often in difficult times) of what great friends are.

I would not be in this program without the support and teachings of Drs. Phil Hampton, Gil Rishton, and Simone Aloisio. They are the ones who prepared me for success at UCI.

Lastly, my Mom, Dad, Brother and rest of the family have been wonderfully supportive during my time in graduate school. Mom and Dad, Thank you for all the love, support and guidance you have provided me with in my life. I can easily say that I am who I am today because of how you raised me. Aaron, you are not only my brother, but one of my best friends; thank you for always being there when I needed you and for being a prime example of what it means to endure and fight through the toughest of times.

CURRICULUM VITAE

JUSTIN ADAM HILF

EDUCATION:

University of California, Irvine February 2016
Ph.D. Candidate, Organic Chemistry

New York University August 2012
MS, Organic Chemistry

University of California, Irvine August 2009 to December 2010
Graduate studies

California State University, Channel Islands May 2009
BS, Chemistry

RESEARCH EXPERIENCE:

Doctoral Research, Advisor: Professor Scott Rychnovsky
University of California, Irvine November 2012 to March 2016
Progress Towards the Total Synthesis of Batrachotoxin and *A New Approach Towards the Synthesis of Substituted Pyridines*

Masters Research, Advisor: Professor Keith Woerpel
New York University November 2009 to July 2012
University of California, Irvine
The Synthesis of 10,12-Peroxycalamenene

Undergraduate Reseach, Advisors: Professor Phil Hampton and Dr. Gilbert Rishton
California State University, Channel Islands August 2007 to May 2009
The Design and Synthesis of Curcumin Analogues to Inhibit β-Secretase

PUBLICATIONS:

Hilf, J. A.; Witthoft, L. W.; Woerpel, K. A. An SN1–type Reaction to Form the 1,2-Dioxepane Ring: The Synthesis of 10,12-Peroxycalamenene, *J. Org. Chem.* **2015**, *80*, 8262–8267.

Hilf, J. A.; Holzwarth, M. S.; Rychnovsky, S. D. A New Approach Towards the Synthesis of Substituted Pyridines, *Manuscript in preparation* **2016**.

RESEARCH SKILLS:

Chemical Instrumentation Experience:
NMR spectroscopy (^{1}H, ^{13}C, ^{19}F, COSY, HMBC, HMQC, DEPT, NOE)
Mass Spectrometry (GCMS, ESI), HPLC and GC, FT-IR spectroscopy and UV/Vis spectroscopy

Small Molecule Synthesis
Research and development of reaction procedures, optimization, and scale up.
Air-free and schlenk line techniques.
Analysis and purification of reaction products through TLC, NMR spectroscopy, column chromatography, and recrystallization.

PRESENTATIONS:

Justin Hilf; *et al.*, Progress Towards the Total Synthesis of Batrachotoxin, 248th American Chemical Society National Meeting, San Francisco, CA, August 2014. (oral presentation)

Justin Hilf; *et al.*, Progress Towards the Total Synthesis of 10,12-Peroxycalamenene, Graduate Student and Postdoctoral Colloquium, May 2012, New York University. (oral presentation)

Justin Hilf; *et al.*, The Design and Synthesis of Curcumin Analogues to Inhibit β-Secretase, 21st Annual California State University Program for Education and Research in Biotechnology Symposium, Los Angeles, CA, January 2009. (poster presentation)

Justin Hilf; *et al.*, The Design and Synthesis of Curcumin Analogues to Inhibit β-Secretase, 42nd American Chemical Society Western Regional Meeting, Las Vegas, NV, September 2008. (poster presentation)

TEACHING EXPERIENCE:

Head Teaching Assistant, UC Irvine
General Chemistry laboratory — Fall 2014, Winter 2015, Spring 2015

Teaching Assistant, UC Irvine
General Chemistry Laboratory — Summer 2014
Organic Chemistry Lecture — Winter 2013, Spring 2013, Summer 2013, Summer 2014
General Chemistry Lecture — Fall 2012, Fall 2013
Organic Chemistry Laboratory — Fall 2009, Winter 2010, Spring 2010

HONORS AND AWARDS: Fall 2005 to Present

Advancement to Candidacy: Pass w/ Distinction
Margaret Strauss Kramer Fellowship
Magna Cum Laude
Program Honors (top graduating student within chemistry department, CSU Channel Islands)
The Alzheimer's Institute Fellowship Scholarship
The Poe Endowed Scholarship
Merck Award (top student in organic chemistry, CSU Channel Islands)
CRC Award (top student in general chemistry, CSU Channel Islands)

REFERENCES:

(*available upon request*)

ABSTRACT OF THE DISSERTATION

Progress Towards the Total Synthesis of Batrachotoxin

And

A Concise Method for the Synthesis of Substituted Pyridines

By

Justin Adam Hilf

Doctor of Philosophy in Chemistry

University of California, Irvine, 2016

Professor Scott D. Rychnovsky, Chair

Part I of this dissertation presents the efforts directed towards the total synthesis of batrachotoxin. The general approach focuses on the construction of the C ring of the steroid backbone through two carbon-carbon bond forming reactions. This approach breaks the complex natural product into two more approachable pieces. The AB ring system was accessed from the Hajos-Parish ketone and was coupled to the elaborated D ring by a conjugate addition/Claisen rearrangement sequence to form one of the desired carbon-carbon bonds. Extensive effort has been made in an attempt to cyclize the C ring.

Part II describes the development of a new approach to the synthesis of substituted pyridines. The method aims to provide a reliable synthesis of a diverse scope of substituted pyridines through a concise three step procedure. Readily available enones are first converted into 1,5-dicarbonyls through a two-step Sakurai allylation/oxidative cleavage sequence, which is followed by subsequent cyclization to the corresponding pyridine using hydroxylamine hydrochloride. A variety of substituted pyridines have been synthesized using this method.

PART I

(Chapter 1 and 2)

Progress Towards the Total Synthesis of Batrachotoxin

CHAPTER 1

Batrachotoxin: Structure, Biological Activity, and Reported Synthetic Work

Introduction and Biological Activity

Batrachotoxin (BTX) is one natural product in a small family of steroidal alkaloids first isolated by Daly and Witkop from poison obtained from the skins of Colombian poison arrow frogs, *Phyllobates aurotaenia*.[1] Secreted by the frogs as a defense mechanism, the poison has been used by the indigenous people of Central and South America for hundreds of years to poison the tips of their blow darts used for hunting.[2] Identified as the most active compound in the poison, only 30 mg of BTX was isolated from the skin extract of 2,400 frogs.[1] Other sources of BTX have also been identified since the original isolation, including the feathers of a New Guinea bird (*Pitohu*) and Melyridae beetles (*Choresine*).[3]

This family of steroidal alkaloids is mainly comprised of batrachotoxin, homobatrachotoxin, and batrachotoxinin A (**1-1**, **1-2**, and **1-3**, respectively),[4] whose complex structures differ only in substitution at the C20 oxygen (Figure 1.1).[5] The shared core of these natural products features a pentacyclic steroidal backbone, a seven-membered oxazapane ring, and a transannular hemiketal, all of which were unambiguously assigned using X-ray crystallography of a C20-*p*-bromobenzoate analogue of batrachotoxinin A.[5-6] As the parent compound of the family, **1-3** exists as the free alcohol at C20, whereas the others are functionalized as a substituted pyrrole ester at this position. These complex alkaloids have received significant attention from the scientific community not only for their unique structures, but also for their potent biological activity.

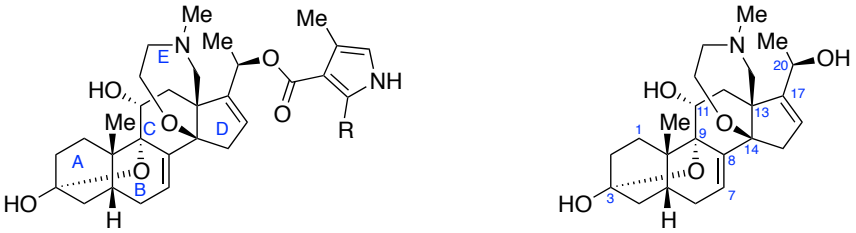

R = Me batrachotoxin (BTX) **1-1**
R = Et homobatrachotoxin **1-2**

batrachotoxinin A **1-3**

Figure 1.1. Batrachotoxin, homobatrachotoxin, and batrachotoxinin A

The biological activity of BTX has been extensively studied over the past 45 years. As one of the most potent non-peptidal neurotoxins known (LD_{50} = 2 μg/kg in mice), BTX is a strong agonist of voltage-gated sodium ion channels (VGSCs), locking them in the "open" position and preventing fast and slow inactivation.[7] Since VGSCs control the generation of action potentials and are important parts of the signal transduction process of membranes of neurons and other cells, the inability to control the ion gradient when BTX is bound often leads to cell death.[8] By better understanding the role of BTX as an agonist, potential advances in treating health conditions associated with VGSCs, including erythromelalgia, epilepsy, and diabetes,[9] can be identified.

Table 1.1. Toxic compounds and their LD_{50} in mice[2, 10]

Compound	LD_{50}, μg/kg
Botulinum Toxin A	0.0012
Batrachotoxin	2
Homobatrachotoxin	3
Tetrodotoxin	8
Strychnine	500
Batrachotoxinin A	1000

Although modeling studies and mutagenesis of VGSCs have helped to shed light on how BTX binds, a complete picture has yet to be reached.[7a,11] Mutagenesis has helped to identify key

interactions between batrachotoxin and site 2 of VGSCs, which explain the dominant structural features responsible for BTXs high affinity (Figure 1.2). The highly oxygenated portion of **1-1**, as well as the amine of the oxazapane ring, provide strong hydrogen bonding networks with site 2 of VGSCs. Pi-stacking interactions between the protein and pyrrole moiety of BTX also help to improve binding, and therefore potency, of the toxin. Loss of the pyrrole ester results in nearly a 1000-fold decrease of potency, as identified by the LD_{50} of batrachotoxinin A. Additional studies of BTX analogues have attributed the activity of the natural product to the E ring amine and ester moiety.[12]

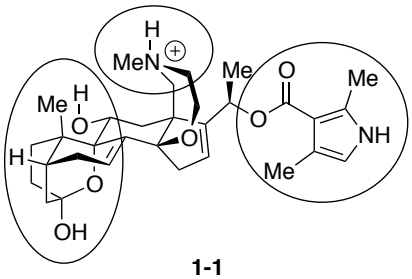

1-1

Figure 1.2. Key structural features of batrachotoxin for VGSC binding

Batrachotoxin has garnered significant attention from the synthetic community since its isolation in 1965. A variety of approaches have been reported in attempts to tackle this complex natural product, with only one total synthesis reported to date. These publications continue to direct and inspire future work on the molecule, including that of the Rychnovsky group.

Kishi's Total Synthesis of (±)-batrachotoxinin A

In 1998, the Kishi group published the first and only total synthesis of batrachotoxinin A.[13] Their retrosynthetic approach is summarized in Scheme 1.1. Key transformations included an oxy-Michael addition of **1-5** to close the E ring and an intramolecular Diels–Alder reaction of **1-7** to form both the C and D rings of the steroid backbone. An advanced AB ring system (**1-8**)

was synthesized from the Wieland–Miescher ketone,[14] which was used as the racemate, but could be used enantiopure to make the synthesis enantioselective.

Scheme 1.1. Kishi's retrosynthetic approach to batrachotoxinin A

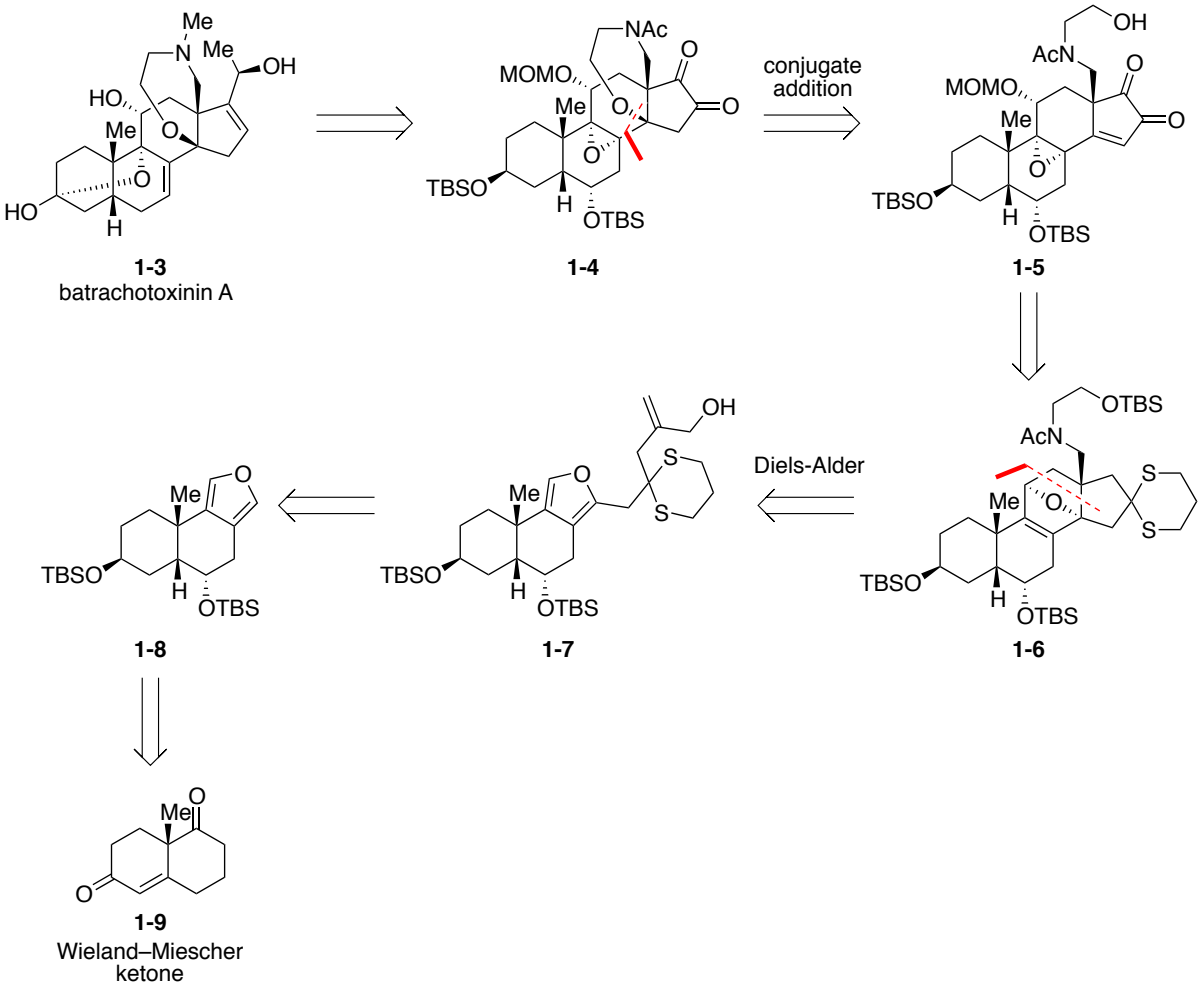

The synthesis began with a selective reduction of the saturated ketone in **1-9** using sodium borohydride, followed by acetylation to provide enone **1-10** (Scheme 1.2). Ketal protection, isomerization of the enone, and subsequent oxidation provided epoxide **1-11**, which could be easily converted to diol **1-12** using a four-step procedure to open the epoxide and reduce the ketal. Silyl protection of the diol, followed by deprotection and oxidation of the acetate protected alcohol afforded ketone **1-13**. The ketone was then converted to the substituted

furan (**1-8**) using a procedure reported by Garst and Spencer,[15] which provided the desired diene functionality needed for the Diels–Alder reaction.

Scheme 1.2. Kishi's synthesis of furan 1-8 from the Wieland–Miescher ketone

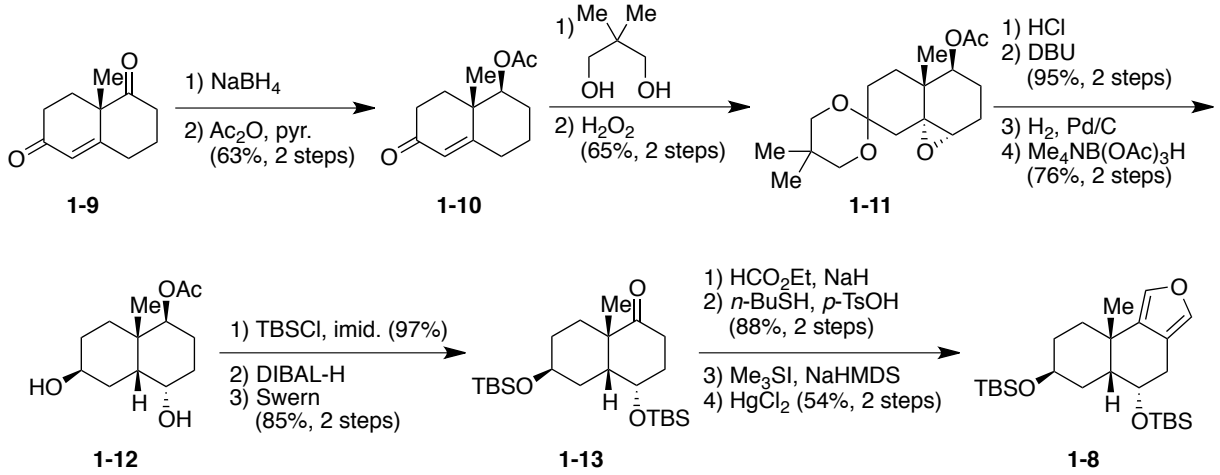

Formylation of furan **1-8**, followed by a Wittig olefination and subsequent alkylation provided dithiane **1-14** (Scheme 1.3). Lithiation of the dithiane was then achieved using *t*-butyl lithium, which was used to alkylate a substituted allyl bromide to afford the Diels–Alder precursor (**1-7**) after deprotection of the primary alcohol. Oxidation of the allylic alcohol to the corresponding enal using MnO_2 activated the dienophile and promoted an intramolecular [4 + 2] cycloaddition to occur. Addition of the dienophile is directed to the top face of the furan due to the ether substitution at C6. Following the cycloaddition, a reductive amination using a protected amino alcohol and subsequent acylation of the resulting amine appended the required four-atom chain for the E ring. With the steroid core complete, attention was directed to closing the E ring. The dithiane of intermediate **1-6** was first deprotected, followed by a base-mediated elimination of the bridging ether to reveal dienone **1-15**. Epoxidation (directed by the allylic alcohol at C11) of **1-15** was then carried out, and after protection of the alcohol and α-oxidation of the diketone, intermediate **1-16** was poised for E ring cyclization.

Scheme 1.3. Kishi's synthesis of the steroidal core

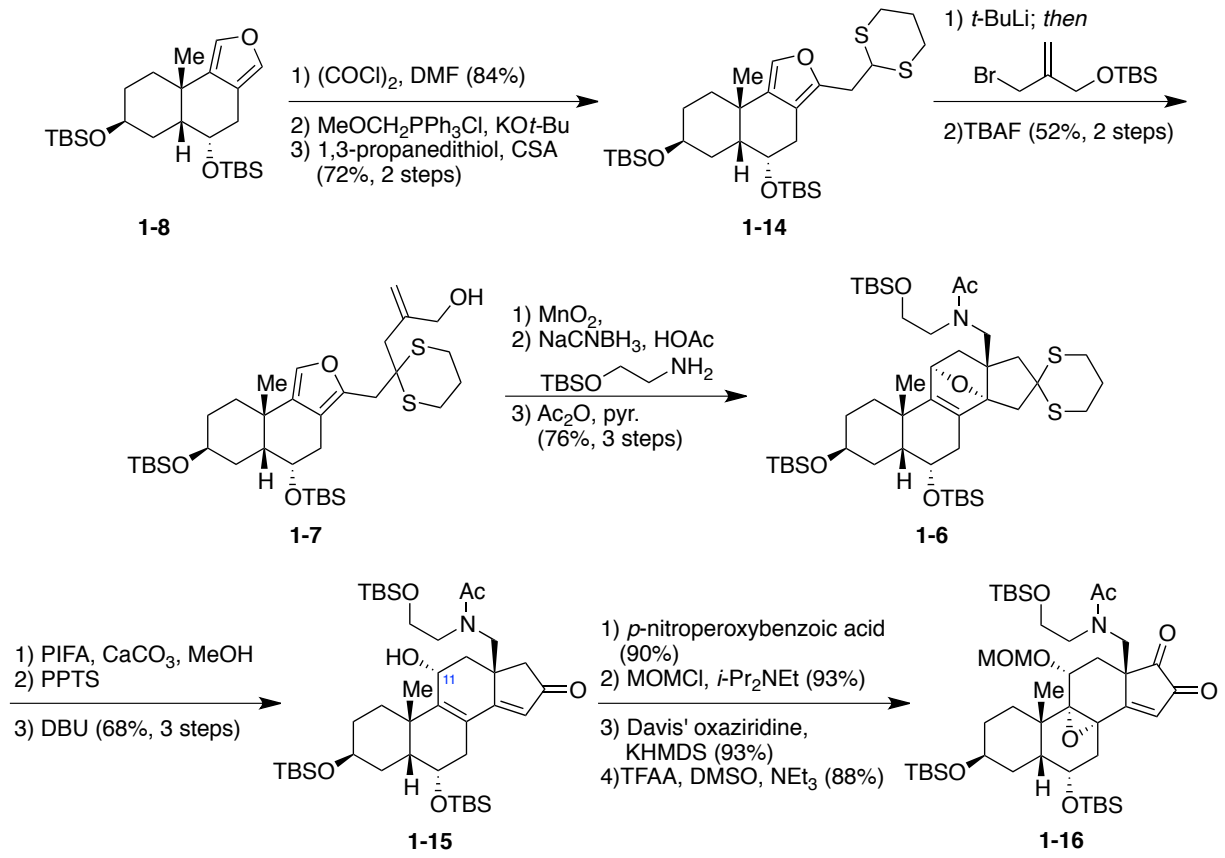

Closure of the E ring was next completed using an oxy-Michael reaction (Scheme 1.4). The primary alcohol of **1-16** was deprotected using TASF, which then underwent a spontaneous conjugate addition in the presence of $PhNTf_2$ to afford the desired enol triflate (**1-17**) in high yield. Hydrogenolysis of the enol triflate was carried out using platinum oxide, and after further oxidation of the system, triketone **1-18** was synthesized. Ketal formation was achieved by first subjecting **1-18** to DBU which induced a base-mediated epoxide opening, followed by methoxy-ketal formation using CSA in methanol. Removal of the C6 ketone was accomplished using a four-step procedure to reduce diketone **1-19**, regioselectively remove the C6 alcohol, and finally oxidize the remaining C17 alcohol to ketone **1-20**. Enol triflate formation and subsequent palladium-catalyzed carbonylation afforded unsaturated amide **1-21**, which could be methylated

to form the desired methyl ketone. After methylation of the E ring amine, zinc borohydride was used to diastereoselectively reduce the ketone to the desired allylic alcohol. A final deprotection of the ketal completed the first and only total synthesis of batrachotoxinin A (**1-3**) in 47 steps and, since the final esterification is a known transformation, a formal synthesis of batrachotoxin.

Scheme 1.4. Kishi's oxy-Michael E ring formation and completion of batrachotoxinin A

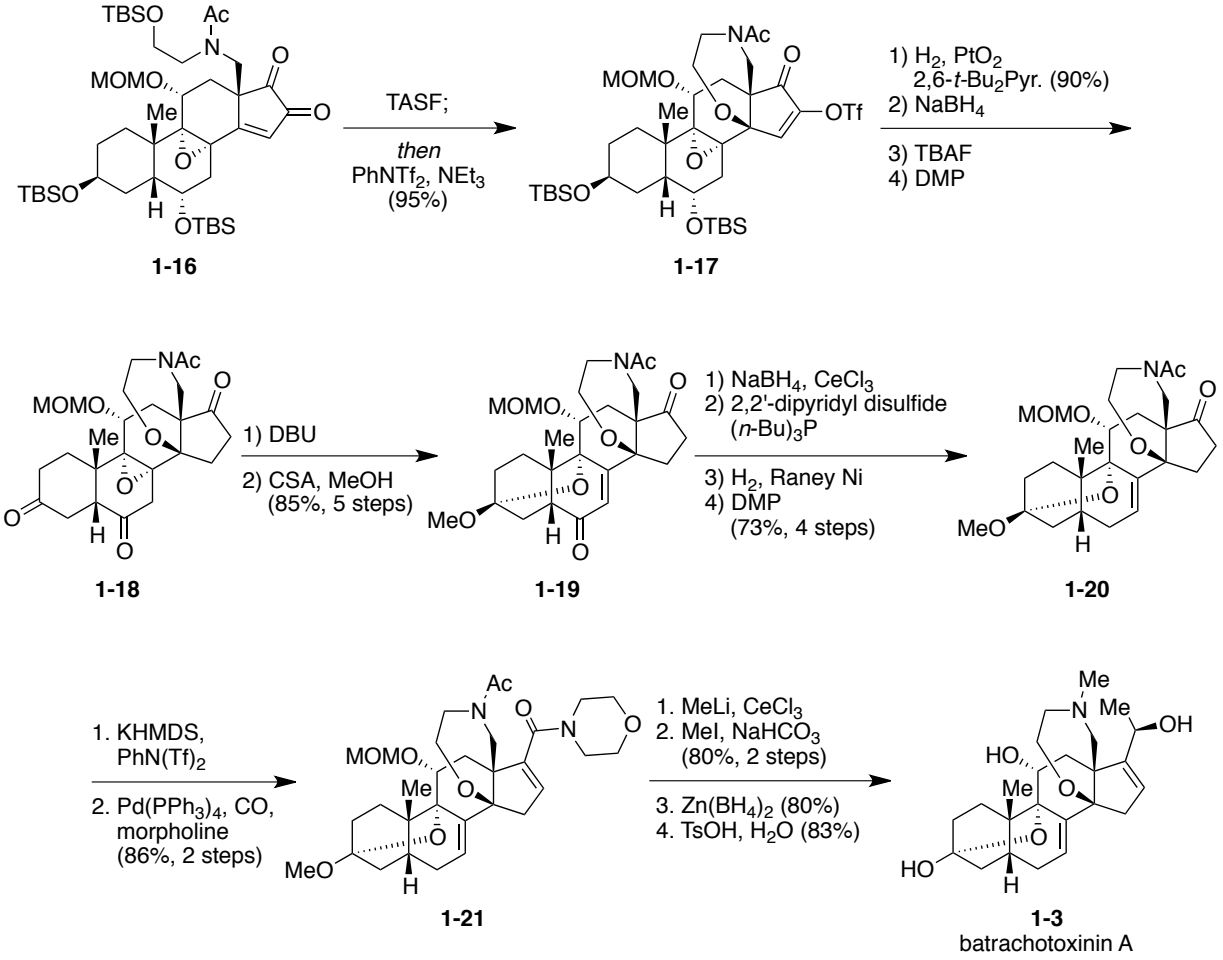

Kishi's total synthesis continues to be the benchmark for synthetic efforts towards BTX. With a longest linear sequence of 47 steps, however, it is an impractical route to producing appreciable quantities of the compound for biological studies. A number of other publications have also described synthetic efforts towards a total synthesis, including early work by Imhof[16] and Magnus,[17] as well as more recent efforts by Deslongchamps,[18] Parsons,[19] and Du Bois.[20]

Their work not only provides valuable information about the reactivity of complex intermediates en route to batrachotoxin, but also provides inspiration for new approaches towards the natural product, including work of our own.

Other synthetic work towards batrachotoxin

Early synthetic work towards batrachotoxinin A was pioneered by Imhof and coworkers, who focused on converting a pre-existing steroid (**1-22**) into an epimer of the complex natural product.[16] Their construction of the E ring from amino alcohol **1-23** provided a notable example for our synthetic endeavors. After a long series of functional group manipulations to install the necessary oxygenation, a reductive amination was used to install the amine needed for the oxazapane ring. The two-carbon unit needed to complete the E ring was installed by acylating amine **1-23** with chloroacetyl chloride. Deprotonation and cyclization of the C14 alcohol furnished the desired oxazapane (**1-24**). After differentiating the alcohols at C7 and C11 through a deprotection/monoprotection sequence, the dehydration of the C7 alcohol provided the desired unsaturation. Reduction of amide **1-25** and deprotection of the ketal afforded the C20 epimer of batrachotoxinin A (**1-26**).

Scheme 1.5. Imhof's partial synthesis of batachotoxinin A

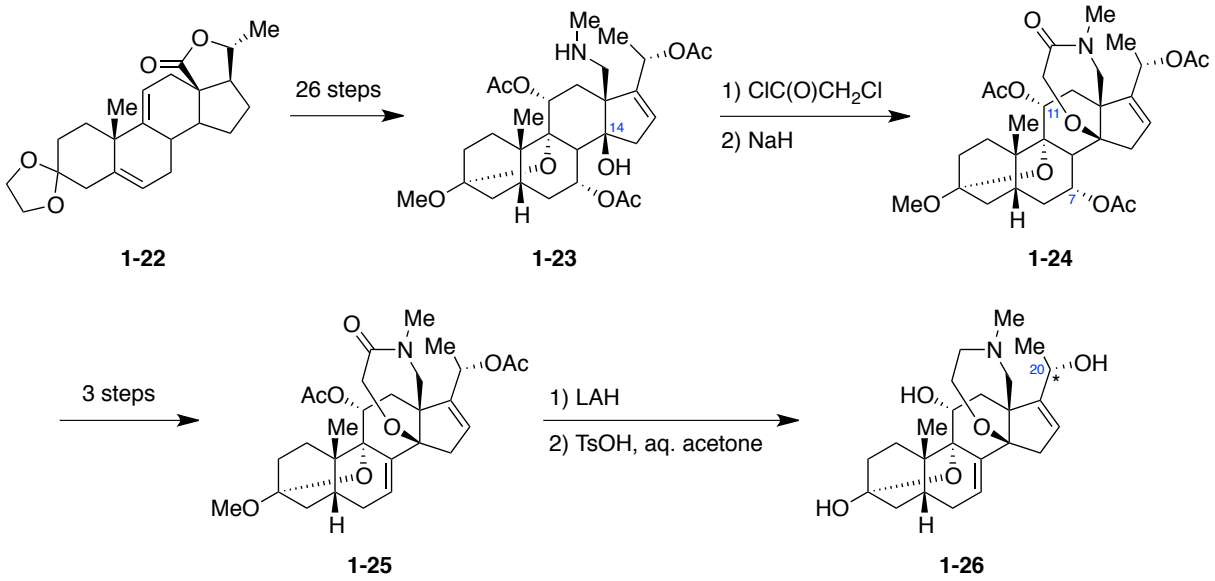

Before Kishi's use of a Diels–Alder reaction to cyclize the C ring, Magnus and coworkers demonstrated the utility of such a reaction for forming the highly substituted cyclohexane C ring.[17] Cis-decalone **1-27**, derived from a common alkaloid precursor, was converted to enyne **1-28** using lithium acetylide and subsequent elimination of the generated tertiary alcohol. Allylic oxidation, followed by reduction of both the alkyne and resulting ketone yielded diene **1-29**. After formation of the ester, the [4 + 2] cycloaddition was carried out to afford the strained lactone (**1-31**). Subsequent treatment with 4-methoxybenzylamine, followed by dihydroxylation and ketal formation provided a highly functionalized ABC ring analogue (**1-32**) of batrachotoxin.

Scheme 1.6. Magnus' patial synthesis of the ABC ring system

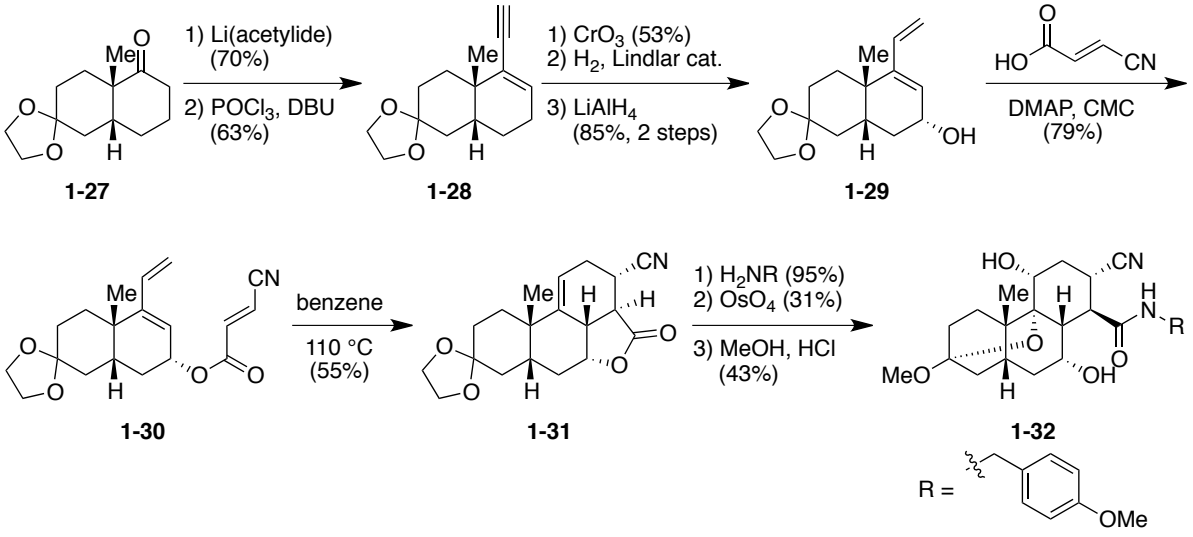

An alternative [4 + 2] cycloaddition, this time to build the B ring, was utilized in Deslongchamps' approach to BTX.[18] Functionalized intermediates **1-33** and **1-34** were coupled to generate **1-35** in 97% yield. The allyl ester was then decarboxylated using tetrakis(triphenylphosphine)palladium, followed by reduction of the aldehyde and acylation of the resulting aldehyde to yield diketone **1-36**. The C ring was then cyclized using an aldol addition to afford steroid **1-37** as a single diastereomer at C14. A similar nucleophilic addition into a D ring ketone has guided our approach to BTX.

Scheme. 1.7. Deslongchamps' partial synthesis of the steroidal backbone

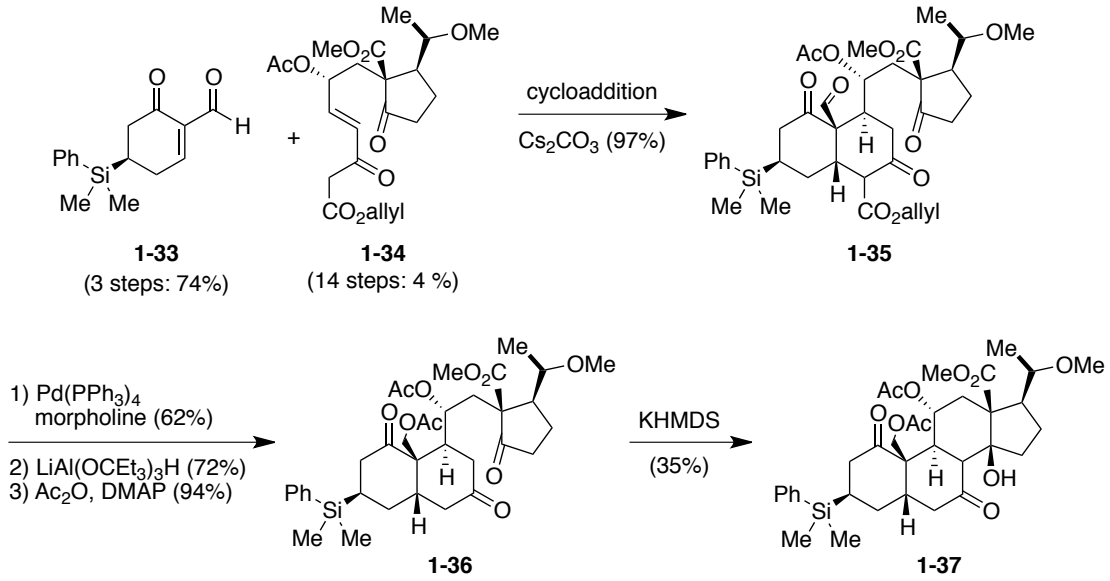

The Rychnovsky group's approach to BTX is most strongly inspired by the work of Parsons and coworkers.[19] α-Bromoenone **1-38**, whose synthesis will be discussed in Chapter 2, is a common intermediate shared between both groups' work towards the natural product. Parsons has demonstrated that alkyne addition can be achieved to obtain propargyl alcohol **1-39** as a single diastereomer. Transannular ketal formation, followed by removal of the trimethylsilyl moiety yields alkyne **1-40**, which can be subsequently hydrogenated to alkene **1-41**. A palladium-mediated annulation with cyclopentenone afforded tetracycle **1-42**. Further elaboration of this steroid-like intermediate has yet to be disclosed.

Scheme 1.8. Parsons' synthesis of a steroid analogue of BTX

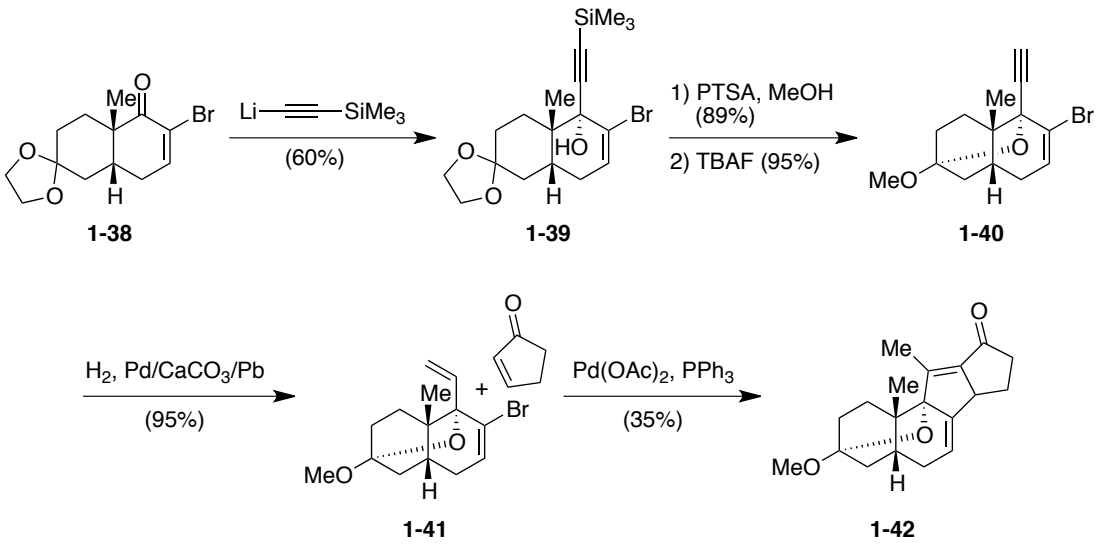

Most recently, Du Bois and coworkers reported synthetic efforts towards racemic batrachotoxin.[20] Their approach focused on construction of the CDE ring system, building the natural product in the other direction when compared to all previous work. This novel approach also allows for the production of CDE ring analogues, since key binding interactions between VGSCs and the CDE ring system's functionality have previously been identified. Nucleophilic addition of 3-bromofuran to aldehyde **1-43**, followed by protection of the generated hemiketal yielded tricycle **1-44** as a 2:1 mixture of the endo vs. exo products. When subjected to *n*-butyllithium, only **1-44-endo** cyclized to afford alcohol **1-45**, which was subsequently alkylated using allyl bromide. Hydrolysis of ketal **1-46** was then achieved using acetyl chloride, and the resulting C ring alcohol was protected as the methoxymethyl ether.

Scheme 1.9. Du Bois' synthesis of the CD ring system as a racemate

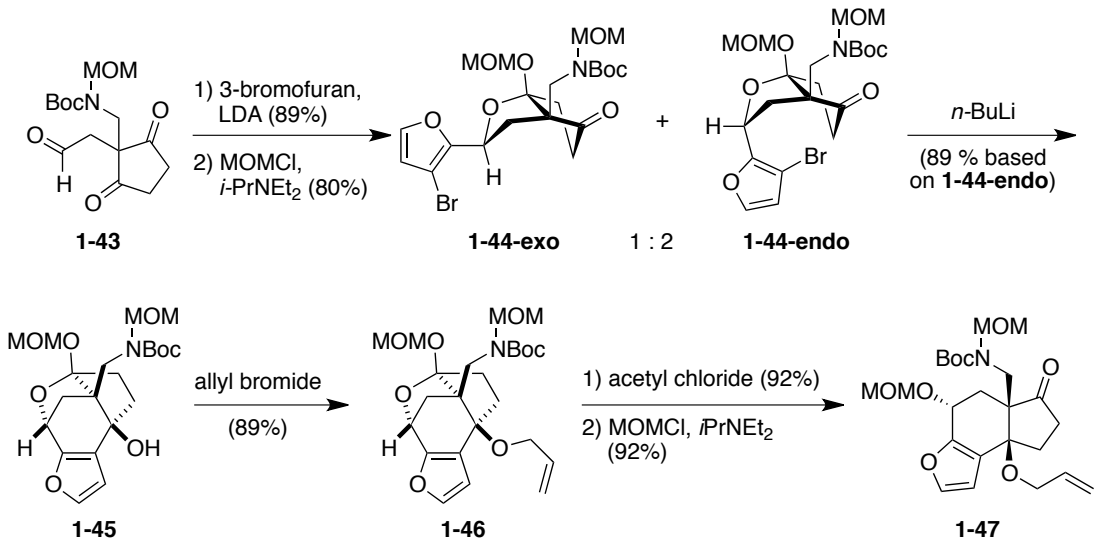

Before cyclizing the E ring, ketone **1-47** was first converted to the enol triflate and subjected to Stille cross-coupling conditions to afford enone **1-48** as the deprotected *N*-Boc amine. Diastereoselctive reduction of the ketone was achieved using DIBAL-H, followed by protection of the resulting alcohol as the silyl ether (**1-49**). To cyclized the E ring, oxidative cleavage of the pendent olefin revealed aldehyde **1-50**, which was subsequently subjected to reductive amination conditions. Reduction of the carbamate afforded oxazapane **1-51**, and thus completed the synthesis of a CDE ring analogue.

Scheme 1.10. Du Bois' synthesis of CDE ring analogue 1-51

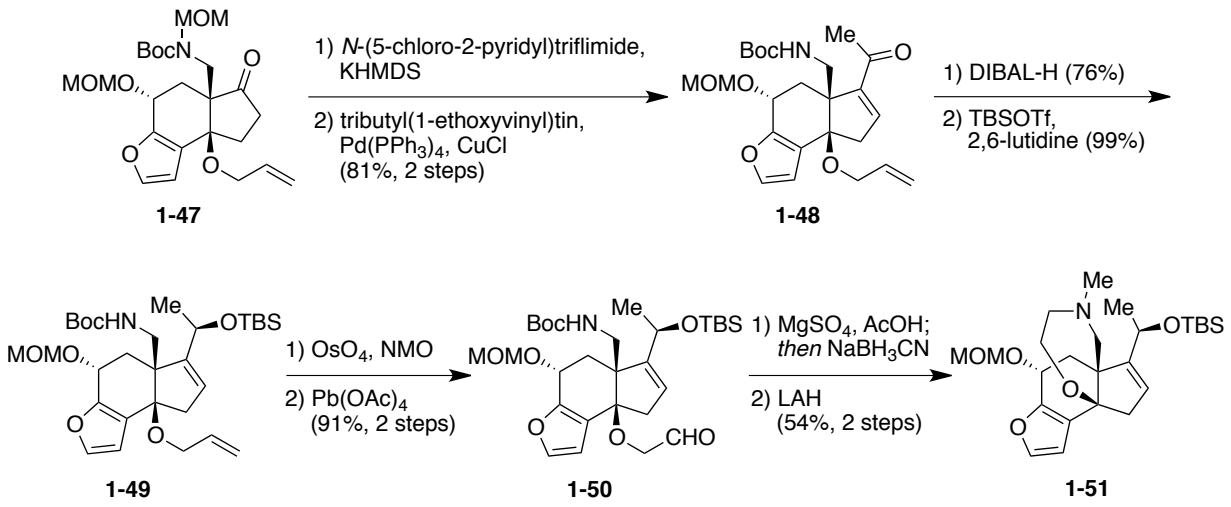

In an attempt to further elaborate **1-51**, various dienophiles were reacted with the furan moiety to afford Diels–Alder adducts **1-52** (Scheme 1.11A). Unfortunately, only modest diastereoselectivity was observed during these transformations. Alternatively, caged ketal **1-46** was reacted with some of the same dienophiles to determine whether the steric bulk of the closed system would have an effect on the diastereoselectivity of the transformation (Scheme 1.11B). These reactions provided the desired diastereomer in >20:1 selectivity. These cycloaddition adducts (**1-53**) can potentially be used to access racemic BTX and other analogues, though no further reports have been disclosed to date.

Scheme 1.11. Du Bois' Diels–Alder reactions of furan intermediates A) 1-51 and B) 1-46

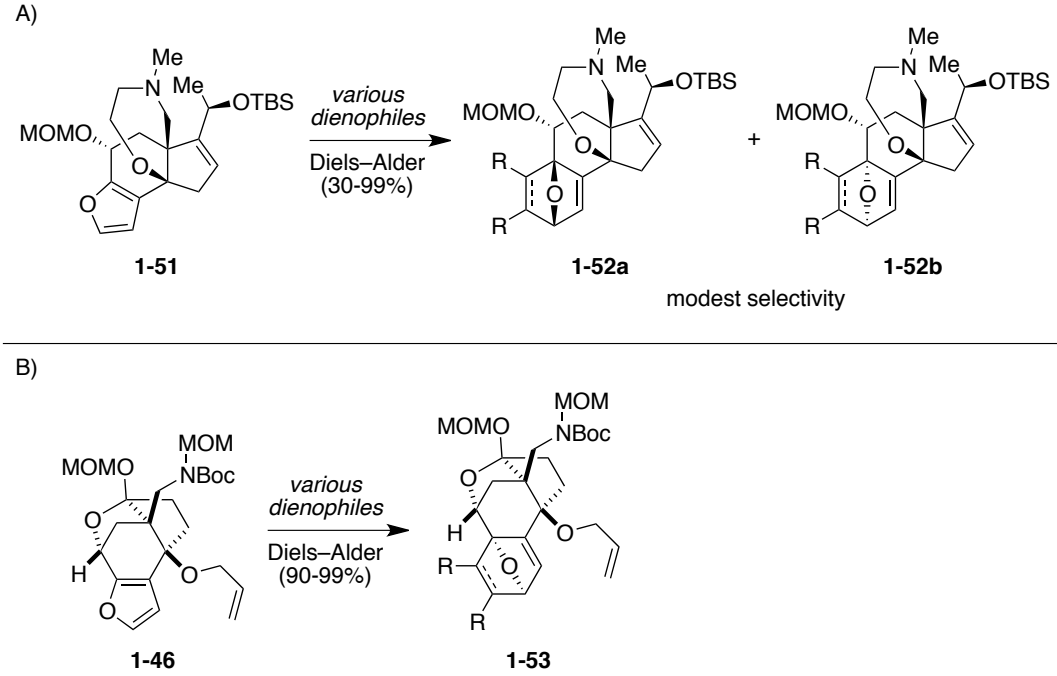

While a number of effective approaches toward the synthesis of batrachotoxin have been reported in the literature, only one total synthesis of racemic batrachotoxin, requiring over 40 linear steps, has been presented to date. An efficient enantioselective synthesis of BTX would be highly valuable in studying voltage-gated sodium ion channels, as well as the structure activity relationship (SAR) that makes batrachotoxin one of the most potent small molecule neurotoxins known.

1. Daly, J. W.; Witkop, B.; Bommer, P.; Biemann, K. *J. Am. Chem. Soc.* **1965**, *87*, 124–126.

2. Daly, J.; Witkop, B. *Clin. Toxicol.* **1971**, *4*, 331–342.

3. (a) Dumbacher, J. P.; Beehler, B. M.; Spande, T. F.; Garraffo, H. M.; Daly, J. W. *Science* **1992**, *258*, 799–801. (b) Dumbacher, J. P.; Wako, A.; Derrickson, S. R.; Samuelson, A.; Spande, T. F.; Daly, J. W. *Proc. Natl. Acad. Sci.* **2004**, *101*, 15857–15860.

4. 4ß-hydroxy analogugues of batrachotoxin and homobatrachotoxin have also been isolated as minor components. see: Tokuyama, T.; Daly, J. W. *Tetrahedron*, **1983**, 39, 41–47.

5. Tokuyama, T.; Daly, J.; Witkop, B. *J. Am. Chem. Soc.* **1969**, *91*, 3931–3938.

6. (a) Tokuyama, T.; Daly, J.; Witkop, B.; Karle, I. L.; Karle, J. *J. Am. Chem. Soc.* **1968**, *90*, 1917–1918. (b) Karle, I. L.; Karle, J. *Acta Cryst.* **1969**, *B25*, 428–434. (c) Gilardi, R. D. *Acta Cryst.* **1970**, *B26*, 440–441.

7. (a) Wang, S.-Y.; Mitchell, J.; Tikhonov, D. B.; Zhorov, B. S.; Wang, G. K. *Mol. Pharmacol.* **2006**, *69*, 788–795. (b) de Lera Ruiz, M.; Kraus, R. L. *J. Med. Chem.* **2015**, *58*, 7093–7118.

8. Bosmans, F.; Maertens, C.; Verdonck, F.; Tytgat, J. *FEBS Letters* **2004**, *577*, 245–248.

9. (a) Han, C.; Rush, A. M.; Dib-Hajj, S. D.; Li, S.; Xu, Z.; Wang, Y.; Tyrrell, L.; Wang, X.; Yang, Y.; Waxman, S. G. *Ann. Neurol.* **2006**, *59*, 553–558. (b) Vanoye, C. G.; Lossin, C.; Rhodes, T. H.; George, A. L. *J. Gen. Physiol.* **2006**, *127*, 1–14.

10. Pearce, L. B.; Borodic, G. E.; First, E. R.; Maccallum, R. D. *Toxicol. Appl. Pharmacol.* **1994**, *128*, 69–77.

11. (a) Wang, G. K.; Quan, C.; Wang, S.-Y. *Mol. Pharmacol.* **1998**, *54*, 389–396. (b) Catterall, W. A.; Cestèle, S.; Yarov-Yarovoy, V.; Yu, F. H.; Konoki, K.; Scheuer, T. *Toxicon* **2007**, *49*, 124–141. (c) Du, Y.; Garden, D. P.; Wang, L.; Zhorov, B. S.; Dong, K. *J. Biol. Chem.* **2011**, *286*, 13151–13160. (d) Nardi, A.; Damann, N.; Hertrampf, T.; Kless, A. *ChemMedChem* **2012**, *7*, 1712–1740.

12. (a) Warnick, J. E.; Albuquerque, E. X.; Onur, R.; Jansson, S. E.; Daly, J.; Tokuyama, T.; Witkop, B. *J. Pharmacol. Exp. Ther.* **1975**, *193*, 232–245. (b) Khodorov, B. I.; Yelin, E. A.; Zaborovskaya, L. D.; Maksudov, M. Z.; Tikhomirova, O. B.; Leonov, V. N. *Cell. Mol. Neurobiol.* **1992**, *12*, 59–81.

13. Kurosu, M.; Marcin, L. R.; Grinsteiner, T. J.; Kishi, Y. *J. Am. Chem. Soc.* **1998**, *120*, 6627–6628.

14. Wieland, P.; Miescher, K. *Helv. Chim. Acta* **1950**, *33*, 2215–2228.

15. Garst, M. E.; Spencer, T. A. *J. Am. Chem. Soc.* **1973**, *95*, 250–252.

16. (a) Imhof, R.; Gössinger, M. E.; Graf, W.; Berner, H.; Berner-Fenz, M. L.; Wehrli, H. *Helv. Chim. Acta* **1972**, *55*, 1151–1153. (b) Imhof, R.; Gössinger, E.; Graf, W.; Berner-Fenz, L.; Berner, H.; Schaufelberger, R.; Wehrli, H. *Helv. Chim. Acta* **1973**, *56*, 139–162.

17. Magnus, P.; Leapheart, T.; Walker, C. *J. Chem. Soc., Chem. Commun.* **1985**, 1185–1186.

18. Trudeau, S.; Deslongchamps, P. *J. Org. Chem.* **2004**, *69*, 832–838.

19. (a) Hudson, P.; Pairaudeau, G.; Parsons, P. J.; Jahans, A. W.; Drew, M. G. B. *Tetrahedron Lett.* **1993**, *34*, 7295–7298. (b) Lacrouts, P.; Parsons, P. J.; Penkett, C. S.; Raza, A. R. *Synlett* **2005**, 2767–2768.

20. Sloan Devlin, A.; Du Bois, J. *Chem. Sci.* **2013**, *4*, 1059–1063.

CHAPTER 2

Progress Towards the Synthesis of the Steroid Backbone of Batrachotoxin

Retrosynthetic Analysis

Work within the Rychnovsky group on batrachotoxin has always been focused on disconnections about the C ring (Scheme 2.1). This approach would break a very complex synthetic target into two more approachable pieces. The AB ring system (**2-2**) would be accessed using similar methods to those previously explored by Kishi[1] and Parsons,[2] while the DE ring scaffold (**2-3**) would provide new challenges.

Scheme 2.1. C ring Disconnection

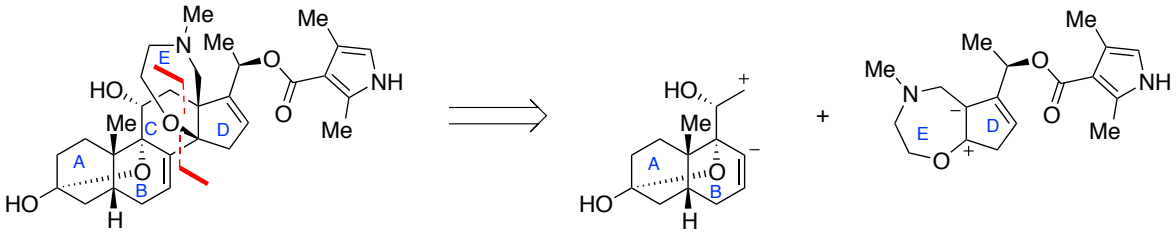

2-1 **2-2** **2-3**

With this key disconnection guiding our approach, a more elaborated retrosynthesis was devised (Scheme 2.2). Installation of the aromatic ester moiety, amide reduction, and deprotection of the hemiketal would provide BTX (**2-1**) from steroid **2-4**, all of which have been previously demonstrated on similar systems.[1] We envisioned that both alcohols in compound **2-4** could come from oxidative cleavage and reduction of the corresponding terminal olefins. A judicious choice of reducing agents could also effect the simultaneous reduction of the amide in **2-5**, assuming that the diastereoselective reduction of both ketones were substrate-controlled. The oxazepinone E ring would be constructed using chemistry similar to that of Imhof and coworkers,[3] returning to *cis*-fused cyanoalcohol **2-6**. Metallation of a vinyl bromide followed by

closure onto the pendant ketone of **2-7** would close the C ring, hopefully with the correct stereochemistry. Finally, alkylation of a functionalized cyclopetanone (**2-9**) using an allylic electrophile (**2-8**) would join the AB and D rings of the steroid.

Scheme 2.2. Elaborated retrosynthetic approach of BTX

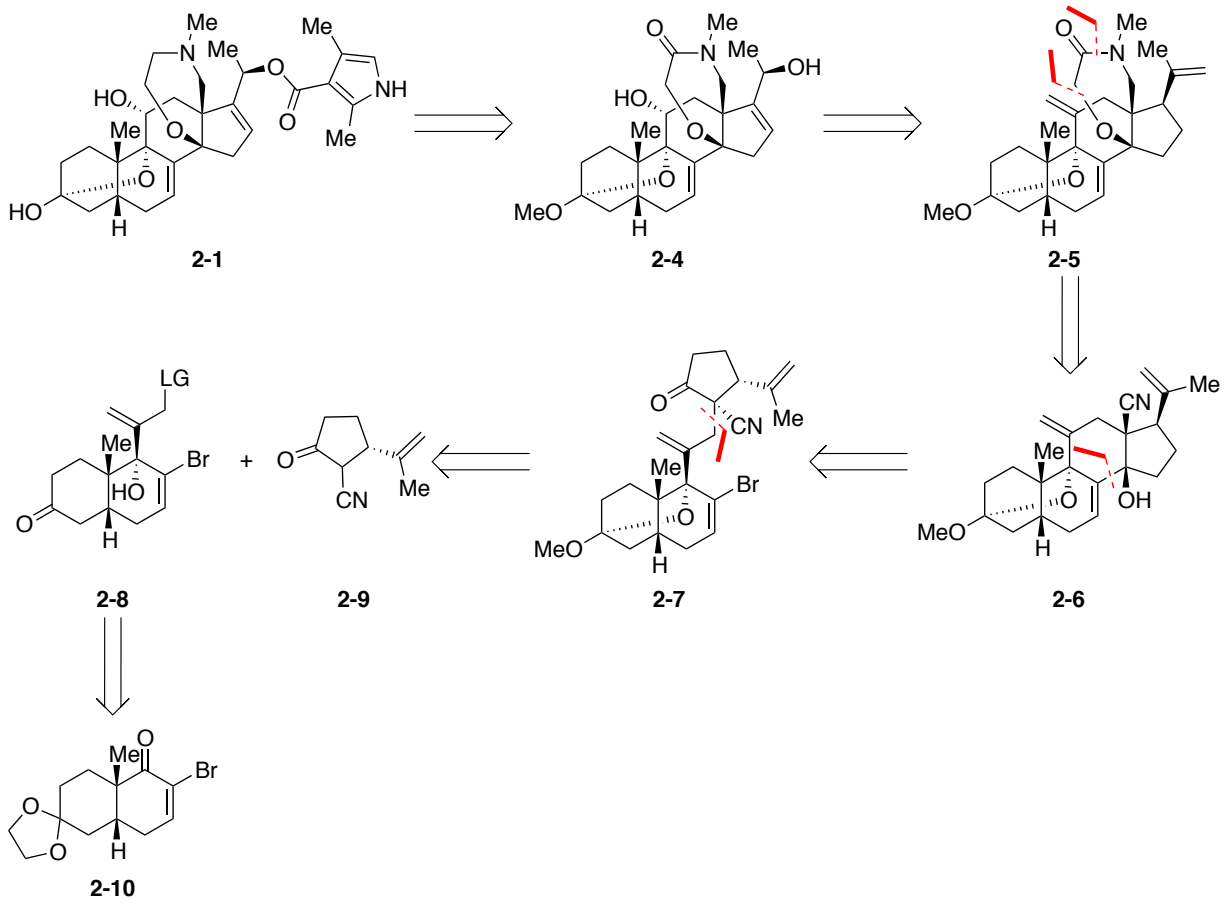

Previous work on BTX, including work within the group performed by Dr. Amber Reilly,[4] Dr. Shinya Yoshida,[5] and Dr. Maureen Reilly,[6] identified the Hajos–Parrish ketone as a suitable chiral starting material. Their combined efforts provided valuable lessons regarding the reactivity and sensitivity of early intermediates towards the synthesis of BTX. Much of their work focused on a variety of AB analogues (Scheme 2.3), with the hope of identifying a suitable motif to couple with an elaborated D ring. By utilizing the alkyne addition and ketal formation of decalone **2-10,** used in Parson's partial synthesis,[2] alkyne **2-11** was successfully converted into a

variety of potentially useful intermediates (**2-12** to **2-15**). Unfortunately, none of these systems proved to be viable, as no successful couplings with a variety of D ring surrogates was achieved. With this knowledge, Dr. Maureen Reilly moved away from alkyne **2-11**, and discovered an alternative addition product that was successfully coupled with D ring **2-9**. It was at this time that I joined the project, and began further exploring the reactivity of these intermediates.

Scheme 2.3. Previous AB ring system analogues

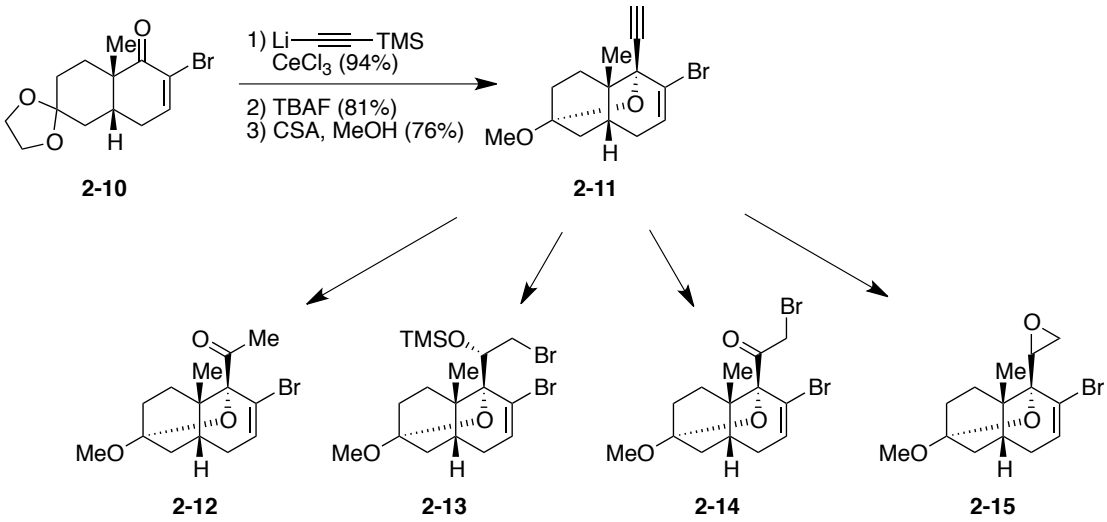

Current Synthetic Work

The synthesis of the AB ring system begins with the Hajos–Parrish ketone (**2-16**).[7] Large-scale preparation of this chiral building block was achieved via an enantioselective Robinson annulation of 2-methyl-1,3-cyclopentanone and methyl vinyl ketone.[8] Hydrogenation of the alkene in the presence of ethylene glycol provided the protected *cis*-hydrindanone (**2-17**). Subsequent silyl enol ether formation using TESOTf afforded **2-18** in 87% yield over 2 steps. This sequence was easily scaled to multi-gram quantities without any issues. Ring expansion of the enol ether to the corresponding α-bromoenone (**2-10**) was successfully carried out through

the addition of dibromocarbene, generated *in situ* using bromoform and base. Use of the triethylsilyl protecting group allowed for smooth conversion to the desired enone, key insight identified by Dr. Shinya Yoshida.[5] Unfortunately, the reaction proved difficult to scale up, so further optimization was necessary.

Scheme 2.4. Synthesis of enone 2-10 from the Hajos–Parrish ketone

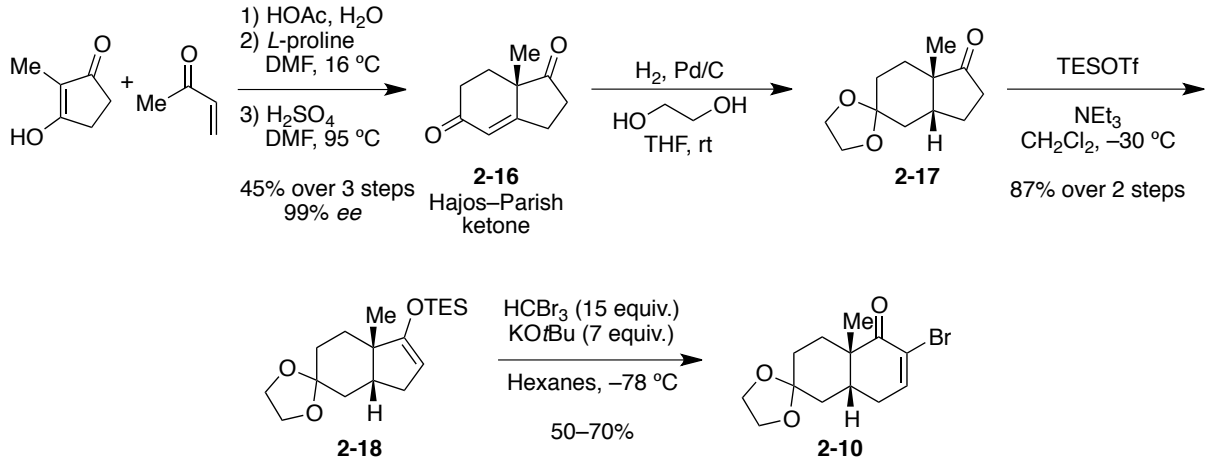

Starting with the previously optimized conditions listed in Scheme 2.4, it was quickly discovered that the quality of reagents played an integral part in the reproducibility of the ring expansion. The use of bromoform without additional purification (Table 2.1, entry 1) completely shut down reactivity, presumably owing to the stabilizers added to most commercially available samples of the reagent to prevent degradation. Using sublimed KO*t*Bu also improved yields. The previously optimized procedures called for the portion-wise addition of the base over 8 hours, which was not only very tedious, but upon scale up, produced an undesired increase in temperature due to the large quantities of reagents used. Considering the decrease in yield (entries 2 to 3 as compared to small scale results, i.e. 50–70%) as the reaction sized increased, further attempts were made to improve the reliability of the reaction. The most significant advance came when distilled bromoform was added to a stirring solution containing the base, opposite that of the previously suggested procedures (entry 5). This change not only improved

yields, but also allowed for reduced reaction times and a decrease of the equivalents of each reagent used, since the bromoform could be added dropwise, allowing for better temperature control. The reaction was now easily scalable, and was run on up to 4 grams of material, with yields of enone **2-10** consistently between 60–65% (entries 6 and 7).

Table 2.1. Ring expansion scale-up optimization

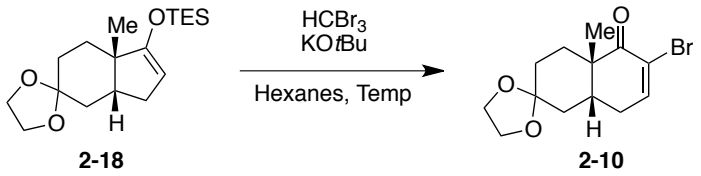

2-18 **2-10**

Entry	Scale (g)	$HCBr_3$ (equiv.)	KO*t*Bu (equiv.)	Time (h)	Temp (°C)	Yield (%)
1[a]	1.0	15[c]	7[d]	8	–78	0
2[a]	0.5	15	7	8	–78	45
3[a]	1.0	15	7	8	–78	38
4[b]	1.0	15	10	3	–78	47
5[b]	0.5	8	8	1.5	–50	60
6[b]	1.5	8	8	2	–50	65
7[b]	4.0	8	8	2	–50	63

[a]base added portion-wise to reaction containing bromoform; [b]bromoform added dropwise to reaction containing base; [c]bromoform was not distilled before use; [d]KO*t*Bu was not sublimed

Attention was next turned to the 1,2-addition of an isopropenyl nucleophile to enone **2-10**. Previous work by Dr. Maureen Reilly had shown that only organolithium reagents could be added regioselectively, albeit in low yields. In an attempt to identify an alternative nucleophile that would improve the outcome of the addition, a variety of metals were screened (Table 2.2). When Grignard reagents were used (entry 1), only the 1,4-addition product (**2-21**) was observed. When $CeCl_3$ or $LaCl_3$ were included to promote 1,2-addition (entries 2 and 3, respectively), no improvement of regioselectivity was observed. The use of zinc reagents offered no improvements (entry 5), while attempts to transmetallate to ytterbium failed altogether (entry 8). Yields of the isopropenyllithium addition consistently fall between 30–40% because of a

competitive lithium-halogen exchange with the vinyl bromide of **2-10**, yielding dehalogenated **2-20**. Since lithium-halogen exchange is a fast process, the temperature of the reaction was increased in the hope that the 1,2-addition would compete with the undesired pathway (entry 7). No change in reactivity was observed, and any future alkylations were carried out using the conditions found in entry 6. This step remains a current bottleneck in the synthesis, but has provided enough material to continue moving forward. It is important to note, however, that these alkylations are in stark contrast to alkynyllithium additions, where yields are in the 90% range.[5-6]

Table 2.2. Isopropenyl nucleophile addition to enone 2-10

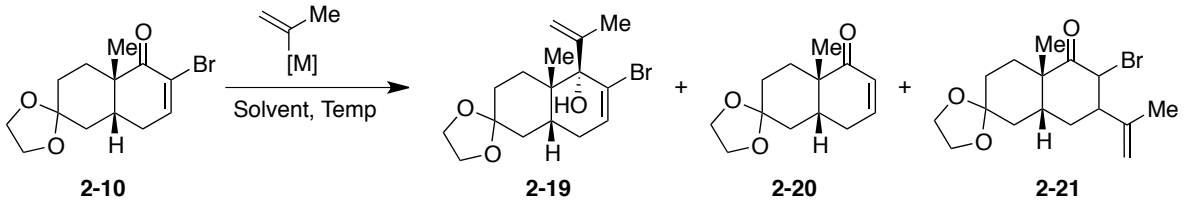

2-10 **2-19** **2-20** **2-21**

Entry	Metal [M]	Additive	Solvent	Temp (°C)	Product(s) (yield)
1	MgBr	-	Et_2O	0-23	**2-21**(92%)
2	MgBr	$CeCl_3$	THF	23	**2-19**(8%), **2-21**(80%)
3	MgBr	$LaCl_3$	THF	23	**2-21**(72%)
4	ZnCl	-	Et2O	–40	N.R.
5	ZnCl	-	THF	23	**2-21**(61%)
6	Li	-	Et_2O/THF	–78	**2-19**(36%) **2-20**(38%)
7	Li	-	Et_2O/THF	–40	**2-19**(33%) **2-20**(40%)
8	Li	$Yb(OTf)_3$	Et_2O	–78	N.R.

A possible alternative to accessing a similar isopropenyl adduct (**2-22**) was envisioned by using one of Dr. Yoshida's intermediates, ketone **2-12** (Scheme 2.5). The alkyne addition product (**2-11**) can be smoothly converted to the corresponding methyl ketone in 83% yield (48% from **2-10**). Olefination of the ketone would then provide **2-22**, though the yields of this reaction would have to be very high in order to compete with the low yield of the single transformation.

Two different olefination reactions were attempted; a methylene Wittig olefination[9] and a titanium-mediated olefination.[10] Unfortunately, neither reaction succeeded in generating the desired product, and this pathway was quickly abandoned.

Scheme 2.5. Alternative route to olefin 2-19

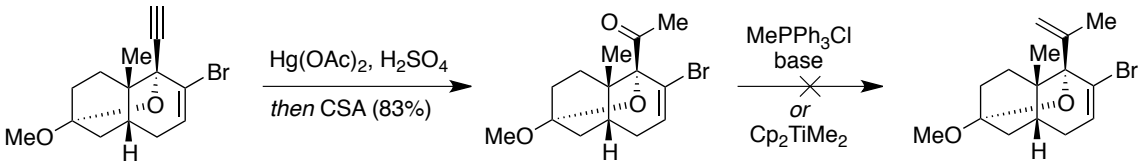

2-11 **2-12** **2-22**

Attention was next focused on synthesizing the D ring. A route to enantiopure vinyl chloride **(*S*)-2-25** was painstakingly pursued by Dr. Maureen Reilly (Scheme 2.6A).[6] Ultimately, a route was selected that provided the desired compound in an overall yield of 12% and 4:1 e.r.. The resolution utilized a CBS reduction/DMP oxidation sequence to enrich **2-9** as the desired enantiomer. In order to progress through the synthesis, and without knowing the stereochemical outcome of future reactions, the racemate of **2-25** was used for further reactions (Scheme 2.6B). In either case, cyclopentenone **2-24** was synthesized from adiponitrile (**2-23**) in 67% yield over two steps; a Thorpe–Ziegler reaction first cyclizes the dinitrile, followed by oxidation to the unsaturated system using phenylselenenyl chloride and hydrogen peroxide. A 1,4-addition using isopropenyl magnesium bromide afforded a racemic mixture of **2-9**. Careful control of the number of equivalents of Grignard reagent was necessary to avoid alkylation of the nitrile. Compound **2-9** could either be generated in enantioenriched form using the previously mentioned resolution, or obtained as the racemate. Finally, the vinyl chloride (**(*rac)*-2-25**) was installed using triphenylphosphine and carbon tetrachloride.

Scheme 2.6. Synthesis of A) enantioenriched D ring and B) racemic D ring

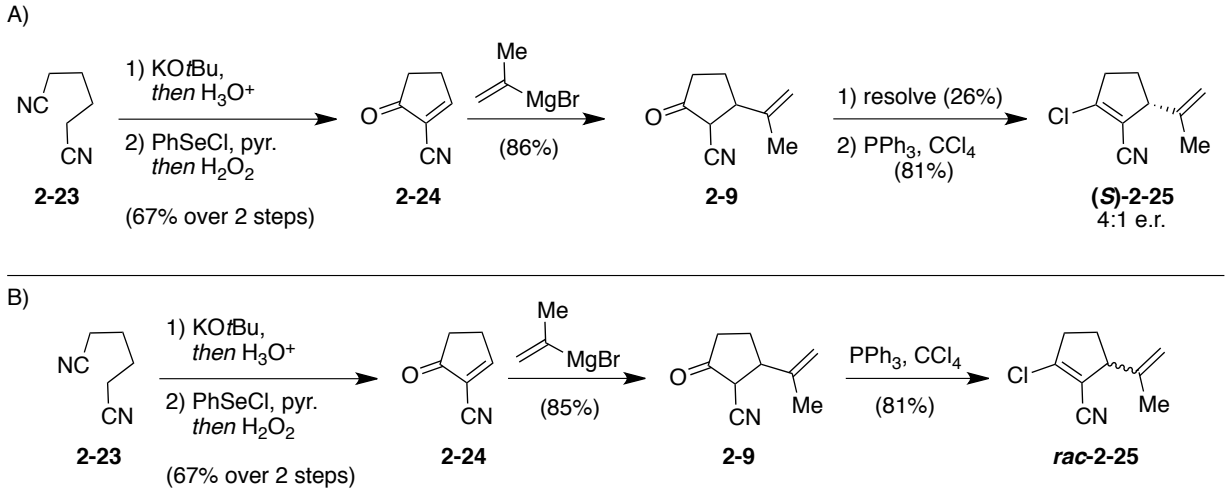

With two possible D ring scaffolds available (**2-9** and **2-25**), two potential pathways for joining the AB and D rings were investigated (Scheme 2.7). Cyclopentanone **2-9** could be either *C*- or *O*-alkylated using a halogenated AB ring system electrophile, both of which are useful compounds. To model whether this transformation could be not only achieved, but also regioselective, **2-9** was reacted with methallyl bromide. These transformations yielded a 2.5:1 mixture of *C*- and *O*-alkylated products, respectively. Most importantly, *C*-alkylated **2-26** was isolated as a single diastereomer,[11] suggesting that a stereoselective alkylation could be achieved using substrate control. Alternatively, vinyl chloride **2-25** could be displaced using a nucleophile. An oxy-Michael/elimination reaction sequence was used to couple **2-25** and methallyl alcohol in the presence of sodium hydride, yielding ether **2-27**. Heating in toluene afforded the Claisen rearrangement product (**2-26**) in 69% yield over the two steps. Once again, the allylation product was obtained as a single diastereomer, similar to the direct alkylation, as well as other reported Claisen rearrangements of similar systems.[12] With both pathways providing similar outcomes, two different AB ring systems were synthesized.

Scheme 2.7. Modeling the D ring alkylation

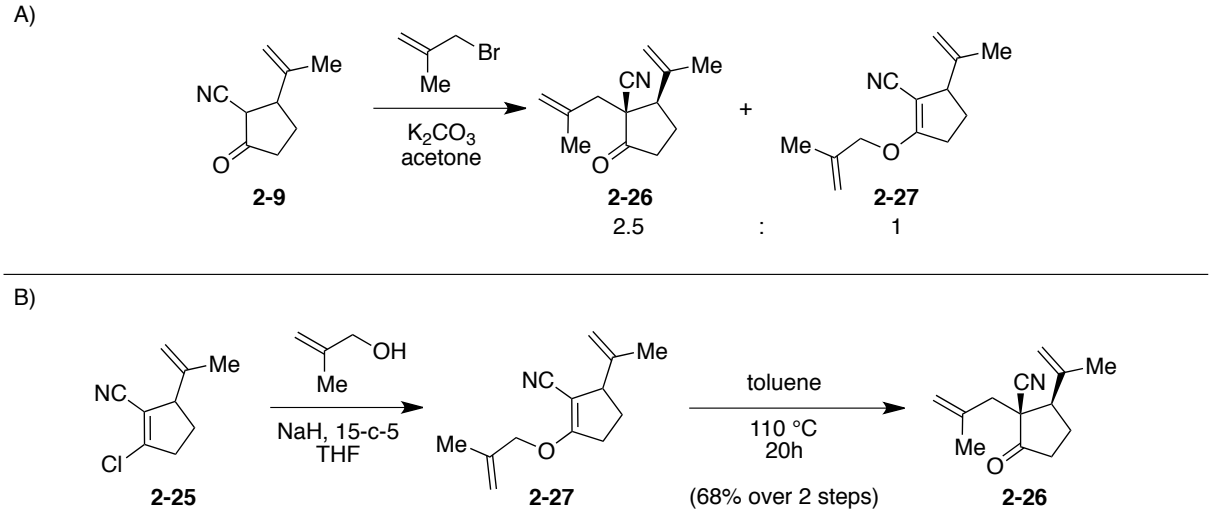

Since methallyl bromide was competent as an alkylating agent for the D ring, allylic bromination of the AB system was explored. Initial attempts to brominate the newly installed isopropenyl moiety of **2-19** utilizing radical-mediated bromination conditions were unsuccessful (Scheme 2.8A).[13] Alternatively, ionic bromination conditions[14] appeared to form the desired bromonium ion intermediate, but did not yield any of the desired allyl bromide (Scheme 2.8B). Instead, small amounts of bromo-epoxides (**2-29** and **2-30**) were isolated, and any attempt to ring-open the epoxide using acid or base decomposed the material. One additional product was identified in trace quantities, and provided promising insight into the desired reactivity. The presence of allyl bromide **2-31** suggested that if the allylic alcohol of **2-19** was tied up through ketal formation, the desired product could be obtained. With this concept in mind, alcohol **2-19** was converted to methyl ketal **2-22** in 86% yield using catalytic amounts of CSA (Scheme 2.8C). Allylic bromination could now be achieved in 75% yield using the same ionic conditions previously attempted on **2-19**. It is important to note that allyl bromide **2-32** exists as a mixture of rotamers, clearly identified in ^{1}H and ^{13}C NMR spectra. This observation suggests that rotation of the allylic bromide moiety is restricted through steric interactions with the cage-like

structure of the closed ketal AB ring system, which may cause issues with reactivity of this moiety.

Scheme 2.8. Allylic bromination of the AB ring system

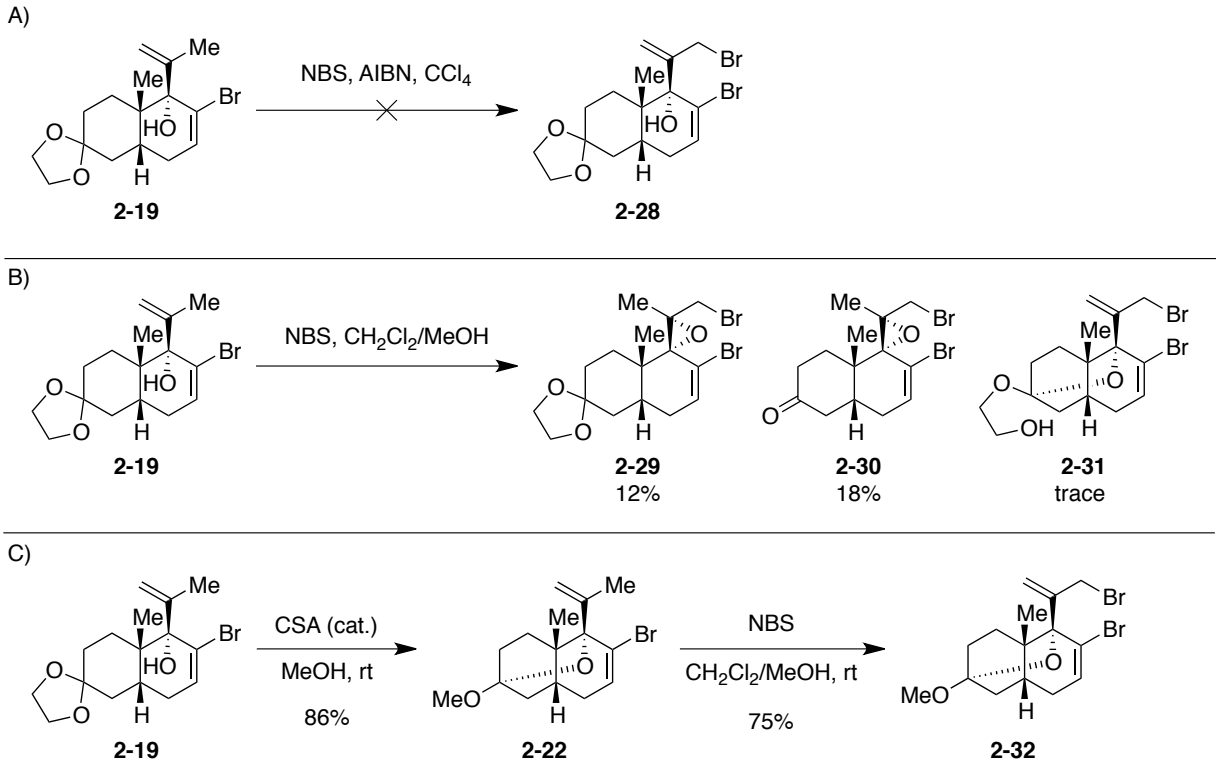

Nevertheless, with allyl bromide **2-32** in hand, alkylation of the D ring could be attempted (Scheme 2.9). The use of conditions similar to those of the model system yielded only trace amounts of *O*-alkylated **2-33**. Small adjustments to base, time, and temperature showed little to no change to the reaction's outcome. More importantly, *C*-alkylation (**2-7**) was never observed, once again suggesting that the steric environment may hinder reactivity around the caged AB system. In addition to the D ring scaffolds described herein, reactions using a more elaborated D ring scaffold were also unsuccessful. With no promising leads for direct allylation of the AB ring, this pathway was abandoned, and an alternative pathway pursued.

Scheme 2.9. Attempted alkylation using allyl bromide 2-32

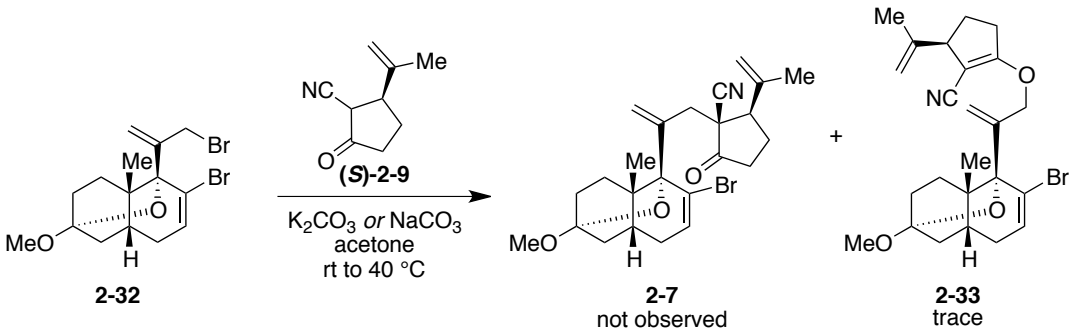

The alternative pathway utilized the Claisen rearrangement demonstrated by the model system in Scheme 2.7B, and required the installation of an allylic alcohol on the AB ring, which would be used to couple to the D ring vinyl chloride (**2-25**). The allylic alcohol was introduced by first epoxidizing the more electron-rich olefin of **2-19** to epoxide **2-34** in 92% yield. Deprotection of the ethylene glycol ketal could then be achieved using catalytic CSA at elevated temperatures to reveal ketone **2-35**. Careful monitoring of this reaction was crucial, as undesired cyclization to the caged methoxy ketal (**2-36**) was occasionally observed in varying amounts. Deprotection of the ketal was important however, since it was somewhat labile under a variety of conditions. Complex mixtures of undesired side products were often obtained from later reactions when deprotection was not completed first. A titanium-mediated epoxide opening was then used to convert **2-35** to allylic alcohol **2-37**, which was immediately coupled with **(*S*)-2-25** to afford the desired Claisen rearrangement precursor, **2-33**, in 78% yield over two steps. Any attempt to carry ketal **2-36** through the same sequence was unsuccessful.

Scheme 2.10. Synthesis of Claisen rearrangement precursor 2-33

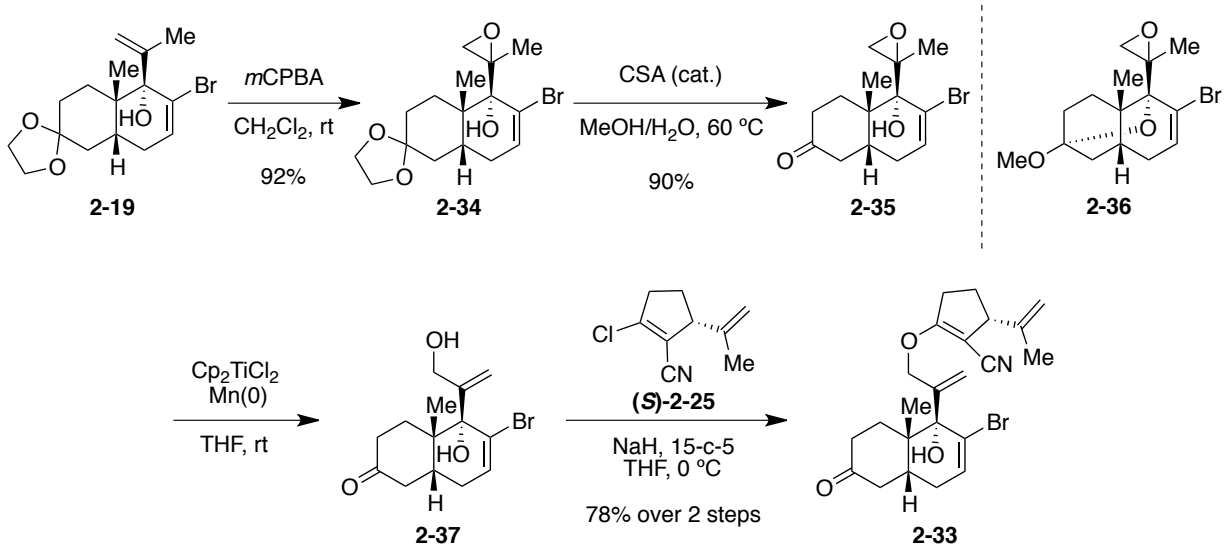

We next investigated the conditions necessary for the desired Claisen rearrangement. The desired product was not observed under the same conditions previously used on the model system (Table 2.3). When the reaction temperature was increased to 132 °C,[4] desired product **2-39** began to form, albeit at a very slow rate.[6] After 6 days of heating, the desired product was isolated in 87% yield (Table 2.3, entry 1). When the temperature was further elevated for long periods of time, the material decomposed. To further investigate this reactivity, a microwave reactor was used to reach elevated temperatures for controlled periods of time. When the temperature was increased from 140 to 180 °C (entries 2 and 3, respectively), 30% of ketone **2-39** was obtained over 2 h. Increasing the reaction time to 6 h yielded 82% of the desired material (entry 4). Reaction times could finally be shortened to under 2 h when the reaction was heated to over 210 °C (entries 6 and 7). These reactions saw slightly diminished yields, with some of the material degrading at such high temperatures. Nevertheless, reaction times for the Claisen rearrangement were greatly improved by switching from standard heating methods to a microwave reactor.

Table 2.3. Claisen rearrangement of ether 2-38

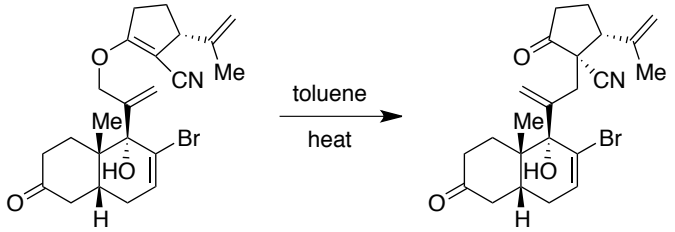

2-38 **2-39**

Entry	Heat Source	Time (h)	Temp (°C)	Yield (%)
1	Al block	144	132	87
2	Microwave	2	140	NR
3	Microwave	2	180	30
4	Microwave	6	180	82
5	Microwave	0.5	210	50
6	Microwave	3	210	85
7	Microwave	1	220	78

Before attempting to cyclize the C ring to obtain steroid **2-6**, methoxy ketal formation was induced. Preliminary cyclization attempts had already been unsuccessful using alcohol **2-39**, possibly due to the presence of the reactive alkoxide generated under basic conditions. Ketal **2-40** was generated in 85% yield using catalytic quantities of CSA (Scheme 2.11). As with other caged AB ring systems generated (i.e. **2-32**), **2-40** exists as a 2:1 mixture of rotamers identified by ^{1}H NMR and confirmed using nOe NMR experiments. Computational analysis of the lowest energy confirmations suggests that one rotamer positions the D ring of **2-40** above the vinyl bromide of the B ring, which brings the two reactive sites within proximity of one another for potential cyclization reactions. The other rotamer forces the D ring away from the reactive site, which may lead to complications during future cyclization attempts.

Scheme 2.11. Preparation for C ring closure

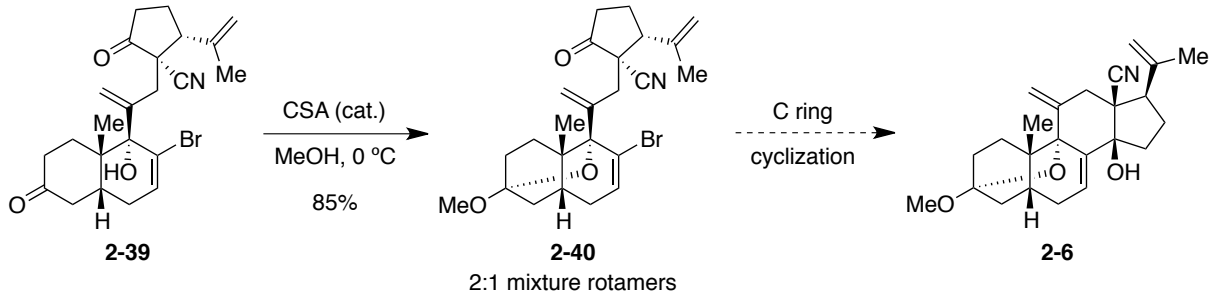

To quickly and efficiently bring material up to the latter stages of the synthesis, racemic D ring was used instead of enantioenriched **(*S*)-2-25**. Coupling of allylic alcohol **2-37** and **rac-2-25**, followed by Claisen rearrangement and subsequent ketal formation generated diastereomers **2-40** and **2-41** (Scheme 2.12). The two diastereomers could be separated using column chromatography, or used as a mixture for C ring cyclization test reactions.[15] It is important to note that both compounds exist as mixtures of slowly interconverting rotamers as discussed above. ^{1}H and ^{13}C NMR spectra are very difficult to interpret, although the vinylogous protons are clearly resolved, providing a handle for interpretation.

Scheme 2.12. Synthesis of ABD ring diastereomers 2-40 and 2-41

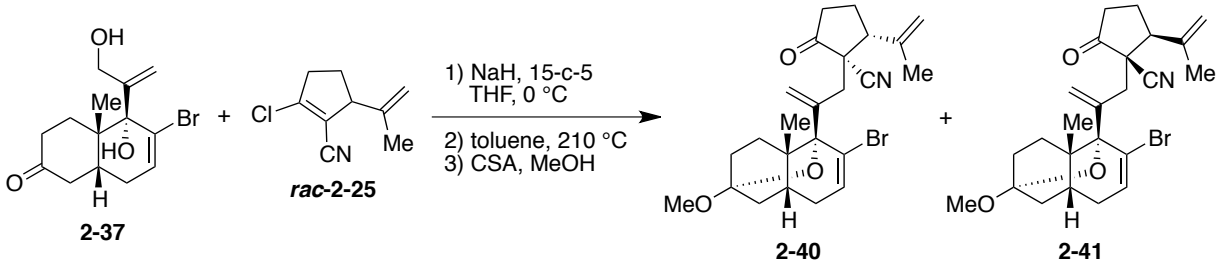

C Ring Cyclization

With compound **2-40** and diastereomer **2-41** in hand, conditions to promote cyclization of the C ring were investigated. Since ketone **2-40** contained the desired stereochemistry about the

nitrile-containing quaternary carbon (C13), special attention was paid to the diagnostic ^{1}H NMR signals for this diastereomer leading to steroid **2-6**. If diastereomer **2-41** cyclized however, we believed that a base-mediated retro-aldol/aldol sequence could correct the stereochemistry, similar to work recently reported by the Inoue and Nagorny groups (Scheme 2.13).[16] This sequence would proceed through a 9-membered ring intermediate (**2-43**), providing steroid **2-44**, which is epimeric at C17. The next few paragraphs will summarize attempted cyclization reactions, with future schemes drawn with a focus on the desired diastereomer, **2-40**, even though most of the reactions run contained a mixture of **2-40** and **2-41**. The outcomes of these reactions are proposed structures based on diagnostic ^{1}H NMR peaks, IR stretches, and mass spectrometry, as all were attempted on small quantities (<10 mg) of starting material.

Scheme 2.13. Proposed outcomes of C ring cyclization reactions

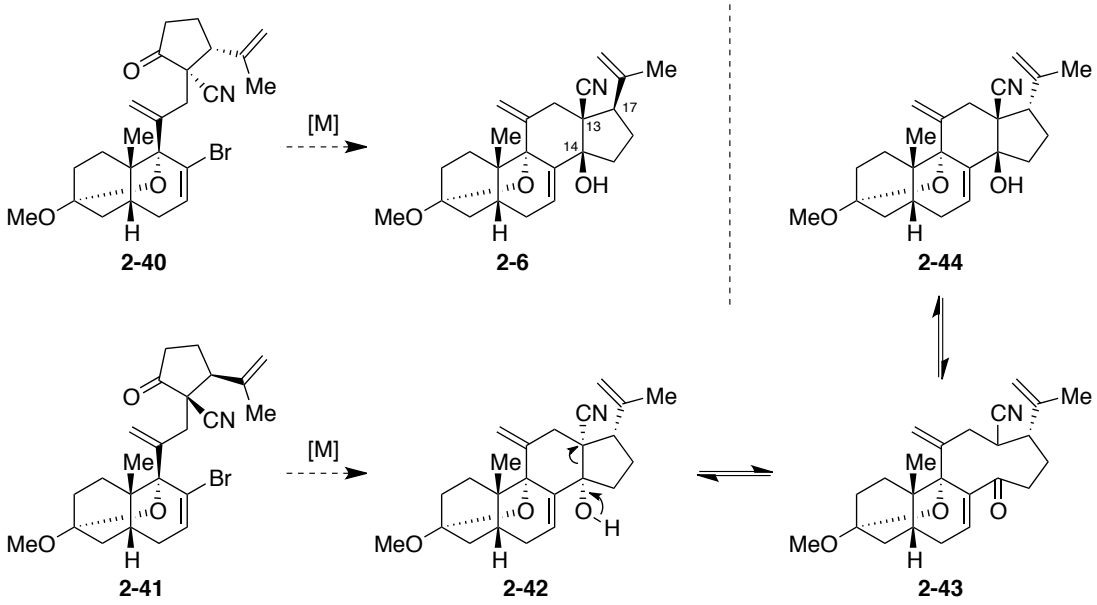

Initial attempts to induce C ring cyclization were centered on metallation of the vinylic bromide of **2-40**. The resulting nucleophile could then add into the pendant cyclopentanone, closing the C ring and forming the steroid backbone of batrachotoxin. Since one face of the D ring is blocked by both the nitrile and isopropenyl moieties, we envisioned that addition of the

nucleophile would occur on the opposite face, providing the desired stereochemistry at C14. Activation of the vinyl bromide was first attempted using Nozaki–Hiyama–Kishi (NHK) conditions (Table 2.4).[17] Although the reaction with $NiCl_2$ and $CrCl_2$ succeeded in reacting with the vinyl bromide, no cyclization product was observed, and only dehalogenated **2-45** was recovered (entry 1). NHK reactions are generally run using more electrophilic carbonyl precursors, such as aldehydes and activated ketones.[18] In our case, it is quite possible that the ketone is not reactive enough for nucleophilc addition to occur under standard NHK conditions. Cyclization was next attempted using *n*- and *t*-butyllithium (entries 2 to 6). In most cases, dehalogenation of the starting material was observed, once again suggesting that the vinyllithium was created, but could not cyclize onto the ketone.

Table 2.4. Attempted C ring cyclizations using metallation protocols

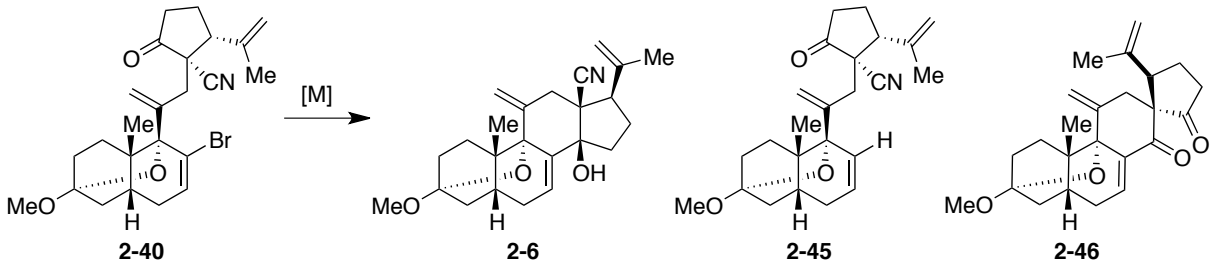

Entry	Metal Source	Solvent	Temp (°C)	Product
1	$NiCl_2/CrCl_2$	DMF	–78 to 23	**2-45**
2	*n*BuLi	THF	–78	**2-45**
3	*n*BuLi	THF	–78 to 0	**2-45**
4	*n*BuLi	Et_2O	–78 to 23	**2-45**
5	*t*BuLi	Et_2O	–78 to 23	Decomp.
6	*t*BuLi	Et_2O	–100	**2-45**
7	Mg^0	THF	66	NR
8	Rieke Mg	THF	66	**2-46**

Two potential problems could explain the inability to cyclize under these conditions: 1) steric hindrance and 2) alpha deprotonation of the ketone. Steric issues surrounding the reactivity

of **2-40** was an expected, yet unavoidable problem when working with this advanced intermediate. We had already observed changes in reactivity between the open and closed forms of the transannular ketal, as well as two distinguishable rotamers when the ketal was formed. Deprotonation alpha to the D ring ketone, however, can potentially be confirmed or dismissed using a deuterium quenching experiment (Scheme 2.14). If deuterium incorporation is identified at alpha to the ketone (**2-47**), then deprotonation is a concern. If the deuterium is only observed at the vinyl position (**2-48**), then deprotonation is unlikely. Deuterium quenching studies will be conducted in the future to better understand the reactivity of intermediates generated using lithiation chemistry. As an alternative to lithiation, activation using magnesium was also attempted. A standard protocol for generating Grignard reagents using magnesium turnings failed to activate the vinyl bromide (Table 2.4, entry 7). Rieke magnesium[19] (magnesium chloride activated with potassium metal) on the other hand, formed the desired Grignard species, which then added into the nitrile to afford diketone **2-46** (entry 8). Although nitrile addition was unexpected, this result suggests that at elevated temperatures, the D ring can come within proximity of the nucleophilic site for cyclization to occur.

Scheme 2.14. Deuterium quenching experiment

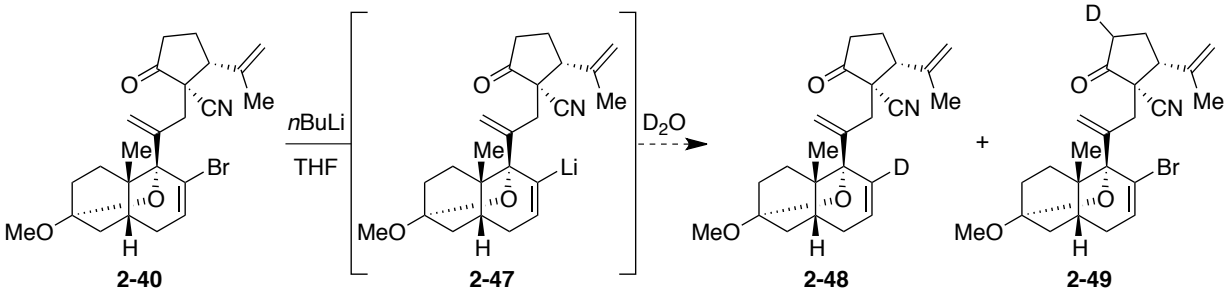

Vinyl halides can also be used to generate a vinyl radical, which could then close the C ring through addition into the ketone, forming an alkoxy radical.[20] Under standard radical initiation conditions, tributyltin radical was used to successfully generate the vinyl radical

intermediate of **2-40** (Scheme 2.15A). Instead of cyclizing onto the ketone as desired, however, a radical-mediated 1,5-nitrile shift occurred, affording compound **2-50**. Nitrile migration could be avoided by first reducing the nitrile to the primary amine, which would need to occur eventually in order to complete the synthesis. Unfortunately, there are no reliable methods for reducing a nitrile in the presence of a ketone, so a sequence of global reduction, oxidation of the alcohol, and protection of the amine would need to be used, adding at least three additional steps before C ring cyclization could be completed. Another potential way of using a radical-based approach would be to generate the alpha-alkoxy radical using samarium diiodide.[21] The radical could the cyclize through a 6-exo trig mechanism, followed by elimination of the bromine to reinstall unsaturation. Unfortunately, when ketone **2-40** was allowed to react with samarium diiodide, only elimination of the nitrile (**2-51**) or reduction of the ketone (**2-52**) was observed (Scheme 2.15B).

Scheme 2.15. Radical-mediated cyclizations

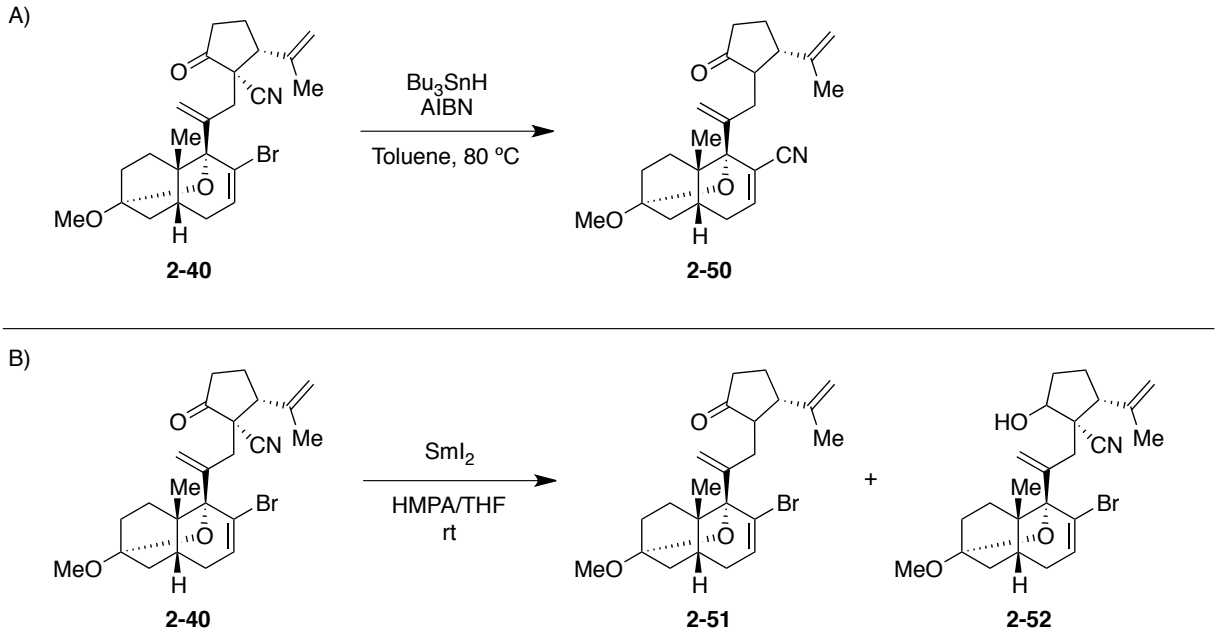

To date, the most promising result for C ring cyclization utilized Heck conditions to achieve ring closure (Scheme 2.16). In order for Heck conditions to provide the desired steroid, the ketone would first need to be converted to an enol ether. This was achieved using TESOTf and base to afford the desired silyl enol ether in 59% yield. After subjecting **2-53** to standard Heck conditions, however, no desired steroid was obtained. Instead, a product was isolated with spectral characteristics consistent with **2-54**, the result of an 8-endo-trig cyclization onto the isopropenyl moiety of the D ring. Although 8-endo-trig cyclizations are disfavored under Balwin's rules, there are enough examples in the literature to suggest that this proposed assignment is not far-fetched.[22] We hypothesized that under the reaction conditions, the triethylsilyl protecting group used was too labile, leading to deprotection before migratory insertion could occur into the enol ether. To test this, ketone **2-40** was subjected to the same reaction conditions, which yielded the same product as was previously isolated for the reaction of **2-53**.

Scheme 2.16. Attempted C ring cyclization using Heck reaction conditions

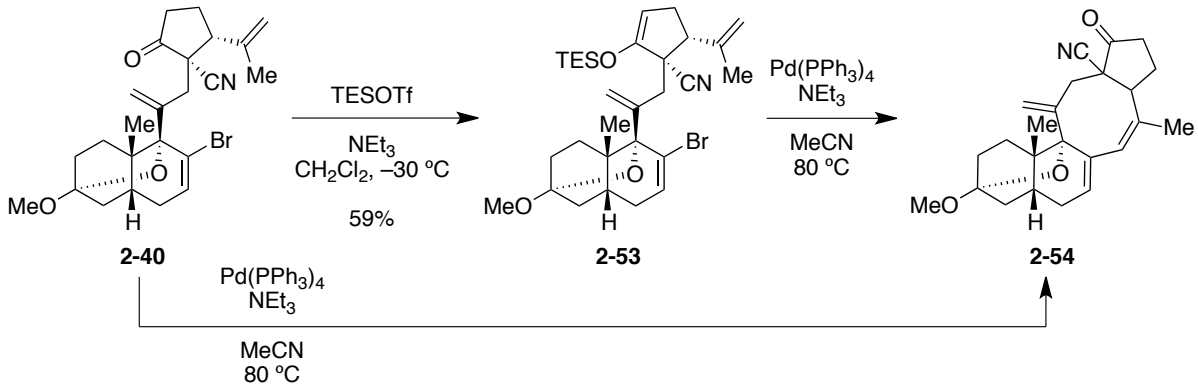

Future Directions

Although all attempts to date have failed to produce the desired steroid core (**2-6**), there are still promising leads for approaching the C ring closure. Metallation reactions have been successful at activating the vinyl bromide, despite some undesired reactivity surrounding the D ring. The nitrile has been the source of some of these issues, and although it is necessary for some of the early reactivity, it does not play a role during the C ring cyclization. As discussed earlier, reduction of the nitrile could be attempted before closure of the C ring, but would likely require a few additional steps, since any reduction of the nitrile would also reduce the D ring ketone. Instead, activation of the ketone using an additive may help to achieve the desired transformation. The addition of $CeCl_3$ has been shown to improve the reactivity of organometallic reagents with ketones in a variety of cases,[23] including work by the Overman group.[24] Future attempts to convert ketone **2-40** to steroid **2-6** would include $CeCl_3$ in reactions using *n*- or *t*-BuLi, which would potentially shut down any undesired enolization of the ketone, improving the chances of steroid formation (Scheme 2.17).

Scheme 2.17. Cerium activation of metallated 2-40

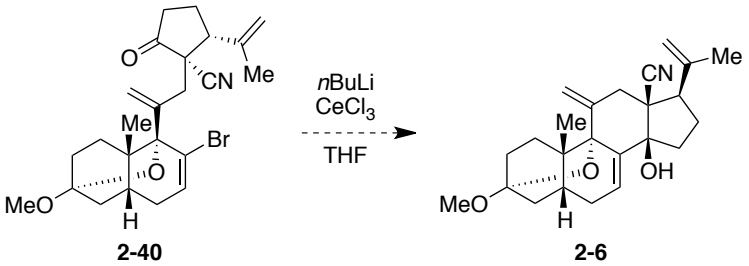

2-40 **2-6**

The Heck reactivity was also a very promising advance towards C ring formation. Although it failed at producing the desired steroid scaffold, it did succeed in forming an alternative ring fusion. As discussed previously, we believed that the chosen protecting group for forming the silyl enol ether was labile under the reaction conditions. A simple alternative would

be to synthesize the same enol ether using a different protecting group (**2-55**). Using a tert-butyldimethylsilyl (TBS) protecting group might provide the stability needed, but may be too sterically bulky, preventing cyclization from occurring. Alternatively, a methyl enol ether, though not useful for progressing through the synthesis, would provide valuable information as to whether such a transformation is viable for the ring closure, as well as the regiochemistry for the resulting alkene (after beta-hydride elimination) of steroid **2-56** (Scheme 2.18).

Scheme 2.18. Alternative Heck reaction scaffolds

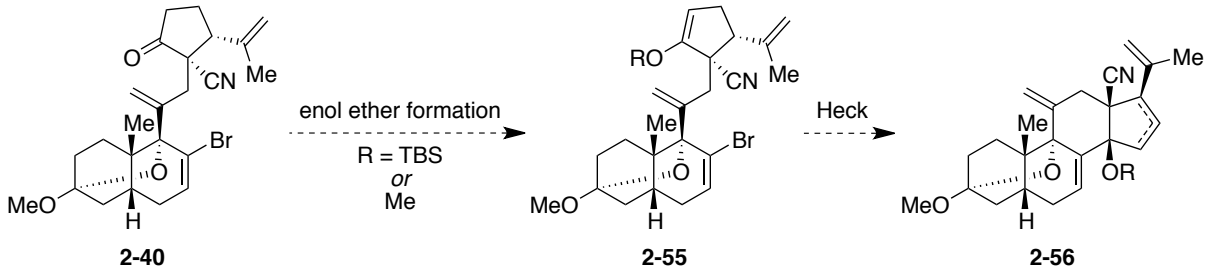

If steroid **2-6** were obtained, installation of the seven-membered E ring would be carried out next. First, reduction of the nitrile followed by methylation of the generated amine would yield an amino alcohol intermediate similar to the one found in Imhof's partial synthesis of BTX.[3] Use of chloroacetyl chloride and base should provide oxazepinone **2-5**. Oxidative cleavage of the two terminal olefins and subsequent reduction would afford diol **2-57**. At this point, the more sterically hindered secondary alcohol would need to be protected, and oxidation of the more accessible alcohol would need to be carried out. This would inevitably require that both be first protected, followed by a deprotection and oxidation of the desired alcohol. If this sequence were successful, further oxidation of ketone **2-58** could be carried out to install unsaturation between C16 and 17 of **2-59**. Reduction of the amide and ketone could be carried out simultaneously, and deprotection of the methyl ketal would generate batrachotoxinin A.

Finally, esterification could be carried out if desired, to afford BTX in an estimated 25 linear steps.

Scheme 2.19. Proposed completion of BTX

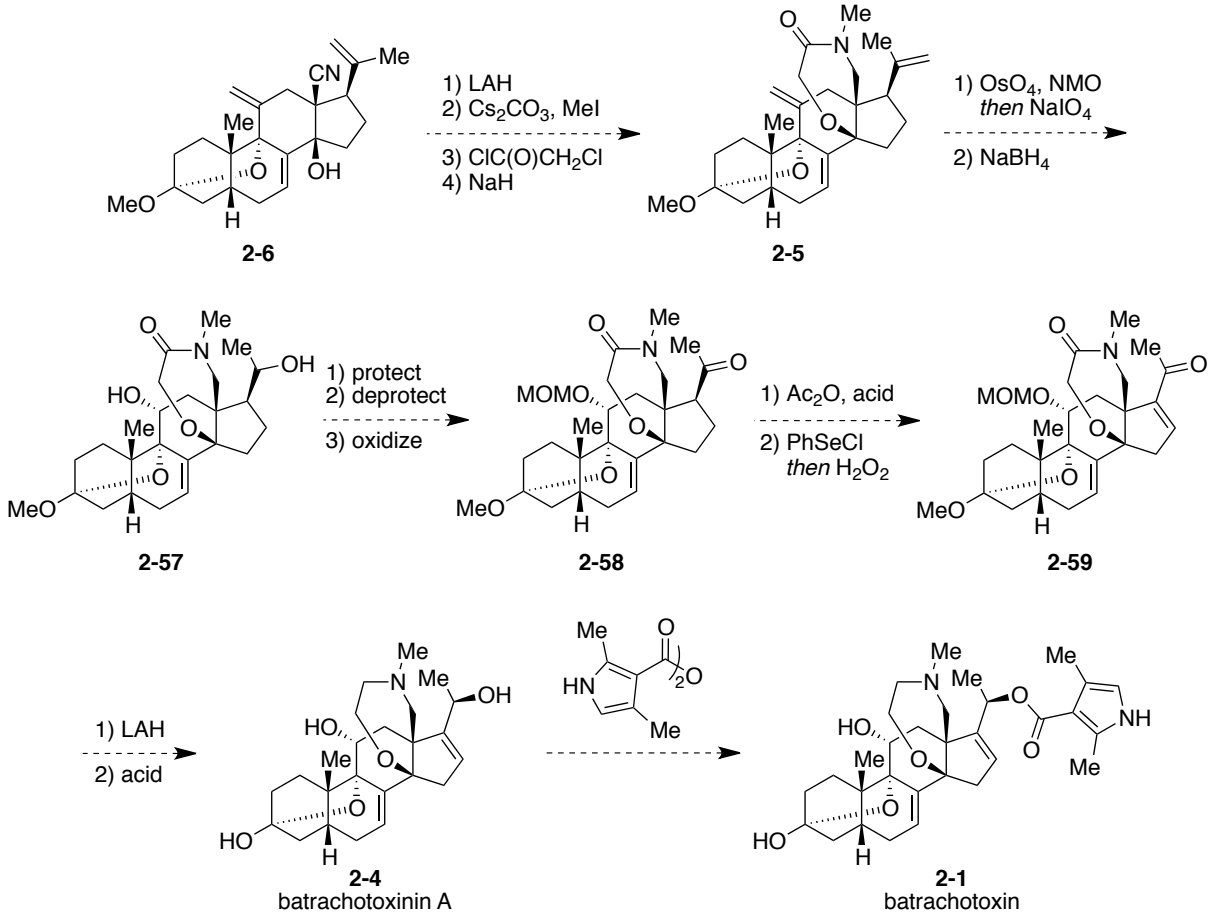

Although significant progress has been made on the route described herein, alternative approaches utilizing other DE ring scaffolds are currently underway. Jacob DeForest has already made noteworthy advances in exploring the reactivity of oxazepinone **2-60**,[25] as well as alternative disconnections centered around the C ring. Other motifs, such as compounds **2-61** and **2-62**, may also provide interesting targets for future work on BTX.

Figure 2.1. Alternative DE ring scaffolds

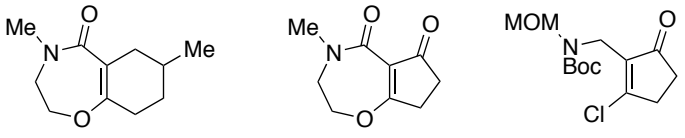

2-60 **2-61** **2-62**

Batrachotoxin has proven to be a challenging synthetic target. As work within the Rychnovsky lab continues to advance, so does the understanding of the limitations on synthetic transformations surrounding this complex natural product. Ultimately, we hope a concise synthesis will not only provide additional material for furthering the understanding of its biological activity, but also provide a pathway for accessing analogues for structure-activity relationship (SAR) studies.

1. Kurosu, M.; Marcin, L. R.; Grinsteiner, T. J.; Kishi, Y. *J. Am. Chem. Soc.* **1998**, *120*, 6627–6628.

2. (a) Hudson, P.; Pairaudeau, G.; Parsons, P. J.; Jahans, A. W.; Drew, M. G. B. *Tetrahedron Lett.* **1993**, *34*, 7295–7298. (b) Lacrouts, P.; Parsons, P. J.; Penkett, C. S.; Raza, A. R. *Synlett* **2005**, *2005*, 2767–2768.

3. (a) Imhof, R.; Gössinger, M. E.; Graf, W.; Berner, H.; Berner-Fenz, M. L.; Wehrli, H. *Helv. Chim. Acta* **1972**, *55*, 1151–1153. (b) Imhof, R.; Gössinger, E.; Graf, W.; Berner-Fenz, L.; Berner, H.; Schaufelberger, R.; Wehrli, H. *Helv. Chim. Acta* **1973**, *56*, 139–162.

4. Reilly, A. Doctoral Thesis. University of California, Irvine, 2010.

5. Yoshida, S., Final Report. University of California, Irvine: 2010.

6. Reilly, M. K. Doctoral Thesis. University of California, Irvine, 2013.

7. Hajos, Z. G.; Parrish, D. R. *J. Org. Chem.* **1974**, *39*, 1615–1621.

8. Hajos, Z. G.; Parrish, D. R. *Org. Synth.* **1985**, *63*, 26–31.

9. Speziale, A. J.; Ratts, K. W.; Bissing, D. E. *Org. Synth.* **1965**, *45*, 33–36.

10. Petasis, N. A.; Bzowej, E. I. *J. Am. Chem. Soc.* **1990**, *112*, 6392–6394.

11. ^{1}H NMR data for compound **2-26** synthesized using direct alkylation matched that of the same compound obtained after the Claisen rearrangement, confirming two as the same diastereomer.

12. (a) Harrington, P. E.; Murai, T.; Chu, C.; Tius, M. A. *J. Am. Chem. Soc.* **2002**, *124*, 10091–10100. (b) Dubé, P.; Toste, F. D. *J. Am. Chem. Soc.* **2006**, *128*, 12062–12063.

13. Djerassi, C. *Chem. Rev.* **1948**, *43*, 271–317.

14. Srikrishna, A.; Anebouselvy, K. *J. Org. Chem.* **2001**, *66*, 7102–7106.

15. Identification of the desired diastereomer (**2-40**) could be achieved using an authentic sample obtained during the synthesis using enantioenriched D ring.

16. (a) Mukai, K.; Urabe, D.; Kasuya, S.; Aoki, N.; Inoue, M. *Angew. Chem. Int. Ed.* **2013**, *52*, 5300–5304. (b) Cichowicz, N. R.; Kaplan, W.; Khomutnyk, Y.; Bhattarai, B.; Sun, Z.; Nagorny, P. *J. Am. Chem. Soc.* **2015**, *137*, 14341–14348.

17. Chen, X.-T.; Bhattacharya, S. K.; Zhou, B.; Gutteridge, C. E.; Pettus, T. R. R.; Danishefsky, S. J. *J. Am. Chem. Soc.* **1999**, *121*, 6563–6579.

18. Fürstner, A. *Chem. Rev.* **1999**, *99*, 991–1046.

19. Rieke, R. D.; Bales, S. E.; Hudnall, P. M.; Burns, T. P.; Poindexter, G. S. *Org. Synth.* **1979**, *59*, 85–92.

20. Jasperse, C. P.; Curran, D. P.; Fevig, T. L. *Chem. Rev.* **1991**, *91*, 1237–1286.

21. Nicolaou, K. C.; Ellery, S. P.; Chen, J. S. *Angew. Chem. Int. Ed.* **2009**, *48*, 7140–7165.

22. (a) Horwell, D. C.; Nichols, P. D.; Ratcliffe, G. S.; Roberts, E. *J. Org. Chem.* **1994**, *59*, 4418–4423. (b) Rigby, J. H.; Hughes, R. C.; Heeg, M. J. *J. Am. Chem. Soc.* **1995**, *117*, 7834–7835. (c) Klein, J. E. M. N.; Műller-Bunz, H.; Ortin, Y.; Evans, P. *Tetrahedron Lett.* **2008**, *49*, 7187–7190.

23. Imamoto, T.; Kusumoto, T.; Tawarayama, Y.; Sugiura, Y.; Mita, T.; Hatanaka, Y.; Yokoyama, M. *J. Org. Chem.* **1984**, *49*, 3904–3912.

24. Martin, C. L.; Overman, L. E.; Rohde, J. M. *J. Am. Chem. Soc.* **2010**, *132*, 4894–4906.

25. DeForest, J. C., Second Year Report. University of California, Irvine: 2014.

Chapter 2:

Experimental section

General Information. ^{1}H NMR and ^{13}C NMR spectra were recorded at ambient temperature using Bruker DRX500 (500 and 125 MHz, respectively) or AVANCE600 (600 and 150 MHz, respectively) spectrometers, as indicated. The data are reported as follows: chemical shift in ppm on a δ scale and referenced to internal tetramethylsilane or residual solvent (^{1}H NMR = TMS: δ 0.00 or $CHCl_3$: δ 7.26; ^{13}C NMR = $CHCl_3$: δ 77.16), multiplicity (appar = apparent, br = broad, s = singlet, d = doublet, t = triplet, q = quartet, quint = quintet, sext = sextet, m = multiplet), coupling constants (Hz), and integration. Infrared (IR) spectra were obtained using a PerkinElmer Frontier FT-IR spectrometer or Varian 640 FT-IR spectrometer. Accurate mass spectra were acquired on a Waters LCT Premier quadrupole time-of-flight spectrometer and were obtained by peak matching. Analytical thin layer chromatography was performed on Merck glass-backed silica gel 60 Å F_{254} plates and visualized by UV light, *p*-anisaldehyde, potassium permanganate, or vanillin. Liquid chromatography was performed using forced flow (flash chromatography) of the indicated solvent system on Merck Geduran silica gel (SiO_2) 60 (40-60 mesh). Optical rotations were measured using a JASCO DIP-370 digital polarimeter. CH_2Cl_2, toluene, DMF, THF, and Et_2O were dried by filtration through alumina according to the method of Grubbs.[1] All reactions were run under an atmosphere of argon in glassware that was flame- or oven-dried, unless otherwise stated. All commercially available reagents were used as received unless stated otherwise. *n*-Butyl lithium and *t*Butyl lithium were titrated with menthol and 1,10-phenanthroline.[2] $CeCl_3$ was dried directly before use at 140 °C overnight under high vacuum. TESOTf , bromoform, and NEt_3 were distilled from CaH_2. KO*t*Bu was sublimed under reduced pressure. Microwave reactions were carried out in a CEM microwave reactor.

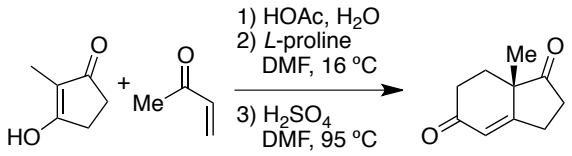

2-16

Hajos–Parrish ketone 2-16. Hajos–Parrish ketone (**2-16**) was prepared on multi-gram scale using the procedure reported by Hajos and Parrish.[3] Isolated as a white crystalline solid: ^{1}H NMR (500 MHz, $CDCl_3$) δ 5.96 (s, 1H), 2.99–2.89 (m, 1H), 2.83–2.69 (m, 2H), 2.58–2.36 (m, 3H), 2.14–2.06 (m, 1H), 1.89–1.79 (m, 1H), 1.31 (s, 3H); ^{13}C NMR (125 MHz, $CDCl_3$) δ 216.7, 198.4, 169.9, 124.1, 48.9, 36.1, 33.1, 29.4, 27.0, 20.8; Accurate Mass (ES/MeOH) *m* / *z* calcd for $C_{10}H_{12}O_2Na$ $(M+Na)^+$ 187.0735, found 187.0738; $[\alpha]_D^{25}$ = +352.3 (c 1.00, Benzene).

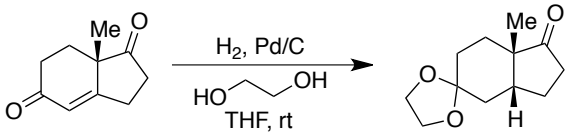

2-16 **2-17**

Ketone 2-17. To a stirring solution of Hajos–Parrish ketone (**2-16**) (10.0 g, 61.0 mmol) in THF (25 mL) was added ethylene glycol (100 ml), followed by 5% Pd/C (0.55 g). The pH of the resulting mixture was adjusted to ~5 using HCl (conc.). The headspace within the flask was purged using hydrogen and the reaction mixture was stirred vigorously at room temperature under a positive pressure of hydrogen (balloon) for 48 h. The resulting mixture was diluted with CH_2Cl_2 and filtered through a plug of Celite, washing with CH_2Cl_2. The filtrate was washed with brine (100 mL) and separated, and the aqueous layer was extracted with CH_2Cl_2 (2 × 100 mL). The combined organic layers were dried over Na_2SO_4 and concentrated *in vacuo*. The resulting crude oil was taken on without further purification. If desired, the oil could be purified by flash chromatography on SiO_2 (hexanes/EtOAc = 80:20) to provide **2-17** as a clear, colorless oil: ^{1}H

NMR (500 MHz, $CDCl_3$) δ 3.97–3.86 (m, 4H), 2.34–2.20 (m, 2H), 2.20– 2.10 (m, 1H), 2.07–1.98 (m, 1H), 1.97–1.90 (m, 1H), 1.89–1.76 (m, 2H), 1.62–1.52 (m, 1H), 1.45–1.34 (m, 3H), 1.03 (s, 3H); ^{13}C NMR (125 MHz, $CDCl_3$) δ 222.0, 108.6, 64.5, 64.3, 48.2, 42.4, 36.1, 34.5, 31.2, 28.1, 23.7, 21.8; Accurate Mass (ES/MeOH) *m* / *z* calcd for $C_{12}H_{18}O_3Na$ $(M+Na)^+$ 233.1154, found 233.1156; $[\alpha]_D^{21}$ = +34.9 (c 2.52, $CHCl_3$).

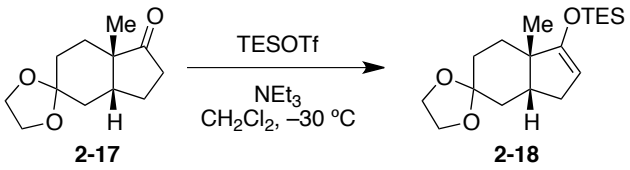

2-17 **2-18**

Silyl enol ether 2-18. To a cooled (–30 °C) solution of crude ketone **2-17** (61.0 mmol) and triethylamine (12.8 mL, 92.0 mmol) in CH_2Cl_2 (250 mL) was added triethylsilyl trifluoromethanesulfonate (TESOTf) (16.6 mL, 73 mmol), and the reaction was stirred for 3 h. Saturated aqueous $NaHCO_3$ (200 mL) was then add, and the resulting mixture was warmed to room temperature. The aqueous layer was extracted with CH_2Cl_2 (2 × 200 mL). The combined organic layers were washed with brine, dried over Na_2SO_4, and concentrated *in vacuo*. The crude oil was purified by flash chromatography on SiO_2 (hexanes/EtOAc = 98:2) to yield 17.3 g (87% over 2 steps) of enol ether **2-18** as a clear, colorless oil: ^1H NMR (500 MHz, $CDCl_3$) δ 4.39 (t, *J* = 2.3 Hz, 1H), 3.97–3.87 (m, 4H), 2.36–2.27 (m, 1H), 2.04–1.97 (m, 1H), 1.91–1.85 (m, 1H), 1.84–1.76 (m, 1H), 1.75–1.67 (m, 1H), 1.64–1.42 (m, 4H), 1.02 (s, 3H), 1.01–0.93 (m, 9H), 0.73–0.60 (m, 6H); ^{13}C NMR (125 MHz, $CDCl_3$) δ 160.1, 109.8, 96.5, 64.3, 64.2, 44.8, 42.3, 37.0, 32.4, 31.5, 30.2, 24.3, 6.9, 5.0; IR (thin film) 3461 (br), 2955, 2877, 1736 cm^{-1}; Accurate Mass (ES/MeOH) *m* / *z* calcd for $C_{18}H_{33}O_3Si$ $(M + H)^+$ 325.2199, found 325.2197; $[\alpha]_D^{23}$ = +40 (c 0.98, $CHCl_3$).

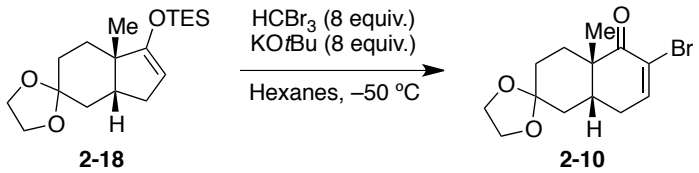

2-18 **2-10**

Bromo enone 2-10. To a cooled (–50 °C) solution of silyl enol ether **2-18** (4.19 g, 12.9 mmol) in hexanes (86 mL, dried over $MgSO_4$) was added KO*t*Bu (5.8 g, 51.7 mmol). To the vigorously stirring suspension was added $CHBr_3$ (9.2 mL, 103.3 mmol) dropwise via syringe pump over 1 h. At the halfway point (30 min), a second portion of KO*t*Bu (5.8 g, 51.7 mmol) was added, followed by the continued addition of the remaining $CHBr_3$. After the bromoform addition was complete, the reaction was allowed to stir for 1 h. The resulting reaction mixture was quenched with brine (200 ml) and warming to room temperature. The reaction was diluted with CH_2Cl_2 (250 mL) and the aqueous layer was separated. The aqueous layer was extracted with CH_2Cl_2 (2 × 100 mL), and the combined organic layers were dried over Na_2SO_4 and concentrated *in vacuo*. The crude oil was purified by flash chromatography on SiO_2 (hexanes/EtOAc = 90:10 → 70:30) to afford 2.45 g (63%) of bromo enone **2-10** as a light yellow solid. ^{1}H NMR (500MHz,$CDCl_3$) δ 7.20 (ddd, *J* = 6.2, 2.6, 1.3 Hz, 1H), 3.96–3.90 (m, 4H), 2.87 (ddd, *J* = 19.7, 5.7, 2.6 Hz, 1H), 2.39 (td, *J* = 13.5, 3.5 Hz, 1H), 2.30–2.22 (m, 1H), 2.13 (dd, *J* = 19.7, 6.1 Hz, 1H), 1.72 (t, *J* = 13.3 Hz, 1H), 1.65–1.44 (m, 3H), 1.42–1.32 (m, 1H), 1.21 (s, 3H); ^{13}C NMR (125 MHz, $CDCl_3$) δ 194.9, 146.8, 135.4, 122.2, 108.9, 64.49, 64.53, 47.6, 40.2, 37.9, 32.2, 32.0, 31.9, 24.4; IR (thin film) 2885, 1687 cm^{-1}; Accurate Mass (ES/MeOH) *m* / *z* calcd for $C_{13}H_{17}BrO_3Na$ $(M + Na)^+$ 323.0259; found, 323.0258; $[\alpha]_D^{21}$ = +22.8 (c 0.865, $CHCl_3$); mp = 95–96 °C.

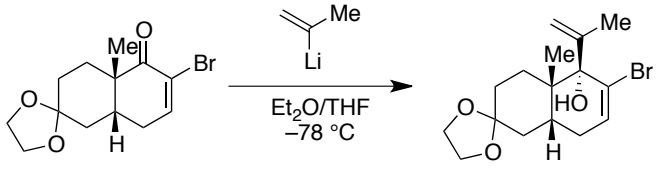

2-10 **2-19**

Isopropenyl lithium. To a cooled (–78 °C) solution of 2-bromopropene (1.9 mL, 21.8 mmol) in Et_2O (26 mL) and THF (2.6 mL) was added *t*butyl lithium (1.4 M in pentanes, 29.6 mL, 41.5 mmol) dropwise via syringe over 10 min. The resulting solution was stirred at –78 °C for 30 min before removing the cooling bath and warming to RT over 1.5 h. The resulting solution was used directly via syringe as a 0.31 M solution of isopropenyl lithium (titrated using menthol and 1,10-phenanthroline).

Isopropenyl alcohol 2-19. To a cooled (–78 °C) solution of enone **2-10** (2.43 g, 8.1 mmol) in Et_2O (40 mL) was added three portions of isopropenyl lithium (10 mL portions, 8.88 mmol total) dropwise. After each portion was added, the reaction was allowed to stir for 10 min. Following the final addition, the reaction was stirred for 20 min before being quenched with the addition of water. The resulting mixture was warmed to room temperature and brine was added (100 mL). The reaction mixture was extracted with EtOAc (3 × 100 mL), and the combined organic layers were dried over Na_2SO_4 and concentrated *in vacuo*. The crude orange oil was purified by flash chromatography on SiO_2 (hexanes/EtOAc w/ 1% NEt_3 = 90:10) to afford the desired compound (**2-19**) in 33% yield as a clear, colorless oil: ^{1}H NMR (500 MHz, $CDCl_3$) δ 6.16 (t, *J* = 4.0 Hz, 1H), 5.13 (m, 2H), 3.97–3.94 (m, 2H), 3.89–3.84 (m, 2H), 2.89 (bs, 1H), 2.15–2.02 (m, 3H), 1.84 (s, 3H), 1.84–1.15 (m, 6H), 1.05 (s, 3H); ^{13}C NMR (125 MHz, $CDCl_3$) δ 147.9, 130.4, 128.4, 115.1, 108.7, 81.3, 64.4, 63.4, 41.6, 35.2, 31.7, 30.0, 29.4, 22.3 (CH3); R*f* = 0.55 (3:1 hexane:EtOAc); IR (thin film) 3480 (br), 2954, 2884 cm-1; Accurate Mass (ES/MeOH) *m* / *z* calcd for $C_{16}H_{23}BrO_3H$ $(M + H)^+$ 343.0909, found 343.0914; $[\alpha]_D^{21}$ = +67.6 (c 1.09, $CHCl_3$).

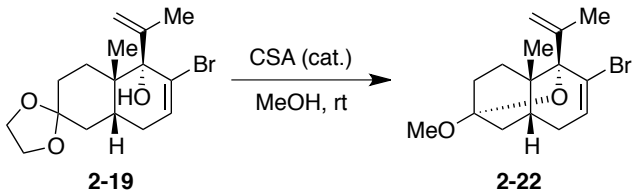

2-19 **2-22**

Transannular ketal 2-22. To a cooled (0 °C) solution of ketal **2-34** (239 mg, 0.7 mmol) in MeOH (12 mL) was added CSA (49 mg, 0.2 mmol). The reaction was stirred for 5 min at 0 °C before being warmed to room temperature over 1 h. Once the reaction was complete, saturated aqueous $NaHCO_3$ (30 mL) was added. The resulting mixture was extracted with CH_2Cl_2 (3 × 30 mL). The combined organic layers were dried over Na_2SO_4 and concentrated *in vacuo*. The resulting oil was purified by flash chromatography on SiO_2 (hexanes/EtOAc w/ 1% NEt_3 = 95:5) to provide 187 mg (86%) of ketal **2-22** as a white solid: ^{1}H NMR (500 MHz, $CDCl_3$) δ 6.17 (d, *J* = 6.5 Hz, 1H), 5.52 (s, 1H), 5.22 (s, 1H), 3.36 (s, 3H), 2.47 (d, *J* = 17.5 Hz, 1H), 2.00–1.82 (m, 6H), 1.81 (s, 3H), 1.55 (dt, *J* = 5.5, 12 Hz, 1H), 1.34–1.27 (m, 1H), 0.89 (s, 3H); ^{13}C NMR (125 MHz, $CDCl_3$) δ ; IR (thin film) 2924, 2852, 1714 cm^{-1}; Accurate Mass (ES/MeOH) *m* / *z* calcd for $C_{15}H_{21}BrO_2Na$ $(M + Na)^+$ 335.0623, found 335.0614.

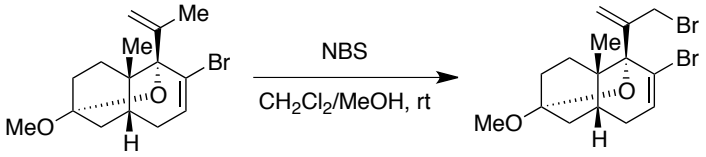

2-22 **2-32**

Allyl bromide 2-32. To a cooled (0 °C) solution of ketal **2-22** (187 mg, 0.6 mmol) in CH_2Cl_2/MeOH (3:2, 6 mL) was added *N*-bromosuccinimide (130 mg, 0.7 mmol). The reaction was stirred for 5 min at 0 °C before being stirred at room temperature for 4.5 h. Once the reaction was complete, water (25 mL) was added. The resulting mixture was extracted with CH_2Cl_2 (3 × 25 mL). The combined organic layers were washed with 5% aqueous NaOH (25 mL), dried over Na_2SO_4, and concentrated *in vacuo*. The resulting oil was purified by flash chromatography on SiO_2 (hexanes/EtOAc w/ 1% NEt_3 = 90:10) to provide 176 mg (75%) of allyl bromide **2-32** as a white solid: Isolated as a 2.5:1 mixture of rotamers (confirmed by nOe): ^{1}H NMR (600 MHz, $CDCl_3$T) δ 6.23 (d, *J* = 5.2 Hz, 1H), 6.17 (d, *J* = 6.3 Hz, 0.4H), 6.02 (s, 1H),

5.94 (s, 1H), 5.77 (s, 0.4H), 5.04 (s, 0.4H), 4.31 (d, J = 12.3 Hz, 1H), 4.22 (s, .8H), 3.65 (d, J = 12.3 Hz, 1H), 3.38 (s, 1.2H), 3.36 (s, 3H), 2.54–2.43 (m, 1.4H), 2.02 (tt, J = 12.4, 3.7 Hz, 0.4H), 1.98–1.85 (m, 6.6H), 1.84–1.76 (m, 2.4H), 1.68–1.56 (m, 1.8H), 1.52–1.43 (m, 0.4H), 1.39–1.32 (m, 1H), 1.00 (s, 3H), 0.87 (s, J = 9.1 Hz, 1.2H); ^{13}C NMR (125 MHz, $CDCl_3$) δ ; IR (thin film) cm^{-1}; Accurate Mass (ES/MeOH) m / z calcd for $C_{15}H_{20}Br_2O_2Na$ $(M + Na)^+$ 412.9728, found 412.9718.

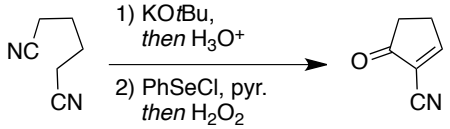

2-23 **2-24**

Cyclopentenone 2-24. To a stirring solution of adiponitrile (**2-23**) (10.0 mL, 89.7 mmol) in THF (300 mL) was added KO*t*Bu (20.1 g, 179 mmol). The reaction was stirred for 1 h at room temperature, during which time it turned into a beige slurry. At the completion of the reaction, the slurry was filtered using a Buchner funnel under a stream of argon. The filtered solid was transferred to a separatory funnel containing 3 M HCl (250 mL) and Et_2O (200 mL). After all of the solid had dissolved, the layers were separated, and the organic layer was washed with brine, dried over Na_2SO_4, and concentrated *in vacuo*. The crude orange oil (carbonitrile) (2.91 g, 26.7 mmol) was taken up in CH_2Cl_2 (17 mL) and placed to the side for later use.

In a separate flask, a solution of phenylselenium chloride (5.11 g, 26.7 mmol) in CH_2Cl_2 (250 mL) was prepared. The solution was cooled to 0 °C and pyridine (2.55 mL, 32 mmol) was added dropwise, and the reaction turned orange. After 15 min of stirring, the carbonitrile solution previously prepared was added dropwise, and the resulting yellow solution was stirred for 15 min at 0 °C. The solution was transferred to a separatory funnel and extracting with 3 M HCl (2 × 60 mL) to remove the pyridine. The organic layer was transferred to a flask and cooled to 0 °C. Portions of 30% H_2O_2 (2.1 mL) were then added to the reaction mixture in 10 min intervals until

the solution went colorless. Once the reaction was complete, the mixture was washed with H_2O (80 mL) and $NaHCO_3$ (80 mL). The organic layer was dried over Na_2SO_4 and concentrated *in vacuo* to afford 6.44 g (67%) of **2-24** as a yellow oil. The crude oil was taken on to the next step immediately, without further purification.

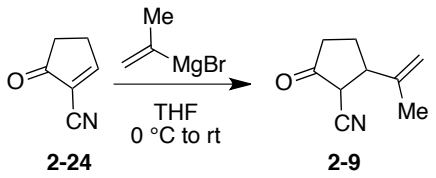

Ketone 2-9. To a cooled (0 °C) solution of enone **2-24** (2.65 g, 24.7 mmol) in THF (124 mL) was added isopropenylmagnesium bromide (0.5 M, 60 mL, 29.7 mmol) via syringe pump over 20 min, causing the reaction solution to turn opaque orange. The reaction was allowed to warm to room temperature and was stirred overnight (15 h). Saturated aqueous NH_4Cl (200 mL) was added to quench the reagents, and the mixture was transferred to a separatory funnel. The layers were separated and the aqueous phase was extracted with EtOAc (2 × 200 mL). The combined organic layers were dried over Na_2SO_4 and concentrated *in vacuo*. The crude residue was purified by flash chromatography on SiO_2 (hexanes/EtOAc = 80:20) to provide 3.17g (86%) of ketone **2-9** as a colorless oil: ^{1}H NMR (500 MHz, $CDCl_3$) δ 5.09 (m, 1H), 4.97 (m, 1H), 3.16 (d, J = 12.5 Hz, 1H), 3.00 (dt, J = 6.5, 12.5 Hz, 1H), 2.60– 2.54 (m, 1H), 2.45–2.37 (m, 1H), 2.34–2.30 (m, 1H), 1.85 (s, 3H), 1.84 (m, 1H); ^{13}C NMR (125 MHz, $CDCl_3$) δ 205.7, 142.0, 116.1, 113.1, 48.9, 44.5, 37.3, 26.7, 20.2; IR (thin film) 3084, 2976, 2886, 2247, 1760 cm^{-1}; Accurate Mass (ES/MeOH) m / z calcd for $C_9H_{11}NONa$ $(M + Na)^+$ 172.0738, found 172.0736.

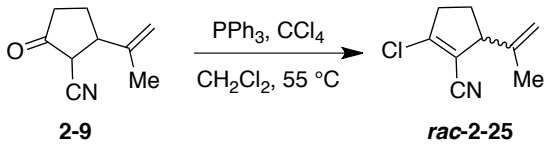

Vinyl chloride *rac*-2-25. To a solution of ketone **2-9** (501 mg, 3.4 mmol) in CH2Cl2 (17 mL) was added triphenylphosphine (1.76 g, 6.8 mmol), followed by carbon tetrachloride (17 mL). The reaction flask was fitted with a condenser and was heated to 55 °C overnight. After stirring for 14 h, the solution was cooled to room temperature and concentrated to provide a black residue. The crude residue was purified by flash chromatography on SiO_2 (hexanes/EtOAc = 60:40) to yield 461 mg (81%) of **2-25** as a yellow oil: ^{1}H NMR (500 MHz, $CDCl_3$) δ 4.86 (s, 1H), 4.83 (s, 1H), 3.58 (m, 1H), 2.80–2.70 (m, 2H), 2.33 (dq, *J* = 6.0, 9.0 Hz, 1H), 1.91 (m, 1H), 1.73 (s, 3H); ^{13}C NMR (125 MHz, $CDCl_3$) δ 150.8, 143.6, 114.2, 114.1, 113.3, 53.3, 38.2, 28.3, 19.4; IR (thin film) 2958, 2927, 2854, 2225 cm^{-1}.

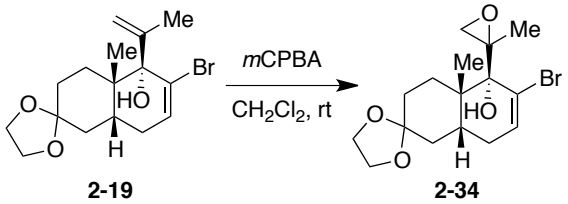

2-19 **2-34**

Epoxide 2-34. To a stirring solution of olefin **2-19** (0.202 g, 0.59 mmol) in CH_2Cl_2 (5.9 mL) was added *m*CPBA (0.158 g, 0.92 mmol). The cloudy mixture was stirred for 24 h. The reaction mixture was then diluted with CH_2Cl_2 (20 mL) and saturated aqueous $NaHCO_3$ (20 mL) was added. The organic layer was separated, and the aqueous layer was washed with CH_2Cl_2 (2 × 20 mL). The combined organic layers were dried over Na_2SO_4 and concentrated *in vacuo*. The resulting mixture was purified by flash chromatography on SiO_2 (hexanes/EtOAc w/ 1% NEt_3 = 80:20) to provide 195 mg (92%) of epoxide **2-34** as a clear colorless film; ^{1}H NMR (500 MHz, $CDCl_3$) δ 6.28 (t, *J* = 4.0 Hz, 1H), 3.96–3.91 (m, 2H), 3.88–3.83 (m, 2H), 3.01 (d, *J* = 4.5 Hz, 1H), 2.96–2.88 (m, 2H), 2.58 (d, *J* = 5.0 Hz, 1H), 2.18–2.15 (m, 1H), 2.04–1.94 (m, 2H), 1.75–1.68 (m, 4H), 1.53 (d, *J* = 14.0 Hz, 1H), 1.41 (s, 3H), 1.13 (s, 3H); ^{13}C NMR (125 MHz, $CDCl_3$) δ 132.0, 125.6, 108.3, 76.3, 64.4, 63.4, 59.3, 49.9, 41.2, 35.7, 35.1, 30.9, 29.7, 26.0, 21.0, 19.3;

IR (thin film) 3499 (br), 3056, 2980, 2939, 2888 cm^{-1}; Accurate Mass (ES/MeOH) *m* / *z* calcd for $C_{16}H_{23}O_4BrNa$ $(M + Na)^+$ 381.0677, found 381.0677; $[\alpha]_D^{21}$ = +43 (c 1.0, $CHCl_3$).

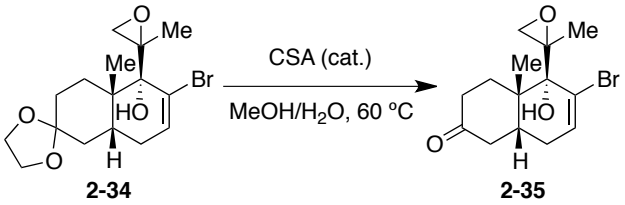

2-34 **2-35**

Ketone 2-35. To a solution of ketal **2-34** (60.0 mg, 0.17 mmol) in MeOH/water (10:1, 3.8 mL) was added CSA (4.1 mg, 0.02 mmol). The reaction was stirred at 60 °C for 1 h. After cooling to room temperature, CH_2Cl_2 (25 mL) was added, followed by saturated aqueous $NaHCO_3$ (20 mL). The organic layer was separated, and the aqueous layer was extracted with CH_2Cl_2 (2 × 20 mL). The combined organic layers were washed with brine, dried over Na_2SO_4 and concentrated *in vacuo*. The resulting yellow oil was purified by flash chromatography on SiO_2 (hexanes/EtOAc w/ 1% NEt_3 = 70:30) to provide 47.9 mg (89%) of ketone **2-35** as a white solid; ^1H NMR (500 MHz, $CDCl_3$) δ 6.28 (dd, *J* = 3, 12.5 Hz, 1H), 3.08 (d, *J* = 4.5 Hz, 1H), 3.06 (s, 1H), 2.68 (dd, *J* = 5.0, 15.5 Hz, 1H), 2.65 (d, *J* = 4.5 Hz, 1H), 2.48–2.35 (m, 3H), 2.21 (td, *J* = 6.0, 19.5 Hz, 1H), 2.12– 2.06 (m, 2H), 1.97 (dt, *J* = 6.0, 8.0 Hz, 1H), 1.88 (ddd, *J* = 3.0, 11.0, 19.0 Hz, 1H), 1.35 (s, 3H), 1.25 (s, 3H); ^{13}C NMR (125 MHz, $CDCl_3$) δ 211.1, 130.4, 127.5, 76.6, 49.7, 42.9, 41.0, 37.7, 37.4, 31.5, 29.8, 28.3, 21.4, 19.0; IR (thin film) 3474 (br), 3064, 2977, 2945, 2883, 2834, 1707 cm^{-1}; Accurate Mass (ES/MeOH) *m* / *z* calcd for $C_{14}H_{19}BrO_3Na$ $(M + Na)^+$ 337.0415, found 337.1413; $[\alpha]_D^{21}$ = +13 (c 2.08, $CHCl_3$); decomposition range = 138–156 °C.

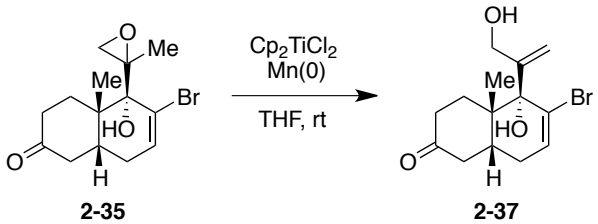

2-35 **2-37**

Allyl alcohol 2-37. To a flame-dried round bottom flask charged with Cp_2TiCl_2 (438 mg, 1.76 mmol) and Mn(0) dust (145 mg, 2.64 mmol) was added THF (27 mL) via syringe. The resulting red solution was stirred at room temperature until it turned green (about 1 h). In a separate scintillation vial, a solution of epoxide **2-35** (119 mg, 0.36 mmol) in THF (9 mL) was prepared with the addition of 4 Å MS. The resulting epoxide solution was added dropwise via syringe to the flask containing the green solution. The vial was rinsed with THF (~0.5 mL), which was added to the reaction flask. The reaction mixture was allowed to stir at room temperature for 2 h, at which point saturated aqueous $NaHCO_3$ (50 mL) was added to quench the reaction. The reaction mixture turned blue following the quench, and was stirred for 1.5 h until the color faded and a white precipitate formed. The reaction mixture was then transferred to a separatory funnel using Et_2O (75 mL) and brine (50 mL). The organic layer was separated, and the aqueous layer was extracted with Et_2O (3 × 50 mL). The combined organic layers were dried over Na_2SO_4 and concentrated *in vacuo* to provide a light yellow oil. The crude oil was used in the next reaction without further purification: ^{1}H NMR (500 MHz, $CDCl_3$) δ 6.12 (dd, *J* = 3.0, 5.0 Hz, 1H), 5.48 (s, 1H), 5.20 (s, 1H), 4.40 (d, *J* = 12.0 Hz, 1H), 4.20 (d, *J* = 12.0 Hz, 1H), 3.80 (br s, 1H), 2.61 (dd, *J* = 5.0, 15.5 Hz, 1H), 2.48–2.36 (m, 2H), 2.22–2.14 (m, 2H), 2.10–2.04 (m, 1H), 1.95–1.83 (m, 3H), 1.62 (br s, 1H), 1.27 (s, 3H); ^{13}C NMR (125 MHz, $CDCl_3$) δ 211.8, 149.6, 130.5, 128.0, 118.7, 81.7, 66.7, 42.8, 41.9, 37.6, 35.1, 31.6, 27.3, 18.7; IR (thin film) 3491 (br), 3083, 2925, 2247, 1761 cm^{-1}; Accurate Mass (ES/MeOH) *m* / *z* calcd for $C_{14}H_{19}BrO_3Na$ $(M + Na)^+$ 337.0415, found 337.0411.

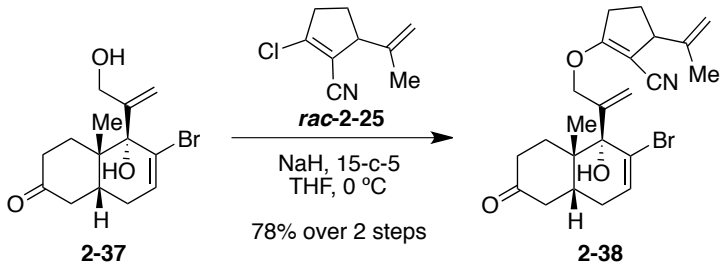

Vinyl ether 2-38. To a cooled (0 °C) solution of allyl alcohol **2-37** (55 mg, 0.17 mmol) in THF (6 mL) was added vinyl chloride **2-25** (47 mg, 0.28 mmol). After stirring the solution for 10 min, 15-crown-5 (0.1 mL, 0.44 mmol) was added followed by NaH (60% in mineral oil, 23 mg, 0.44 mmol). The resulting yellow mixture was warmed to room temperature and stirred for 3 h. The reaction was then cooled to 0 °C and quenched with water (10 mL). The resulting reaction mixture was extracted with EtOAc (3 × 50 mL), dried over Na_2SO_4, and concentrated *in vacuo*. The crude oil was purified by flash chromatography on SiO_2 (hexanes/EtOAc w/ 1% NEt_3 = 100:0 → 75:25 → 70:30) to yield 60.6 mg (78% over 2 steps) of vinyl ether **2-38** as a white film; 1:1 mixture of diastereomers: ^{1}H NMR (500 MHz, $CDCl_3$) δ 6.18 (s, 1H), 5.65 (s, 0.5H), 5.63 (s, 0.5H), 5.40 (s, 1H), 5.22–4.97 (m, 1H), 4.92–4.88 (m, 1H), 4.88 (s, 1H), 4.85 (s, 1H), 3.52 (app t, *J* = 7.0 Hz, 1H), 2.64–2.33 (m, 7H), 2.28–2.21 (td, *J* = 5.0, 14.0 Hz, 1H), 2.19–2.08 (m, 3H), 1.95–1.83 (m, 2H), 1.72 (s, 3H), 1.66 (br s, 1H), 1.29 (s, 3H); ^{13}C NMR (125 MHz, $CDCl_3$) δ 211.5, 172.2, 172.1, 145.05, 145.04, 145.00, 144.98, 129.31, 129.26, 129.03, 128.99, 119.9, 119.8, 119.4, 117.0, 112.3, 112.2, 84.5, 84.4, 81.0, 72.3, 72.2, 51.7, 51.6, 42.6, 41.8, 39.7, 37.7, 35.4, 35.3, 32.8, 32.7, 32.5, 32.4, 31.6, 31.0, 27.5, 26.4, 25.3, 19.13, 19.07; IR (thin film) 3449 (br), 2923, 2850, 2206, 1711 cm^{-1}; Accurate Mass (ES/MeOH) *m* / *z* calcd for $C_{23}H_{28}BrNO_3Na$ $(M + Na)^+$ 468.1150, found 468.1116.

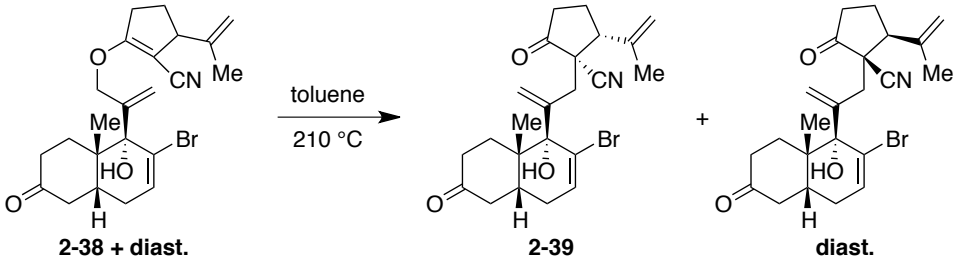

Ketone 2-39. To a microwave vial equipped with a silicon carbide pellet was added vinyl ether **2-38** (58.1 mg, 0.13 mmol) as a solution in toluene (4.3 mL). The reaction was heated to 210 °C and held at that temperature for 3 h. The reaction was quickly cooled to room temperature and the toluene was evaporated under reduced pressure to yield a brown oil. The crude oil was purified by flash chromatography on SiO_2 (hexanes/EtOAc w/ 1% NEt_3 = 75:25 → 70:30) to yield 49.2 mg (85%) of ketone **2-39** as a white film; 1:1 mixture of diastereomers: ^{1}H NMR (500 MHz, $CDCl_3$) δ; ^{13}C NMR (125 MHz, $CDCl_3$) δ; IR (thin film) 3449 (br), 3473 (br), 2954, 2922, 2239, 1750, 1709 cm^{-1}; Accurate Mass (ES/MeOH) *m* / *z* calcd for $C_{23}H_{28}BrNO_3Na$ $(M + Na)^+$ 468.1150, found 468.1139.

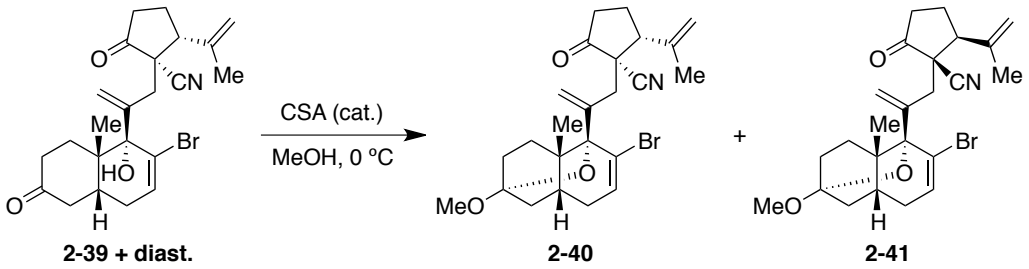

Ketal 2-39. To a cooled (0 °C) solution of ketone **2-39** (49.2 mg, 0.11 mmol) in MeOH (2 mL) was added CSA (8 mg, 0.03 mmol). The reaction was stirred for 5 min at 0 °C before being warmed to room temperature over 2 h. Once the reaction was complete, saturated aqueous $NaHCO_3$ (5 mL) was added. The resulting mixture was extracted with CH_2Cl_2 (3 × 5 mL). The combined organic layers were dried over Na_2SO_4 and concentrated *in vacuo*. The resulting oil was purified by flash chromatography on SiO_2 (hexanes/EtOAc w/ 1% NEt_3 = 85:15) to provide

43 mg (85%) of ketal **2-22** as a white solid; Complex mixture of diastereomers and rotamers: ^{1}H NMR (500 MHz, $CDCl_3$) δ; ^{13}C NMR (125 MHz, $CDCl_3$) δ; IR (thin film) cm^{-1}; Accurate Mass (ES/MeOH) *m* / *z* calcd for $C_{24}H_{30}BrNO_3Na$ $(M + Na)^+$ 482.1307, found 482.1288.

---

1. Pangborn, A. B.; Giardello, M. A.; Grubbs, R. H.; Rosen, R. K.; Timmers, F. J. *Organometallics* **1996**, *15*, 1518–1520.

2. Bowen, M. E.; Aavula, B. R.; Mash, E. A. *Org. Chem. Soc.* **2002**, *67*, 9087–9088.

3. Hajos, Z. G.; Parrish, D. R. *Org. Synth.* **1985**, *63*, 26–31.

PART II

(Chapter 3)

A Concise Method for the Synthesis of Substituted Pyridines

CHAPTER 3

A Concise Method for the Synthesis of Substituted Pyridines

Introduction and Background

Pyridine rings, as well as pyridine-containing polycycles, are commonly found in pharmaceutical lead compounds, and are well represented in clinically approved pharmaceuticals (Figure 3.1).[1] These compounds have drawn inspiration from naturally occurring pyridine-containing molecules, including vitamins B_3 and B_6, as well as NADP and nicotine.[2] With such a diverse set of possible substitution patterns and functionality, coupled with the biological activity possessed by pyridine-containing compounds, the synthesis of pyridines has garnered the attention of chemists for over a century.[3] The Rychnovsky group's interest in synthetic pyridines arose from the desire to synthesize a confidential 2,4-diaryl substituted pyridine (**3-1**).

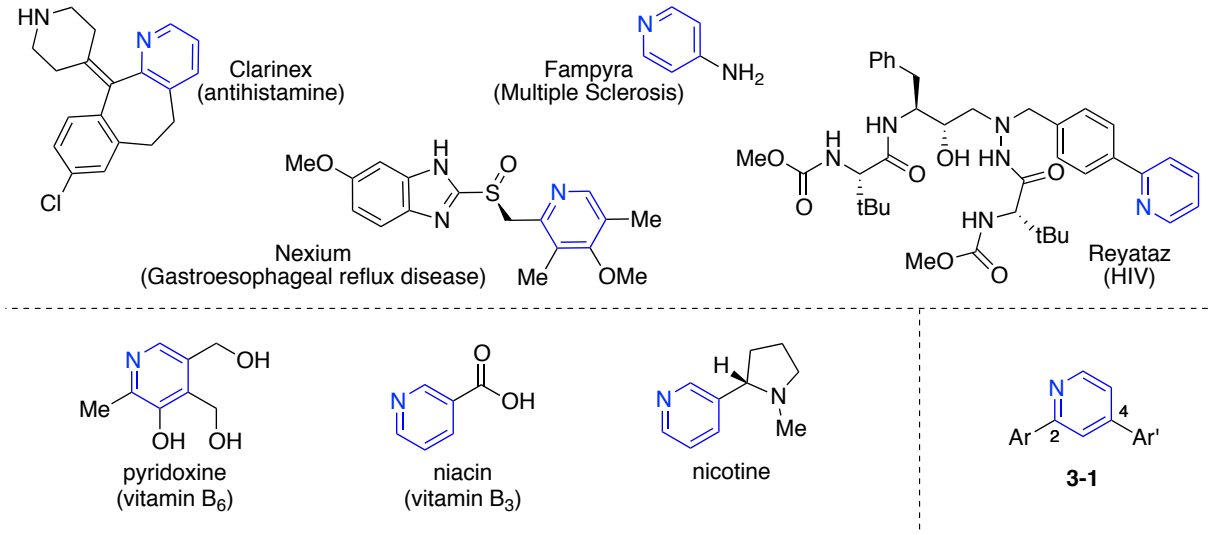

Figure 3.1. Pyridine containing pharmaceuticals and natural products, and our medicinal chemistry motif, 3-1

The synthesis of substituted pyridines is commonly approached in one of two ways: 1) construction of the pyridine ring from functionalized precursors,[4] or 2) site-specific functionalization of an existing pyridine.[5] Reactions in which the pyridine ring is formed include classic named reactions, such as the Kröhnke,[6] Hantzsch,[7] and Chichibabin[8] syntheses, as well as routes based on modern transition metal catalysis.[9] When choosing one of these methods for the synthesis of a desired pyridine, one must consider the substitution pattern the method generates, as well as the functional group tolerance of the reaction sequence and the ease with which the starting materials are obtained. Since no one method exists to generate all possible substitution patterns and functionality conceivable between the five available positions around the pyridine ring, options for methods to utilize are quickly limited to a few reported procedures. In our case, a 2,4-substituted pyridine was targeted by Dr. Michael Holzwarth for a medicinal chemistry collaboration, reducing the number of potentially useful methods to only a handful of examples, two of which are outlined in the following few paragraphs.

In 1988, Ciufolini and coworkers reported a method utilizing a hetero-Diels–Alder reaction to generate acetal intermediates **3-4**, which could easily be converted to the corresponding substituted pyridine via a modified Knoevenagel–Stobbe reaction[10] using hydroxylamine hydrochloride (Table 3.1).[11] The [4 + 2] cycloaddition was carried out between enones **3-2** and ethyl vinyl ether (**3-3**, where R^3 = H) in the presence of a ytterbium catalyst to generate the six-membered ring acetals (**3-4**). This chemistry was successful in generating a variety of substrates including those found in Table 3.1. Aromatic (**3-5a**) and heteroaromatic (**3-5c,f**) substituents were tolerated in this transformation, as well as alkyl and styrenyl substituents (**3-5d** and **3-5e**, respectively). Substitution at the 6-position of the pyridine could additionally be achieved with the use of ethyl isopropenyl ether (**3-3**, where R^3 = Me) to afford 2,4,6-substituted

pyridines **3-5b** and **3-5g**. Yields for this method ranged from 25–40% for the more complex substrates (including those with alkyl substitution), and 81–86% for the simple aromatic systems. Bergman and coworkers elaborated on the substrate scope, showing that 2,2'-bipyridines could be synthesized using the same method.[12] This two-step procedure was of interest to us because it utilized easily accessible enone substrates to functionalize the 2- and 4-positions (R^1 and R^2, respectively) of the resulting pyridine, which made obtaining the necessary starting materials for our system relatively straightforward. It had also been used in the synthesis of a variety of natural products, showing its utility and versatility for generating complex systems.[13] Unfortunately, the initial Diels–Alder reaction was unsuccessful in our case, blocking the synthesis of the desired pyridine and forcing Dr. Michael Holzwath to investigate alternative methods.

Table 3.1. Ciufolini's approach to substituted pyridines

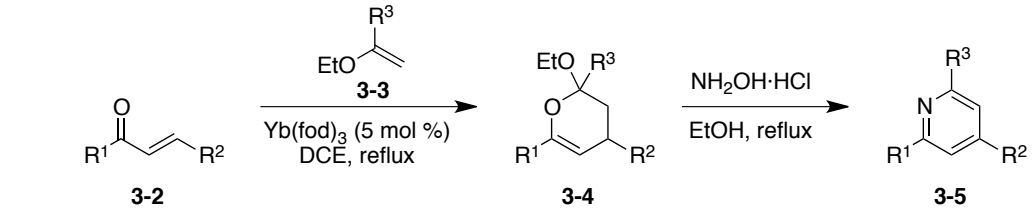

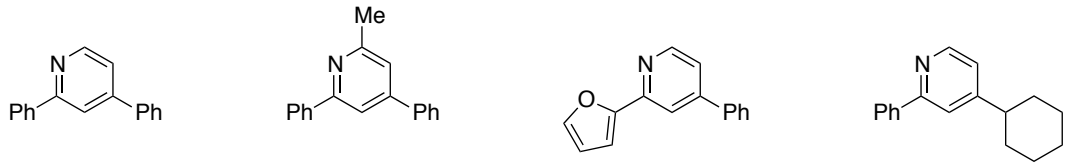

3-5a 81%

3-5b 82%

3-5c 86%

3-5d 40%

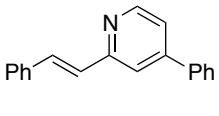

3-5e 84%

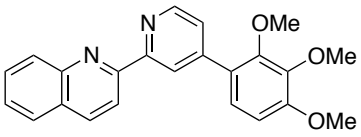

3-5f 25-30%

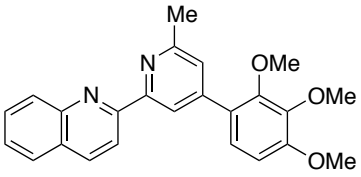

3-5g 25-30%

A method focusing on the synthesis of 2,4-substituted pyridines was reported by Yoshikai and Wei in 2013.[14] A formal [3 + 3] condensation reaction of O-acetyl oximes (**3-6**) and enals (**3-7**) was carried out using a combination of copper(I) redox catalysis and iminium organocatalysis, allowing for the modular synthesis of substituted pyridines (**3-8**) under relatively mild conditions (Scheme 3.1). The authors proposed that the copper catalyst first reduces the oxime N−O bond, generating a nucleophilic copper(II) enamine (**3-9**).[15] A 1,4-addition of the enamine to the α,β-unsaturated iminium ion (**3-10**, formed from the enal starting material) and subsequent cyclization forms a dihydropyridine intermediate (**3-11**). Oxidation of the dihydropyridine intermediate is achieved using the copper(II) species generated during nucleophilic addition of the enamine, to yield the desired pyridine product and regenerate the copper(I) catalyst.

Scheme 3.1. A formal [3 + 3] condensation approach to substituted pyridines

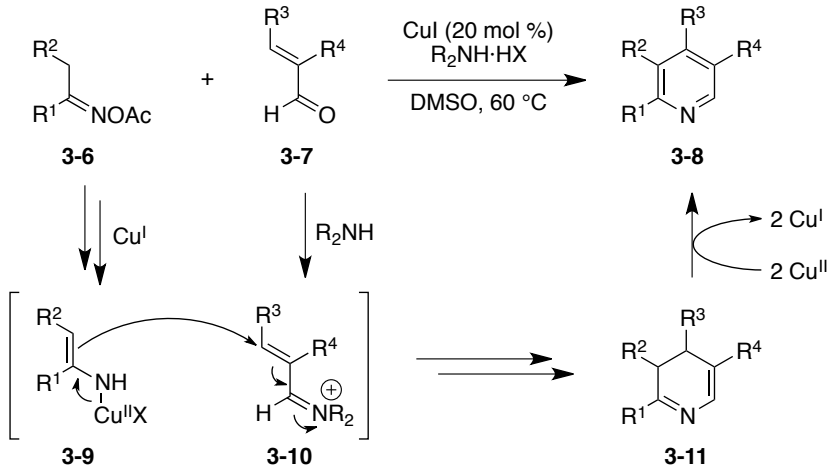

The [3 + 3] condensation reaction was used to successfully synthesize a variety of substituted pyridines, a selection of which are found in Table 3.2. Diaryl-substituted pyridines (i.e. **3-8a,b,h**) were well represented, including electron rich and electron poor systems in both the R^1 and R^3 positions in yields ranging from 48% to 87%. Heterocycles were also tolerated using this method (**3-8c,d**). The use of oximes with R^2 substitution allowed for the synthesis of

2,3,4-substituted pyridines, including cyclic systems like **3-8e**. Some alkyl-substituted oximes could be used, though symmetry was usually necessary to avoid regioselectivity concerns, generating pyridines with alkyl groups at the 2-position (**3-8f**). Ester-substituted pyridines (**3-8g**) could also be synthesized, albeit in slightly diminished yields. Finally, 5-substitution was introduced using α-functionalized enals, allowing for the synthesis of highly substituted pyridines (**3-8i**) in a single transformation and with predictable regiochemistry. One limitation to this method is the inability to introduce substitution at the 6-position, exemplified by pyridine **3-8j**. Only trace quantities of the desired cyclization product was observed when enones were used in place of enals. Another drawback to using this method is the necessary synthesis of starting materials. Additional transformations to commercially available stating materials, though not difficult, nor lengthy by any measure, would inevitably take time and resources to carry out. For this reason, as well as the fact that he already had the desired enone starting material, Dr. Michael Holzwarth never considered this method.

Table 3.2. Substrate scope of the [3 + 3] condensation method

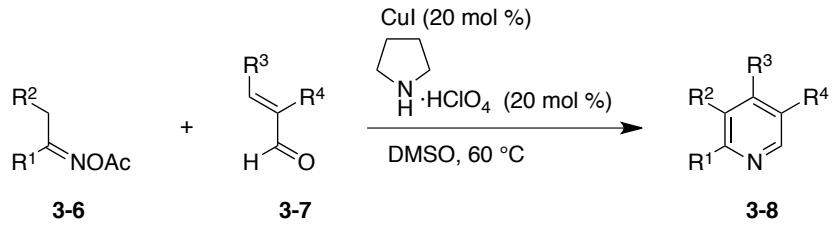

3-6 **3-7** **3-8**

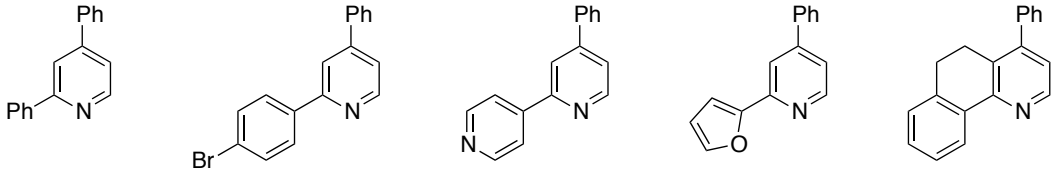

3-8a 75%

3-8b 78%

3-8c 42%

3-8d 66%

3-8e 65%

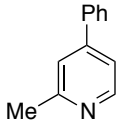

3-8f 65%

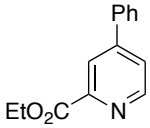

3-8g 52%

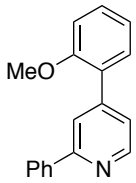

3-8h 87%

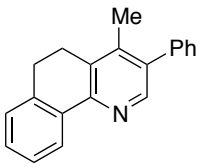

3-8i 36%

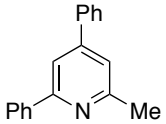

3-8j ≤5%

As previously mentioned, another route to accessing substituted pyridines is through site-specific functionalization of existing pyridines.[5] Some methods have been developed to functionalize pyridines with heteroatoms, such as oxygen, nitrogen, silicon, and sulfur, while others aim to halogenate them. Functionalizing pyridines with carbon is most commonly achieved using standard cross-coupling reactions, including but not limited to Suzuki and Negishi couplings,[16] but can also carried out through C–H bond activation.[17] Most of the time, these methods are employed when the starting materials to make the desired substitutions are commercially available, making them quick and affordable routes. This can quickly change however, when differentially substituted pyridine starting materials need to be synthesized or purchased, as this can take time and resources, or be very costly, as was the case with our desired

substrate. Nevertheless, the following are literature examples of how these methods can be used to generate 2,4-substituted pyridines.

Chemoselective cross-coupling reactions can be useful for controlling the reactivity of polyhalogenated systems, as exemplified by work by the Duan group[18] and Finney group.[19] In Duan's example, synthesis of the starting material, 2-bromo-4-iodopyridine (**3-12**), was accomplished in either a single step or over three steps from 2-bromopyridine in 40% or 56% yield, respectively (Scheme 3.2). For this report, the authors chose aryl Grignard reagents as the cross-coupling partners in Kumada couplings[20] owing to the availability of the starting materials. Reactions run at –40 °C allowed for the chemoselective reaction of the iodide in the presence of the bromide, yielding bromopyridine **3-14**. Simply increasing the reaction temperature by 20 °C and including a new coupling partner (**3-15**), afforded 2,4-diaryl-substituted pyridine **3-16** in 60% yield over 2 steps.

Scheme 3.2. Duan's cross-coupling method for 2,4-diaryl substituted pyridines

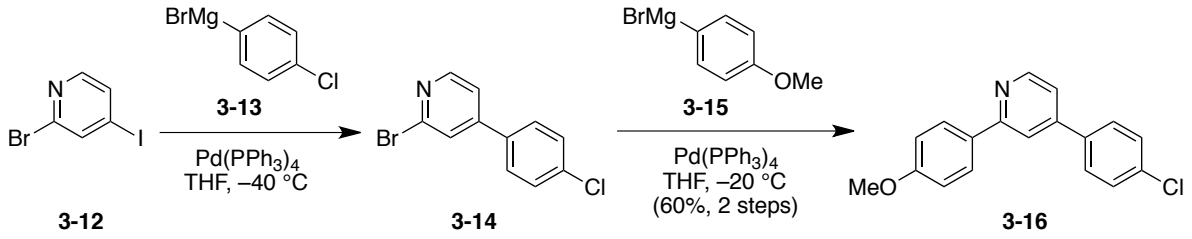

Similarly, Finney utilized reactivity differences in Negishi[21] and Suzuki[22] reactions to accomplish the first and second cross-coupling reactions of pyridine **3-18**, respectively (Scheme 3.3). This synthesis, as with the previous example from Duan, demonstrates the difficulty in obtaining useful starting materials in high yields. Starting from citrazinic acid (**3-17**), pyridine **3-18** was synthesized in 34% yield over four steps. Reaction of the iodide with phenylzinc chloride under Negishi conditions afforded dichloropyridine **3-19** in very high yield. Monofunctionalization of **3-19** was achieved using arylboronic acid **3-20** as the limiting reagent,

providing pyridine **3-21**, which contains a chloride as a functional handle for further manipulation. Alternatively, the dichloride was converted to triflate **3-22** over three steps, followed by cross-coupling to yield 2,4-disubstituted pyridine **2-23**. Although cross-coupling reactions are high-yielding, dependable reactions, syntheses of complex substituted pyridines are sometime tedious and low-yielding when differentiated starting materials are unavailable.

Scheme 3.3. Finney's method to di- and tri-substituted pyridines using cross-coupling reactions

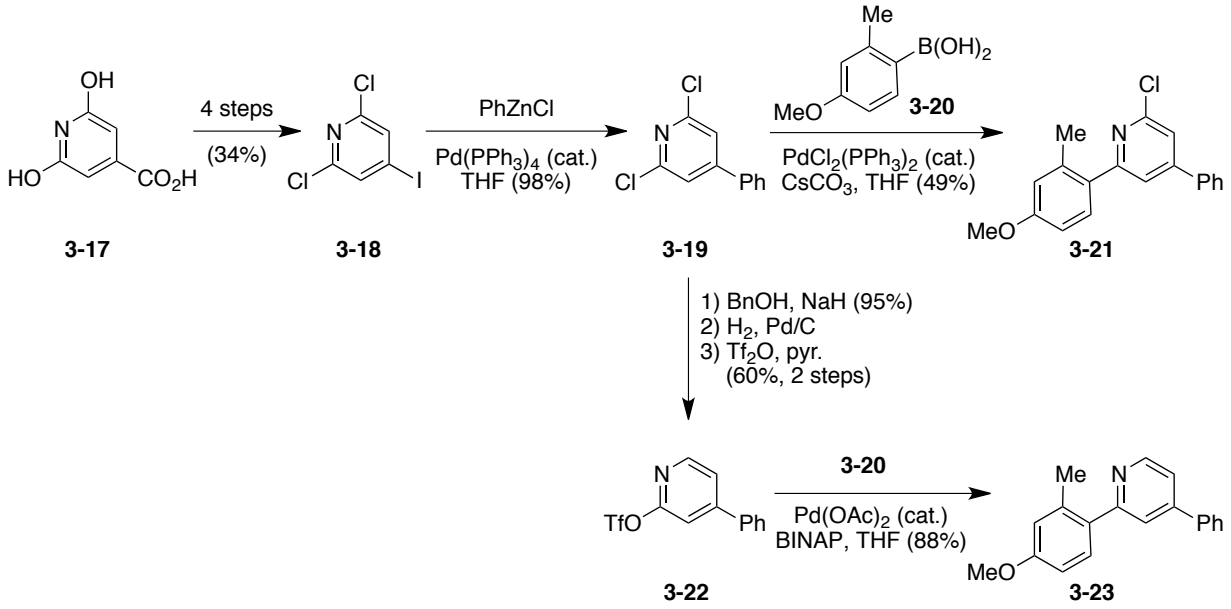

With a biaryl enone precursor already in hand from previous attempts at pyridine cyclizations, Dr. Michael Holzwarth developed a new route from several reliable reactions that allowed for the construction of the requisite pyridine target. During this process, we quickly identified the utility of the designed sequence, and decided to pursue the method for publication. It was at this time that I joined the project, to both optimize reaction conditions and explore the substrate scope of the methodology.

Current Method

The method by design, utilizes robust chemistry to provide a simple, yet reliable way of accessing substituted pyridines from starting materials that are commercially available or easily synthesized. The general approach is outlined in Scheme 3.4. Condensation of a functionalized 1,5-dicarbonyl (**3-25**) would provide pyridines using well-established cyclization chemistry. The dicarbonyl intermediate could be accessed from enones (**3-26**), a motif commonly synthesized through a variety of methods, including aldol condensations,[23] cross-metathesis reactions,[24] and HWE olefinations.[25] In order to introduce the two carbon unit needed, we envisioned a two-step procedure, by first introducing an allylic nucleophile to the Michael acceptor, followed by oxidative cleavage of the resulting olefin.

Scheme 3.4. Retrosynthetic approach to pyridines from enones and allyl nucleophiles

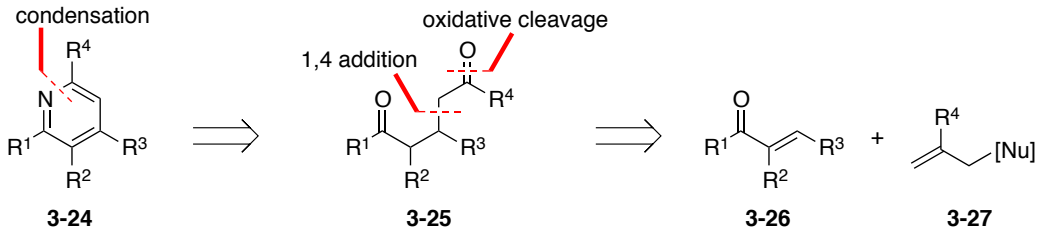

Initial studies focused on a general procedure for converting enones (chalcone derivatives) to the desired pyridine (Scheme 3.5). Optimization of the sequence was accomplished using chalcone (**3-28**) as the enone precursor. The conjugate addition was achieved by reacting enone **3-28** with commercially available allyltrimethylsilane (**3-29**) under modified Hosomi–Sakurai reaction conditions.[26] A variety of Lewis acids and additives can be used to effect this transformation, including but not limited to aluminum trichloride,[27] fluoride,[28] iodine,[29] and indium trichloride,[30] but titanium tetrachloride was found to work best for most of the substrates tested during the course of our investigation.[31] One could also envision the use of organometallic reagents, such as organocuprates, for allylic conjugate additions.[32] Although

these reactions would achieve the necessary transformation, the allylsilanes used in Sakurai additions provided a bench stable reagent. Additionally, the titanium tetrachloride could be used without purification, simplifying the reaction setup. Following the allylation, oxidative cleavage of olefin **3-30** was carried out using ozone.[33] Other oxidations were also competent in this sequence, including Johnson–Lemieux conditions,[34] but the ozonolysis procedure provided the desired crude aldehyde **3-31** with good purity and minimal side products. Finally, the cyclization of aldehyde **3-31** was carried out using hydroxylamine hydrochloride[10] at elevated temperatures to provide pyridine **3-32** in high yields.[35] Several solvents were investigated for the cyclization, and acetonitrile was found to be superior to alcohol solvents with respect to scope and yield. In an attempt to identify whether the reaction sequence could be telescoped, we determined that the sequence requires two purifications using column chromatography: once after oxidation of the olefin, and another following the cyclization. In many cases, the first purification can be omitted, albeit with diminished yields.[36]

Scheme 3.5. Optimized synthetic route to pyridines using chalcone and allyltrimethylsilane

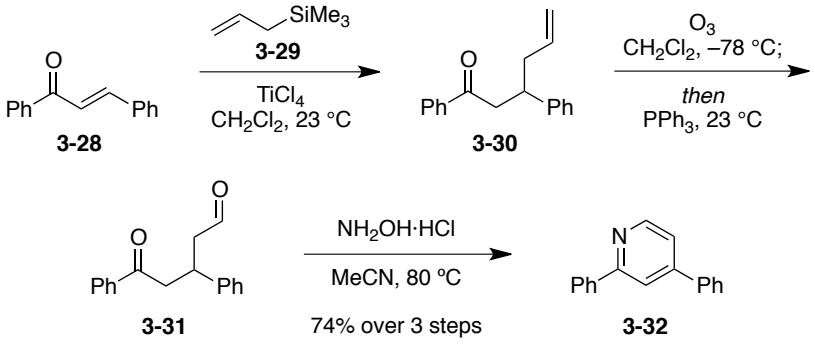

With an optimized procedure in hand, the substrate scope was explored. Sakurai reactions using allyltrimethylsilane (**3-29**) were the primary focus, yielding pyridines without substitution at the 5 and 6 positions (Table 3.3). Reactions using aryl-aryl disubstituted enones provided 2,4-substituted pyridines (**3-34a-g**) in 60–80% yield. The three-step sequence was tolerant of a

variety of substitution patterns and substituents, including electron-donating and -withdrawing groups. More notably, halogenated aromatic systems could be used (**3-34b,c**) without concern for the loss of the halogen, since no transition metal catalysts are used in the sequence. These substrates also provide a handle for further functionalization using traditional cross-coupling reactions. 2,2'-Bipyridines (**3-34h**) can also be synthesized using this method, similar to those synthesized by Bergman and coworkers.[12] Alkyl-substituted pyridines (**3-34i-k**) can also be produced using the same three-step procedure, albeit in slightly diminished yields.

Table 3.3. Scope of 2,4-substituted pyridines

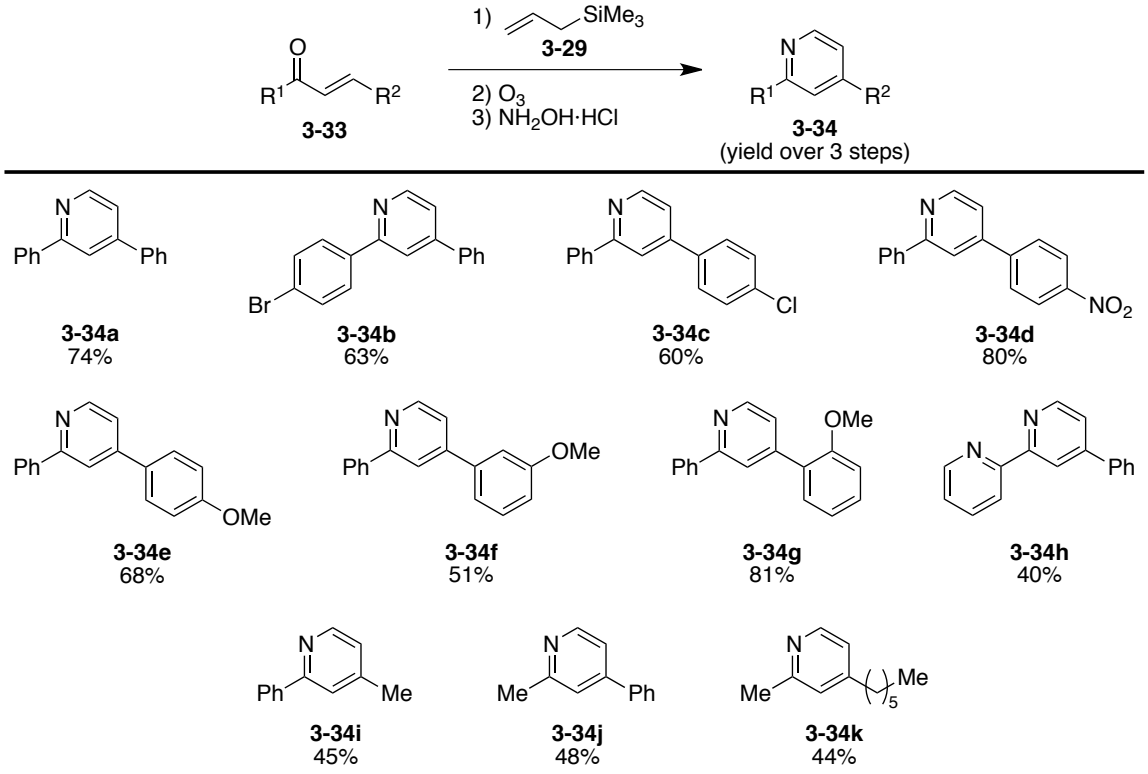

Substitution at the 3-position of the pyridine can be introduced through the use of α-substituted enones. This modification allows for the synthesis of polycyclic pyridines, as demonstrated by **3-36a-c**, as well as 2,3,4-trisubstituted pyridines **3-36d**. A fluorine atom on the enone is compatible with the sequence and leads to a 3-fluoropyridine **3-36e** in good yield.[37] The

method can be used with a variety of simple substituents to produce disubstituted and trisubstituted pyridine rings.

Table 3.4. Scope of 2,3,4-substituted pyridines

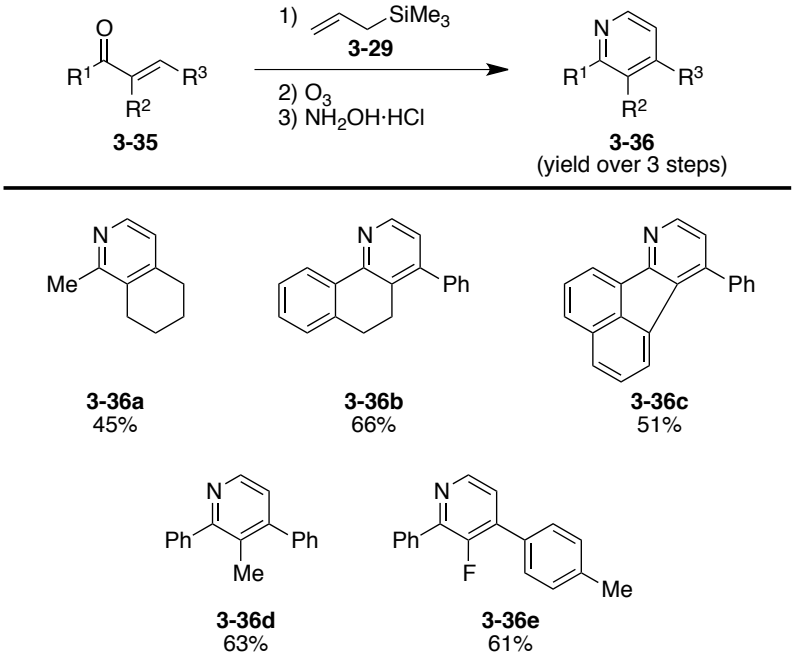

Further investigation of the scope of the method was directed at the allylsilane component, which can carry additional substituents. Substituted allylsilanes are most often synthesized using (trimethylsilyl)methylmagnesium chloride, typically through double addition/elimination reactions of esters, or cross-coupling reactions of vinyl halides or enol triflates.[38] Commercially available methallyltrimethylsilane (**3-38**) was evaluated in order to introduce a methyl group at the 6-position of the constructed pyridine ring. The Hosomi–Sakurai reactions using methallyltrimethylsilane, however, were not as widely successful as those using allyltrimethylsilane. At this time, it is unclear as to why these reactions were difficult to carry out, though some effort was directed at investigating this problem. The reaction time, temperature, and order of addition of reagents were all explored, but no conclusions could be made. In cases where the Hosomi–Sakurai addition worked well, however, the oxidation and

cyclization reactions proceeded uneventfully to provide the desired pyridines (Table 3.5). Pyridine **3-39c** offers an example of a tetrasubstituted pyridine prepared by this strategy.

Table 3.5. Scope of 6-substituted pyridines

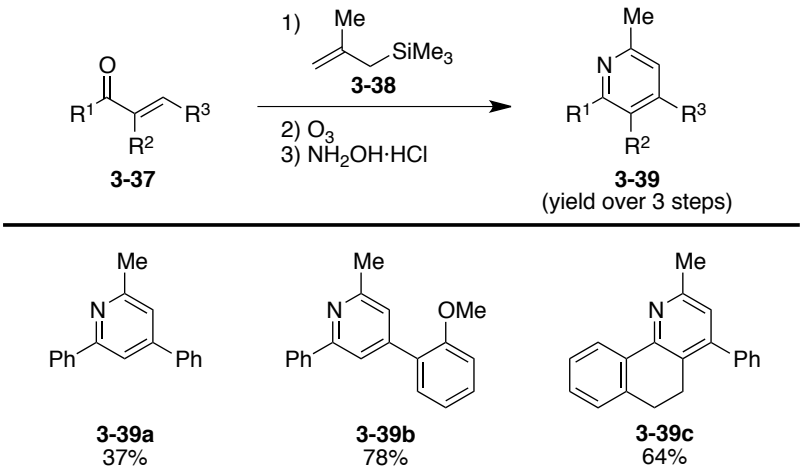

Not all substrates subjected to this method were successfully converted to the corresponding pyridine. Though every 1,5-dicarbonyl compound was easily cyclized using hydroxylamine hydrochloride, some substrates were unable to undergo Hosomi–Sakurai addition (Table 3.6). Enol ether **3-40a** provided a complex mixture of products, including β-elimination of the ethyl ether, which could then undergo a second allyl addition. Compounds **3-40b-d** also provided complex mixtures of products with no evidence of the desired addition products. Although these substrates did not work under the optimized conditions determined for our method, other Lewis acids could potentially improve the reactivity of some, if not all, of these substrates. As previously mentioned, other allylic nucleophiles could also be added to these α,β-unsaturated enones as a direct extension of this method, if these substrates were desired.

Table 3.6. Substrates that did not undergo successful Hosomi–Sakurai additions

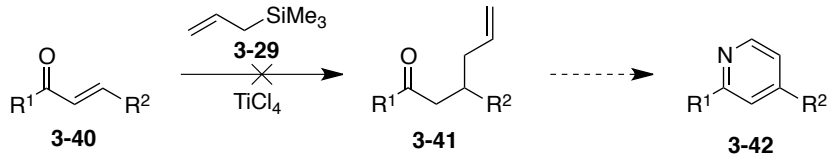

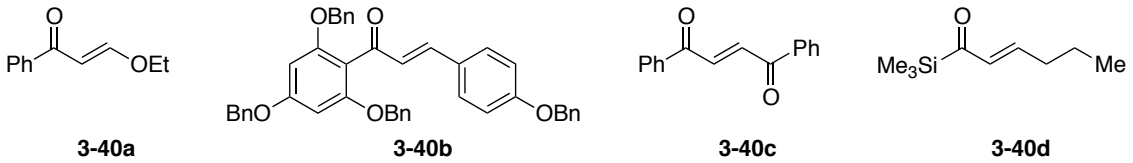

Substrates that did not successfully undergo oxidative cleavage can be found in Table 3.7. The pendant olefins of cyclohexanones **3-43a** and **b**, as well as trifluoroketone **3-43e**, reacted with ozone, as evidenced by the disappearance of vinylic proton signals in ^{1}H NMR spectra obtained of the crude reaction mixture. Only trace amounts of aldehyde could be identified, however, presumably due to an aldol cyclization of the ketone into the generated aldehyde, or lactol formation. Oxidation of the sulfur of benzothiophene **3-43c** during ozonolysis provided a complex mixture of products, none of which were obtained in high yield. Finally, no desired aldehyde product was identified after attempted oxidative cleavage of β-keto ester **3-43d**, presumable due to over oxidation of the enol resonance structures.

Table 3.7. Substrates that did not successfully undergo oxidative cleavage using ozonolysis

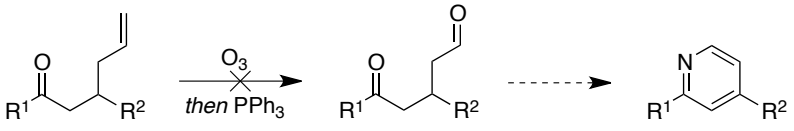

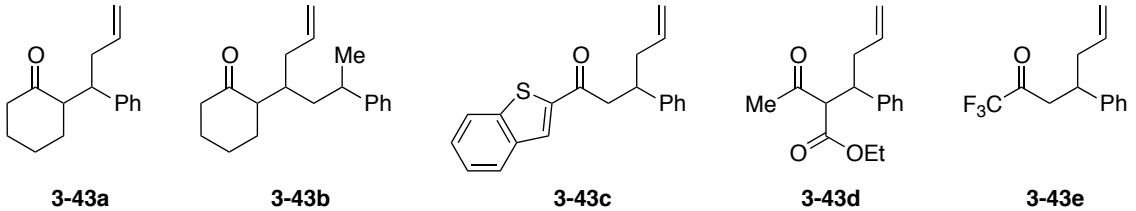

To complete the substrate scope, we wanted to determine whether multiple pyridine rings could be formed during a single sequence using this method. Pyridine rings have been identified as excellent ligands for first-row transition metals. For many applications in this area, multiple pyridine rings are desirable and act as polydentate ligands. We have already demonstrated that the method can be used to generate 2,2'-bipyridines (**3-34h**), using pyridine-substituted enones as starting materials. The construction of bis-pyridines, however, was explored using symmetric bis-enones, in which both pyridine rings would be formed simultaneously (Scheme 3-6). Bis-enone **3-46** underwent two Hosomi–Sakurai additions successfully, generating **3-47**. Subsequent oxidation gave the bis-aldehyde (**3-48**), which was cyclized under standard conditions using hydroxylamine hydrochloride to afford bis-pyridine **3-49** in 41% yield. As a direct extension of this chemistry, bis-enone **3-50**, with an existing pyridine ring at the center of the system, was used to assemble a tris-pyridine ligand (**3-51**) in 21% yield over three steps using this method. This approach provides an alternative route for generating polydentate pyridine ligands.[39]

Scheme 3.6. Synthesis of bis- and tris-pyridines from bis-enones

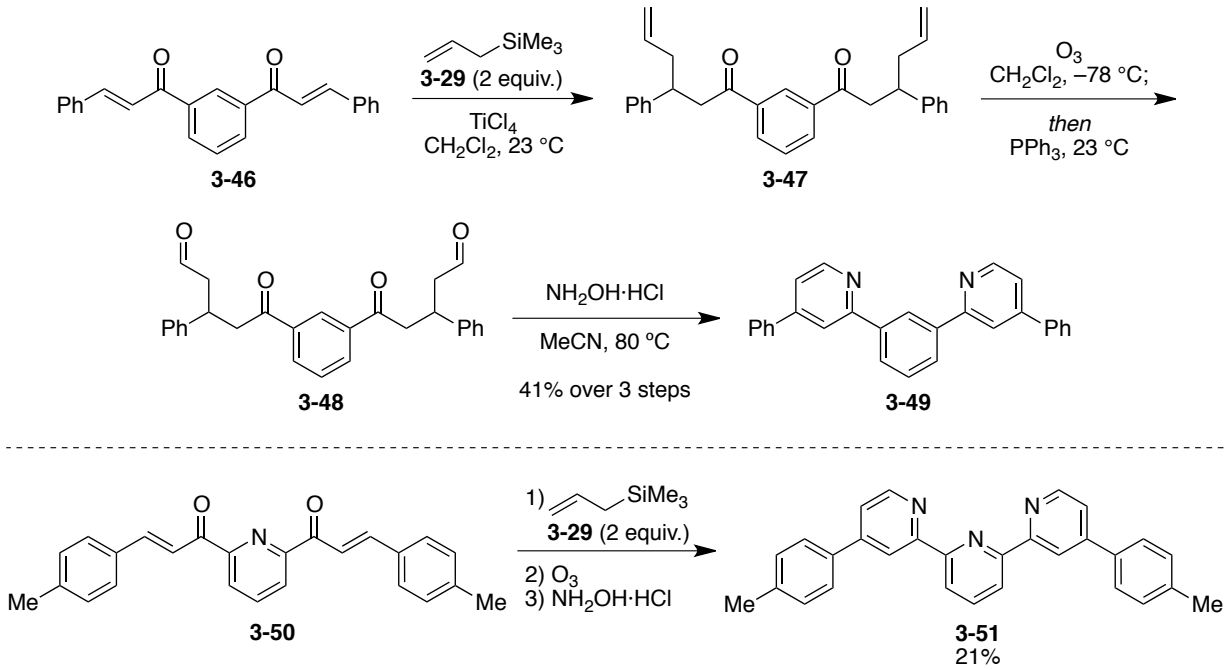

Conclusion

A simple method for the construction of highly substituted pyridine rings was developed utilizing enones as the starting material. These building blocks are either commercially available or easily synthesized with many substitution patterns. A Hosomi–Sakurai addition with allylsilanes provided a robust pathway for installing the remaining carbon atoms for the ring. Oxidative cleavage of the resulting terminal olefin, and subsequent cyclization of the intermediate 1,5-dicarbonyl structure using hydroxylamine hydrochloride completes the synthesis. The method has a reasonable scope, uses simple and reliable steps, and should be useful for the preparation of new bioactive materials or transition metal ligands.

1. (a) Baumann, M.; Baxendale, I. R. *Beilstein J. Org. Chem.* **2013**, *9*, 2265–2319. (b) Afzal, O.; Kumar, S.; Haider, M. R.; Ali, M. R.; Kumar, R.; Jaggi, M.; Bawa, S. *Eur. J. Med. Chem.* **2015**, *97*, 871–910. (c) Shiro, T.; Fukaya, T.; Tobe, M. *Eur. J. Med. Chem.* **2015**, *97*, 397–408.

2. Kiuru, P.; Yli-Kauhaluoma, J., Pyridine and Its Derivatives. In *Heterocycles in Natural Product Synthesis*, Wiley-VCH Verlag GmbH & Co. KGaA: 2011; pp 267–297.

3. (a) Henry, G. D. *Tetrahedron* **2004**, *60*, 6043–6061. (b) Wagner, F. F.; Comins, D. L. *Tetrahedron* **2007**, *63*, 8065–8082.

4. Keller, P. A.; Abdel-Hamid, M. K.; Abdel-Megeed, A. M., Chapter 2 - Ring Synthesis. In *Pyridines: from lab to production*, Scriven, E. F., Ed. Academic Press: Oxford, 2013; pp 15–152.

5. Gribble, G. W.; Fu, L.; Lin, Q.-X., Chapter 3 - Attachment at Ring Positions In *Pyridines: from lab to production*, Scriven, E. F., Ed. Academic Press: Oxford, 2013; pp 153–373.

6. (a) Zecher, W.; Kröhnke, F. *Chem. Ber.* **1961**, *94*, 690–697. (b) Zecher, W.; Kröhnke, F. *Chem. Ber.* **1961**, *94*, 698–706.

7. Hantzsch, A. *Chem. Ber.* **1881**, *14*, 1637–1638.

8. Tschitschibabin, A. E. *J. Prakt. Chem.* **1924**, *107*, 122–128.

9. (a) Wang, Y.-F.; Chiba, S. *J. Am. Chem. Soc.* **2009**, *131*, 12570–12572. (b) Martin, R. M.; Bergman, R. G.; Ellman, J. A. *J. Org. Chem.* **2012**, *77*, 2501–2507. (c) Neely, J. M.; Rovis, T. *J. Am. Chem. Soc.* **2013**, *135*, 66–69. (d) He, Z.; Dobrovolsky, D.; Trinchera, P.; Yudin, A. K. *Org. Lett.* **2013**, *15*, 334–337. (e) Hardegger, L. A.; Habegger, J.; Donohoe, T. J. *Org. Lett.* **2015**, *17*, 3222–3225.

10. (a) Knoevenagel, E.; Weissgerber, R. *Chem. Ber.* **1893**, *26*, 436–441. (b) Stobbe, H.; Striegler, C. *J. Prakt. Chem.* **1912**, *86*, 241–250.

11. Ciufolini, M. A.; Byrne, N. E. *J. Chem. Soc., Chem. Commun.* **1988**, 1230–1231.

12. Cordaro, J. G.; McCusker, J. K.; Bergman, R. G. *Chem. Commun.* **2002**, 1496–1497.

13. (a) Ciufolini, M. A.; Byrne, N. E. *Tetrahedron Lett.* **1989**, *30*, 5559–5562. (b) Ciufolini, M. A.; Byrne, N. E. *J. Am. Chem. Soc.* **1991**, *113*, 8016–8024. (c) Ciufolini, M. A.; Shen, Y.-C. *Tetrahedron Lett.* **1995**, *36*, 4709–4712. (d) Ciufolini, M. A.; Shen, Y.-C.; Bishop, M. J. *J. Am. Chem. Soc.* **1995**, *117*, 12460–12469.

14. Wei, Y.; Yoshikai, N. *J. Am. Chem. Soc.* **2013**, *135*, 3756–3759.

15. Ren, Z.-H.; Zhang, Z.-Y.; Yang, B.-Q.; Wang, Y.-Y.; Guan, Z.-H. *Org. Lett.* **2011**, *13*, 5394–5397.

16. Johansson Seechurn, C. C. C.; Kitching, M. O.; Colacot, T. J.; Snieckus, V. *Angew. Chem. Int. Ed.* **2012**, *51*, 5062–5085.

17. Lewis, J. C.; Bergman, R. G.; Ellman, J. A. *J. Am. Chem. Soc.* **2007**, *129*, 5332–5333.

18. Duan, X.-F.; Li, X.-H.; Li, F.-Y.; Huang, C.-H. *Synthesis* **2004**, *2004*, 2614–2616.

19. Mello, J. V.; Finney, N. S. *Org. Lett.* **2001**, *3*, 4263–4265.

20. (a) Tamao, K.; Sumitani, K.; Kumada, M. *J. Am. Chem. Soc.* **1972**, *94*, 4374–4376. (b) Knappke, C. E. I.; Jacobi von Wangelin, A. *Chem. Soc. Rev.* **2011**, *40*, 4948–4962.

21. Negishi, E.; King, A. O.; Okukado, N. *J. Org. Chem.* **1977**, *42*, 1821–1823.

22. Miyaura, N.; Suzuki, A. *Chem. Rev.* **1995**, *95*, 2457–2483.

23. Nielsen, A. T.; Houlihan, W. J., The Aldol Condensation. In *Organic Reactions*, John Wiley & Sons, Inc.: 2004.

24. Connon, S. J.; Blechert, S. *Angew. Chem. Int. Ed.* **2003**, *42*, 1900–1923.

25. Maryanoff, B. E.; Reitz, A. B. *Chem. Rev.* **1989**, *89*, 863–927.

26. Hosomi, A.; Sakurai, H. *J. Am. Chem. Soc.* **1977**, *99*, 1673–1675.

27. Ojima, I.; Kumagai, M.; Miyazawa, Y. *Tetrahedron Lett.* **1977**, *18*, 1385–1388.

28. Majetich, G.; Casares, A. M.; Chapman, D.; Behnke, M. *Tetrahedron Lett.* **1983**, *24*, 1909–1912.

29. Yadav, J. S.; Reddy, B. V. S.; Sadasiv, K.; Satheesh, G. *Tetrahedron Lett.* **2002**, *43*, 9695–9697.

30. (a) Lee, P. H.; Lee, K.; Sung, S.-y.; Chang, S. *J. Org. Chem.* **2001**, *66*, 8646–8649. (b) Lee, P. H.; Seomoon, D.; Kim, S.; Nagaiah, K.; Damle, S. V.; Lee, K. *Synthesis* **2003**, *2003*, 2189–2193.

31. Indium trichloride worked well for chalcone derivatives, but reactions of alkyl substituted enones were lower yielding and provided complex mixtures of products in our hands.

32. Lipshutz, B. H.; Sengupta, S., Organocopper Reagents: Substitution, Conjugate Addition, Carbo/Metallocupration, and Other Reactions. In *Organic Reactions*, John Wiley & Sons, Inc.: 2004.

33. (a) Caron, S.; Dugger, R. W.; Ruggeri, S. G.; Ragan, J. A.; Ripin, D. H. B. *Chem. Rev.* **2006**, *106*, 2943–2989. (b) Bailey, P. S. *Chem. Rev.* **1958**, *58*, 925–1010.

34. Pappo, R.; Allen, J. D. S.; Lemieux, R. U.; Johnson, W. S. *J. Org. Chem.* **1956**, *21*, 478–479.

35. Although never explored, ammonium acetate or ammonia could also be used to afford the pyridine cyclization from 1,5-dicarbonyls. see ref. 4 for additional details.

36. An isolated yield of 44% was obtained when the reaction sequence was fully telescoped.

37. Chen, S.; Bergman, R. G.; Ellman, J. A. *Org. Lett.* **2015**, *17*, 2567–2569.

38. Ager, D. J.; Yorimitsu, H.; Oshima, K., Trimethylsilylmethylmagnesium Chloride. In *Encyclopedia of Reagents for Organic Synthesis*, John Wiley & Sons, Ltd: 2001.

39. Hommes, P.; Reissig, H.-U. *Eur. J. Org. Chem.* **2016**, *2016*, 338–342.

Chapter 3:

Experimental Section

General Information. ^{1}H NMR and ^{13}C NMR spectra were recorded at ambient temperature using Bruker DRX500 (500 and 125 MHz, respectively) or AVANCE600 (600 and 150 MHz, respectively) spectrometers, as indicated. The data are reported as follows: chemical shift in ppm on a δ scale and referenced to internal tetramethylsilane or residual solvent (^{1}H NMR = TMS: δ 0.00 or $CHCl_3$: δ 7.26; ^{13}C NMR = $CHCl_3$: δ 77.16), multiplicity (appar = apparent, br = broad, s = singlet, d = doublet, t = triplet, q = quartet, quint = quintet, sext = sextet, m = multiplet), coupling constants (Hz), and integration. Infrared (IR) spectra were obtained using a PerkinElmer Frontier FT-IR spectrometer. Accurate mass spectra were acquired on a Waters LCT Premier quadrupole time-of-flight spectrometer and were obtained by peak matching. Analytical thin layer chromatography was performed on Merck glass-backed silica gel 60 Å F_{254} plates and visualized by UV light, *p*-anisaldehyde, potassium permanganate, or vanillin. Liquid chromatography was performed using forced flow (flash chromatography) of the indicated solvent system on Merck Geduran silica gel (SiO_2) 60 (40-60 mesh). CH_2Cl_2 was dried by filtration through alumina according to the method of Grubbs.[1] All reactions using CH_2Cl_2 as solvents were run under an atmosphere of argon in glassware that was flame- or oven-dried, unless otherwise stated. All commercially available reagents were used as received unless stated otherwise.

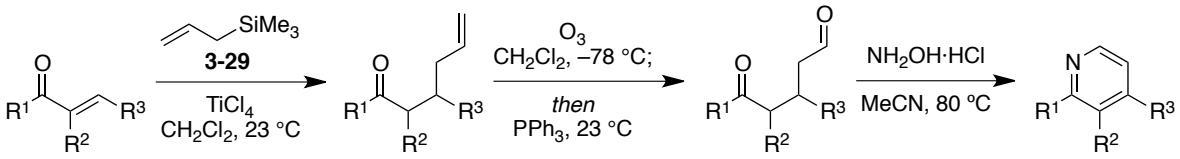

General procedure using allyltrimethylsilane (3-29): Hosomi–Sakurai addition. To a stirring solution of enone (1 mmol) in CH_2Cl_2 (1.5 mL) was added titanium tetrachloride (1.2 mmol) as a single portion and the solution turned dark red. A separate solution of allyltrimethylsilane (**3-29**) (1.3 mmol) in CH_2Cl_2 (1.5 mL) was prepared, and then added as a single portion to the stirring enone solution. The reaction mixture was allowed to stir at room temperature for 2 h. Once the reaction was complete, the reagents were quenched with the slow addition of H_2O (3 ml), resulting in a cloudy biphasic solution. The phases were separated, and the aqueous layer was extracted with CH_2Cl_2 (3 × 2 mL). The combined organic layers were dried over Na_2SO_4, run through a plug of silica gel, and concentrated *in vacuo*. The resulting crude oil was taken on to the next step without further purification.

General procedure: ozonolysis. A stirring solution of olefin (1 mmol) in CH_2Cl_2 (7 mL) was cooled to –78 °C. Ozone was then bubbled through the solution until a blue color persisted for 1 min. Oxygen was then bubbled through the solution for 5 min to displace any remaining ozone in solution. Triphenylphosphine (1.5 mmol) was then added, and the reaction was capped and stirred overnight at room temperature. Once the reaction was complete, the solvent was evaporated and PPh_3 and $OPPh_3$ were removed using flash chromatography on SiO_2 (hexanes/EtOAc = 75:25). All fractions not containing PPh_3 and $OPPh_3$ were combined, concentrated, and carried on to the next step.

General procedure: cyclization of the pyridine ring. To a scintillation vial containing a solution of aldehyde (1 mmol) in acetonitrile (12 mL) was added hydroxylamine hydrochloride (3 mmol). After capping the vial, the reaction was heated to 80 °C, where it was left to stir overnight. The next day, the reaction was cooled to room temperature, and the MeCN was removed under reduced pressure. The dark-colored solid was then dissolved in 10 mL of saturated aqueous K_2CO_3/H_2O (1:1), and was extracted with EtOAc (3 × 5 mL). The combined organic layers were dried over Na_2SO_4 and concentrated *in vacuo*. The crude residue was purified using flash chromatography on SiO_2 (hexanes/EtOAc = 70:30) to afford the desired pyridine. All yields presented are over the three steps.

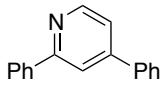

3-34a

2,4-diphenylpyridine (3-34a). Colorless oil (74%): ^{1}H NMR (500 MHz, $CDCl_3$) δ 8.72 (d, *J* = 5.0 Hz, 1H), 8.04 (d, *J* = 7.3 Hz, 2H), 7.91 (s, 1H), 7.67 (d, *J* = 6.8 Hz, 2H), 7.50–7.41 (m, 7H); ^{13}C NMR (125 MHz, $CDCl_3$) δ 158.1, 150.1, 149.3, 139.5, 138.6, 129.16, 129.07, 128.8, 127.12, 127.07, 120.3, 118.8; ^{1}H and ^{13}C NMR spectral data are in agreement with previously reported literature data.[2]

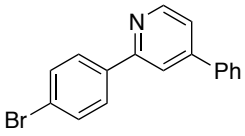

3-34b

2-(4-bromophenyl)-4-phenylpyridine (3-34b). White solid (80%): ^{1}H NMR (500 MHz, $CDCl_3$) δ 8.72 (d, *J* = 5.1 Hz, 1H), 7.93 (d, *J* = 8.7 Hz, 2H), 7.88 (s, 1H), 7.67 (dd, *J* = 7.2, 1.1 Hz, 2H), 7.61 (d, *J* = 8.7 Hz, 2H), 7.54–7.42 (m, 4H); ^{13}C NMR (125 MHz, $CDCl_3$) δ 1567.0, 150.3, 149.6, 138.5, 132.0, 129.3, 128.7, 127.2, 123.7, 120.7, 118.6; ^{1}H and ^{13}C NMR spectral data are in agreement with previously reported literature data.[2]

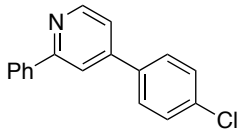

3-34c

4-(4-chlorophenyl)-2-phenylpyridine (3-34c). Brown oil (60%): ^{1}H NMR (500 MHz, $CDCl_3$) δ 8.70 (d, *J* = 5.2 Hz, 1H), 8.06–7.97 (m, 2H), 7.83 (d, *J* = 0.8 Hz, 1H), 7.58–7.54 (m, 2H), 7.51–7.39 (m, 5H), 7.36–7.32 (m, 1H); ^{13}C NMR (125 MHz, $CDCl_3$) δ 158.3, 150.3, 148.0, 139.3, 136.9, 135.3, 129.4, 129.2, 128.9, 128.4, 127.1, 120.0, 118.5; ^{1}H and ^{13}C NMR spectral data are in agreement with previously reported literature data.[3]

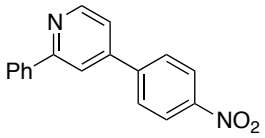

3-34d

4-(4-nitrophenyl)-2-phenylpyridine (3-34d). White solid (80%): ^{1}H NMR (500 MHz, $CDCl_3$) δ 8.82 (d, *J* = 4.5 Hz, 1H), 8.38 (d, *J* = 8.8 Hz, 2H), 8.06 (d, *J* = 7.1 Hz, 2H), 7.94 (s, 1H), 7.85 (d, *J* = 8.8 Hz, 2H), 7.52 (t, *J* = 7.1 Hz, 2H), 7.47 (m, 2H); ^{13}C NMR (125 MHz, $CDCl_3$) δ 158.8, 150.7, 148.4, 147.1, 145.1, 139.1, 129.6, 129.1, 128.3, 127.2, 124.5, 120.4, 118.9; ^{1}H and ^{13}C NMR spectral data are in agreement with previously reported literature data.[4]

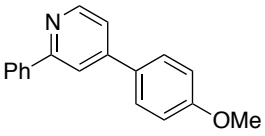

3-34e

4-(4-methoxyphenyl)-2-phenylpyridine (3-34e). Light brown oil (68%): ^{1}H NMR (500 MHz, $CDCl_3$) δ 8.70 (d, *J* = 5.1 Hz, 1H), 8.04–8.03 (m, 2H), 7.89 (s, 1H), 7.65 (d, *J* = 8.8 Hz, 2H), 7.51–7.41 (m, 4H), 7.03 (d, *J* = 8.8 Hz, 2H), 3.86 (s, 3H); ^{13}C NMR (125 MHz, $CDCl_3$) δ 160.7, 158.2, 150.2, 148.9, 139.8, 130.9, 129.1, 128.9, 128.4, 127.2, 119.9, 118.4, 114.7, 55.6; ^{1}H and ^{13}C NMR spectral data are in agreement with previously reported literature data.[2]

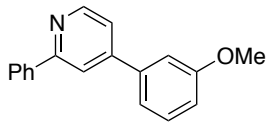

3-34f

4-(3-methoxyphenyl)-2-phenylpyridine (3-34f). Brown oil (51%): ^{1}H NMR (500 MHz, $CDCl_3$) δ 8.74 (d, *J* = 5.1 Hz, 1H), 8.07 (d, *J* = 7.1 Hz, 2H), 7.93 (s, 1H), 7.51 (t, *J* = 7.1 Hz, 2H), 7.47–7.39 (m, 3H), 7.28 (d, *J* = 8.3 Hz, 1H), 7.23–7.21 (m, 1H), 7.00 (dd, *J* = 8.3, 2.5 Hz, 1H), 3.88 (s, 3H); ^{13}C NMR (125 MHz, $CDCl_3$) δ 160.2, 158.1, 150.1, 149.2, 140.1, 139.5, 130.2, 129.1, 128.8, 127.1, 120.4, 119.6, 118.9, 114.3, 113.0, 55.4; IR (thin film) 1593, 1543, 1210, 772, 691 cm^{-1}; Accurate Mass (ES/MeOH) *m* / *z* calcd for $C_{18}H_{15}NONa$ $(M + Na)^+$ 284.1051, found 284.1049.

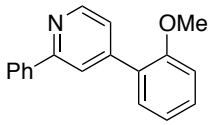

3-34g

4-(2-methoxyphenyl)-2-phenylpyridine (3-34g). Light pink oil (81%): ^{1}H NMR (500 MHz, $CDCl_3$) δ 8.72 (d, *J* = 5.1 Hz, 1H), 8.06–8.00 (m, 2H), 7.90 (s, 1H), 7.49 (t, *J* = 7.5 Hz, 2H), 7.45–7.38 (m, 4H), 7.09 (t, *J* = 7.5 Hz, 1H), 7.04 (d, *J* = 8.1 Hz, 1H), 3.86 (s, 3H); ^{13}C NMR (125 MHz, $CDCl_3$) δ 157.5, 156.7, 149.5, 147.3, 139.9, 130.6, 130.3, 128.9, 128.8, 128.2, 127.2, 123.0, 121.6, 121.2, 111.6, 55.8; ^{1}H and ^{13}C NMR spectral data are in agreement with previously reported literature data.[2]

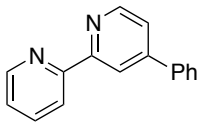

3-34h

4-phenyl-2,2'-bipyridine (3-34h). Light yellow oil (40%): ^{1}H NMR (500 MHz, $CDCl_3$) δ 8.75–8.64 (m, 3H), 8.45 (d, *J* = 8.0 Hz, 1H), 7.81 (td, *J* = 7.5, 1.8 Hz, 1H), 7.75 (m, 2H), 7.52 (dd, *J* =

5.1, 1.9 Hz, 1H), 7.50–7.45 (m, 2H), 7.45–7.39 (m, 1H), 7.30 (ddd, J = 7.5, 4.8, 1.1 Hz, 1H); ^{13}C NMR (125 MHz, $CDCl_3$) δ 156.7, 156.2, 149.7, 149.4, 149.3, 138.3, 137.0, 129.1, 129.1, 127.2, 123.9, 121.7, 121.3, 119.1; IR (thin film) 3055, 1582, 1456, 1389, 759, 694 cm^{-1}; Accurate Mass (ES/MeOH) m / z calcd for $C_{16}H_{12}N_2H$ $(M + H)^+$ 233.1079, found 233.1069.

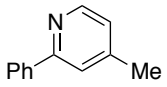

3-34i

4-methyl-2-phenylpyridine (3-34i). Colorless oil (45%): ^{1}H NMR (500 MHz, $CDCl_3$) δ 8.55 (d, J = 4.8 Hz, 1H), 7.97 (d, J = 8.2 Hz, 2H), 7.55 (s, 1H), 7.47 (t, J = 7.4 Hz, 2H), 7.45–7.37 (m, 1H), 7.06 (d, J = 4.4 Hz, 1H), 2.42 (s, 3H); ^{13}C NMR (125 MHz, $CDCl_3$) δ 157.5, 149.6, 147.9, 139.7, 129.0, 128.8, 127.1, 123.3, 121.7, 21.4; ^{1}H and ^{13}C NMR spectral data are in agreement with previously reported literature data.[3]

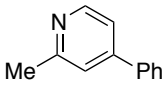

3-34j

2-methyl-4-phenylpyridine (3-34j). Orange oil (48%): ^{1}H NMR (500 MHz, $CDCl_3$) δ 8.53 (d, J = 5.3 Hz, 1H), 7.61 (d, J = 8.5 Hz, 2H), 7.50–7.44 (m, 2H), 7.41 (m, 1H), 7.36 (s, 1H), 7.30 (d, J = 5.3 Hz, 1H), 2.62 (s, 3H); ^{13}C NMR (125 MHz, $CDCl_3$) δ 158.9, 149.7, 148.8, 138.5, 129.1, 129.0, 127.1, 121.3, 119.0, 24.7; ^{1}H and ^{13}C NMR spectral data are in agreement with previously reported literature data.[2]

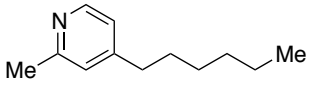

3-34k

4-hexyl-2-methylpyridine (3-34k). Brown oil (44%): ^{1}H NMR (500 MHz, $CDCl_3$) δ 8.36 (d, J = 5.1 Hz, 1H), 6.97 (s, 1H), 6.91 (d, J = 5.1 Hz, 1H), 2.57–2.53 (t, J = 7.5 Hz, 2H), 2.52 (s, 3H), 1.60 (dt, J = 15.2, 7.5 Hz, 2H), 1.37–1.21 (m, 6H), 0.88 (t, J = 6.6 Hz, 3H); ^{13}C NMR (125 MHz,

$CDCl_3$) δ 158.2, 152.3, 149.0, 123.6, 121.2, 35.4, 31.8, 30.5, 29.0, 24.4, 22.7, 14.2; IR (thin film) 2926, 2856, 1604, 1456 cm^{-1}; Accurate Mass (ES/MeOH) *m* / *z* calcd for $C_{12}H_{19}NH$ $(M + H)^+$ 178.1596, found 178.1604.

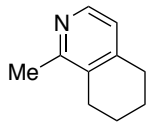

3-36a

1-methyl-5,6,7,8-tetrahydroisoquinoline (3-36a). Light orange oil (45%): ^1H NMR (500 MHz, $CDCl_3$) δ 8.16 (d, *J* = 5.1 Hz, 1H), 6.83 (d, *J* = 5.1 Hz, 1H), 2.72 (t, *J* = 6.3 Hz, 2H), 2.62 (t, *J* = 6.4 Hz, 2H), 2.43 (s, 3H), 1.89–1.82 (m, 2H), 1.81–1.72 (m, 2H); ^{13}C NMR (125 MHz, $CDCl_3$) δ 157.1, 146.0, 145.3, 131.0, 122.2, 29.5, 26.1, 23.1, 22.3, 22.2; IR (thin film) 2928, 1587, 1428, 1411, 834, 807 cm^{-1}; Accurate Mass (ES/MeOH) *m* / *z* calcd for C10H13NH $(M + H)^+$ 148.1126, found 148.1123.

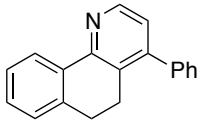

3-36b

4-phenyl-5,6-dihydrobenzo[*h*]quinoline (3-36b). Tan solid (66%): ^1H NMR (500 MHz, $CDCl_3$) δ 8.55 (d, *J* = 4.9 Hz, 1H), 8.36 (dd, *J* = 7.7, 1.0 Hz, 1H), 7.46–7.28 (m, 7H), 7.19 (d, *J* = 7.4 Hz, 1H), 7.09 (d, *J* = 4.9 Hz, 1H), 2.90–2.87 (m, 2H), 2.80–2.78 (m, 2H); ^{13}C NMR (125 MHz, $CDCl_3$) δ; ^1H and ^{13}C NMR spectral data are in agreement with previously reported literature data.[2]

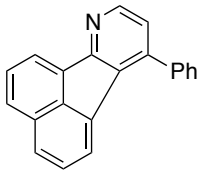

3-36c

10-phenylacenaphtho[1,2-*b*]pyridine (3-36c). Orange solid (51%): ^{1}H NMR (500 MHz, $CDCl_3$) δ 8.61 (d, *J* = 5.1 Hz, 1H), 8.35 (d, *J* = 6.9 Hz, 1H), 7.98 (d, *J* = 8.1 Hz, 1H), 7.88 (d, *J* = 8.0 Hz, 1H), 7.76 (t, *J* = 7.5 Hz, 1H), 7.67 (dd, *J* = 8.0, 1.7 Hz, 2H), 7.61–7.53 (m, 3H), 7.52–7.42 (m, 2H), 7.18 (d, *J* = 5.1 Hz, 1H); ^{13}C NMR (125 MHz, $CDCl_3$) δ 159.7, 147.8, 145.7, 138.7, 135.3, 133.5, 132.3, 131.0, 129.8, 129.0, 128.9, 128.6, 128.4, 128.0, 127.8, 123.9, 123.0, 121.9; IR (thin film) 3053, 1428, 825, 776, 763, 701 cm^{-1}; Accurate Mass (ES/MeOH) *m* / *z* calcd for $C_{21}H_{13}NH$ $(M + H)^+$ 280.1126, found 280.1123.

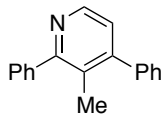

3-36d

3-methyl-2,4-diphenylpyridine (3-36d). Brown oil (63%): ^{1}H NMR (500 MHz, $CDCl_3$) δ 8.57 (d, *J* = 5.0 Hz, 1H), 7.57 (d, *J* = 8.2 Hz, 2H), 7.51–7.44 (m, 4H), 7.44–7.35 (m, 4H), 7.16 (d, *J* = 5.0 Hz, 1H), 2.23 (s, 3H); ^{13}C NMR (125 MHz, $CDCl_3$) δ 159.8, 151.0, 146.5, 141.1, 139.9, 129.2, 128.8, 128.6, 128.5, 128.2, 128.0, 123.3, 18.1; ^{1}H and ^{13}C NMR spectral data are in agreement with previously reported literature data.[2]

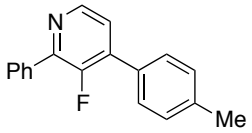

3-36e

3-fluoro-2-phenyl-4-(*p*-tolyl)pyridine (3-36e). Tan solid (61%): ^{1}H NMR (500 MHz, $CDCl_3$) δ 8.53 (d, *J* = 4.8 Hz, 1H), 7.98 (d, *J* = 7.3 Hz, 2H), 7.55 (dd, *J* = 7.9, 1.2 Hz, 2H), 7.51 (t, *J* = 7.3 Hz, 2H), 7.48–7.43 (m, 1H), 7.37–7.28 (m, 3H), 2.44 (s, 3H); ^{13}C NMR (125 MHz, $CDCl_3$) δ 154.7 (d, *J* = 260.8 Hz), 147.2 (d, *J* = 13.0 Hz), 145.4 (d, *J* = 6.7 Hz), 139.4, 137.4 (d, *J* = 13.0 Hz), 135.8 (d, *J* = 4.9 Hz), 130.6, 130.0, 129.6, 129.2, 129.15 (d, *J* = 5.5 Hz), 129.0 (d, *J* = 3.2 Hz), 128.9, 128.5, 127.1 (d, *J* = 18.4 Hz), 123.7, 21.4; ^{19}F NMR (376 MHz, $CDCl_3$) δ –130.65;

IR (thin film) 2915, 1597, 1396, 1204, 815, 750, 695, 497 cm^{-1}; Accurate Mass (ES/MeOH) *m* / *z* calcd for $C_{18}H_{14}FNNa$ $(M + Na)^+$ 286.1008, found 286.1019.

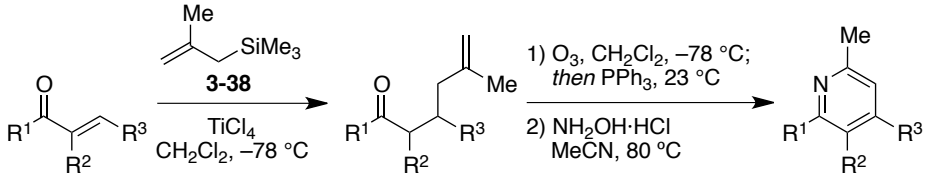

General procedure using methallyltrimethylsilane (3-38): Hosomi–Sakurai addition. To a cooled (–78 °C) solution of enone (1 mmol) in CH_2Cl_2 (4 mL) was added titanium tetrachloride (1.2 mmol) dropwise and the solution turned red. A separate solution of methallyltrimethylsilane (**3-38**) (1.4 mmol) in CH_2Cl_2 (1.5 mL) was prepared, and then added dropwise to the stirring enone solution after it had stirred for 10 min. The reaction mixture was allowed to stir at –78 °C for 2 h. Once the reaction was complete, the reagents were quenched with the slow addition of H_2O (3 ml) and warmed to room temperature, resulting in a cloudy biphasic solution. The phases were separated, and the aqueous layer was extracted with CH_2Cl_2 (3 × 2 mL). The combined organic layers were dried over Na_2SO_4, run through a plug of silica gel, and concentrated *in vacuo*. The resulting crude oil was taken on to the next step without further purification.

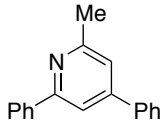

3-39a

2-methyl-4,6-diphenylpyridine (3-39a). Brown oil (37%): ^{1}H NMR (500 MHz, $CDCl_3$) δ 8.01 (d, *J* = 7.1 Hz, 2H), 7.67 (s, 1H), 7.61 (d, *J* = 7.1 Hz, 2H), 7.45–7.35 (m, 5H), 2.65 (s, 3H); ^{13}C NMR (125 MHz, $CDCl_3$) δ; ^{1}H and ^{13}C NMR spectral data are in agreement with previously reported literature data.[5]

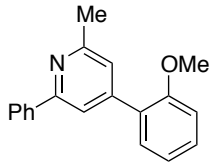

3-39b

4-(2-methoxyphenyl)-2-methyl-6-phenylpyridine (3-39b). Colorless oil (78%): ^{1}H NMR (500 MHz, $CDCl_3$) δ 8.00 (d, *J* = 8.2 Hz, 2H), 7.68 (s, 1H), 7.46 (t, *J* = 7.5 Hz, 2H), 7.42–7.34 (m, 3H), 7.26 (s, 1H), 7.06 (t, *J* = 7.5 Hz, 1H), 7.01 (d, *J* = 8.2 Hz, 1H), 3.84 (s, 3H), 2.67 (s, 3H); ^{13}C NMR (125 MHz, $CDCl_3$) δ 158.2, 157.0, 156.7, 147.4, 140.3, 130.6, 130.0, 128.8, 128.7, 128.5, 127.3, 122.4, 121.1, 118.9, 111.5, 55.7, 25.0; IR (thin film) 1604, 1399, 1246, 1024, 751, 693 cm^{-1}; Accurate Mass (ES/MeOH) *m* / *z* calcd for $C_{19}H_{17}NONa$ $(M + Na)^+$ 298.1208, found 298.1204.

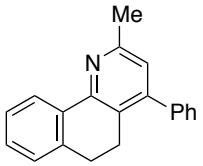

3-39c

2-methyl-4-phenyl-5,6-dihydrobenzo[*h*]quinoline (3-39c). Orange oil (64%): ^{1}H NMR (500 MHz, $CDCl_3$) δ 8.38 (d, *J* = 7.6 Hz, 1H), 7.46 (m, 2H), 7.43–7.38 (m, 1H), 7.35 (m, 3H), 7.30 (td, *J* = 7.4, 1.3 Hz, 1H), 7.20 (d, *J* = 7.4 Hz, 1H), 7.00 (s, 1H), 2.88–2.83 (m, 2H), 2.83–2.77 (m, 2H), 2.63 (s, 3H); ^{13}C NMR (125 MHz, $CDCl_3$) δ; IR (thin film) 2927, 1590, 1547, 1497, 750, 701 cm^{-1}; Accurate Mass (ES/MeOH) *m* / *z* calcd for $C_{20}H_{17}NH$ $(M + H)^+$ 272.1439, found 272.1426.

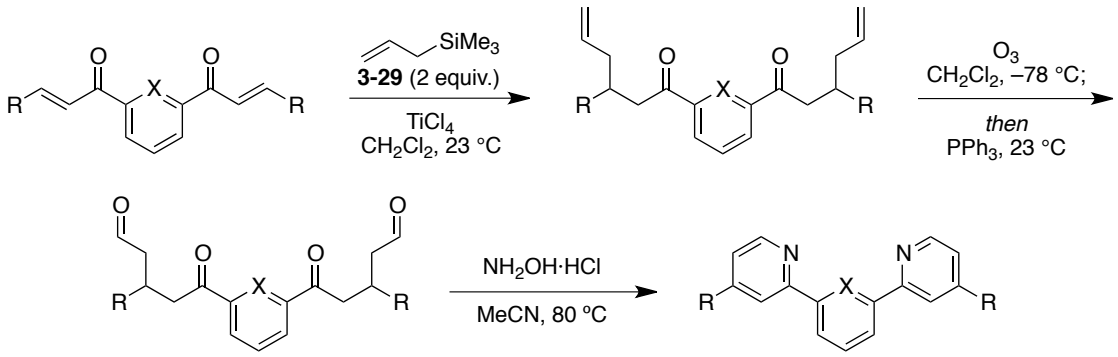

General procedure using bis-enones: Hosomi–Sakurai addition. To a stirring solution of bis-enone (0.5 mmol) in CH_2Cl_2 (1.5 mL) was added titanium tetrachloride (1.2 mmol) as a single portion and the solution turned dark red. A separate solution of allyltrimethylsilane (**3-29**) (1.3 mmol) in CH_2Cl_2 (1.5 mL) was prepared, and then added as a single portion to the stirring enone solution. The reaction mixture was allowed to stir at room temperature for 2 h. Once the reaction was complete, the reagents were quenched with the slow addition of H_2O (3 ml), resulting in a cloudy biphasic solution. The phases were separated, and the aqueous layer was extracted with CH_2Cl_2 (3 × 2 mL). The combined organic layers were dried over Na_2SO_4, run through a plug of silica gel, and concentrated *in vacuo*. The resulting crude oil was taken on to the next step without further purification.

General procedure using bis-enones: ozonolysis. A stirring solution of bis-olefin (0.5 mmol) in CH_2Cl_2 (7 mL) was cooled to –78 °C. Ozone was then bubbled through the solution until a blue color persisted for 1 min. Oxygen was then bubbled through the solution for 5 min to displace any remaining ozone in solution. Triphenylphosphine (1.5 mmol) was then added, and the reaction was capped and stirred overnight at room temperature. Once the reaction was complete, the solvent was evaporated and PPh_3 and $OPPh_3$ were removed using flash chromatography on

SiO_2 (hexanes/EtOAc = 75:25). All fractions not containing PPh_3 and $OPPh_3$ were combined, concentrated, and carried on to the next step.

General procedure using bis-enones: cyclization of the pyridine rings. To a scintillation vial containing a solution of bis-aldehyde (0.5 mmol) in acetonitrile (12 mL) was added hydroxylamine hydrochloride (3 mmol). After capping the vial, the reaction was heated to 80 °C, where it was left to stir overnight. The next day, the reaction was cooled to room temperature, and the MeCN was removed under reduced pressure. The dark-colored solid was then dissolved in 10 mL of saturated aqueous K_2CO_3/H_2O (1:1), and was extracted with EtOAc (3 × 5 mL). The combined organic layers were dried over Na_2SO_4 and concentrated *in vacuo*. The crude residue was purified using flash chromatography on SiO_2 (hexanes/EtOAc = 70:30) to afford the desired bis-pyridine. All yields presented are over the three steps.

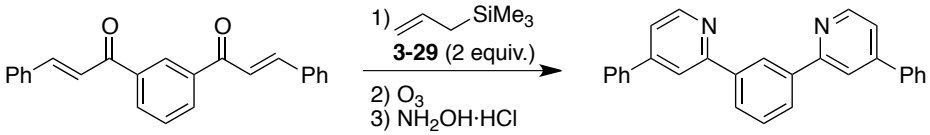

3-46 **3-49**

1,3-bis(4-phenylpyridin-2-yl)benzene (3-49). Light red oil (41%): ^{1}H NMR (500 MHz, $CDCl_3$) δ 8.77 (d, *J* = 5.1 Hz, 2H), 8.71 (s, 1H), 8.14 (dd, *J* = 7.8, 1.8 Hz, 2H), 8.05 (s, 2H), 7.72 (m, 4H), 7.64 (t, *J* = 7.8 Hz, 1H), 7.58–7.41 (m, 8H); ^{13}C NMR (125 MHz, $CDCl_3$) δ 158.1, 150.3, 149.6, 140.3, 138.7, 129.4, 129.3, 129.2, 127.9, 127.3, 125.9, 120.6, 119.1; IR (thin film) 1592, 1542, 758, 728, 692, 613 cm^{-1}; Accurate Mass (ES/MeOH) *m* / *z* calcd for $C_{28}H_{20}N_2H$ $(M + H)^+$ 385.1705, found 385.1694.

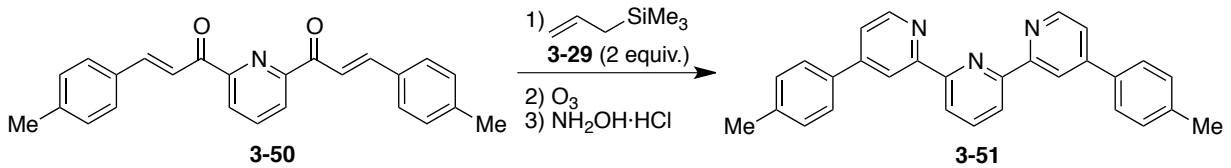

3-50 **3-51**

4,4''-di-*p*-tolyl-2,2':6',2''-terpyridine (3-51). Tan solid (21%): ^{1}H NMR (500 MHz, $CDCl_3$) δ 8.86 (d, *J* = 1.1 Hz, 2H), 8.73 (d, *J* = 5.1 Hz, 2H), 8.49 (d, *J* = 7.8 Hz, 2H), 7.99 (t, *J* = 7.8 Hz, 1H), 7.70 (d, *J* = 8.0 Hz, 4H), 7.55 (dd, *J* = 5.1, 1.8 Hz, 2H), 7.33 (d, *J* = 8.0 Hz, 4H), 2.45 (s, *J* = 10.6 Hz, 6H); ^{13}C NMR (125 MHz, $CDCl_3$) δ 156.9, 155.6, 149.7, 149.2, 139.3, 138.1, 135.7, 130.0, 127.1, 121.6, 121.4, 119.1, 21.4; IR (thin film) 2920, 1572, 1383, 802, 453 cm^{-1}; Accurate Mass (ES/MeOH) *m* / *z* calcd for $C_{29}H_{23}N_3Na$ $(M + Na)^+$ 436.1790, found 436.1782.

---

1. Pangborn, A. B.; Giardello, M. A.; Grubbs, R. H.; Rosen, R. K.; Timmers, F. J. *Organometallics* **1996**, *15*, 1518–1520.

2. Wei, Y.; Yoshikai, N. *J. Am. Chem. Soc.* **2013**, *135*, 3756–3759.

3. Wang, S.-W.; Guo, W.-S.; Wen, L.-R.; Li, M. *RSC Adv.* **2014**, *4*, 59218–59220.

4. Zu, L.; Xie, H.; Li, H.; Wang, J.; Yu, X.; Wang, W. *Chem. Eur. J.* **2008**, *14*, 6333–6335.

5. Zhu, C.; Bi, B.; Ding, Y.; Zhang, T.; Chen, Q.-Y. *Tetrahedron* **2015**, *71*, 9251–9257.

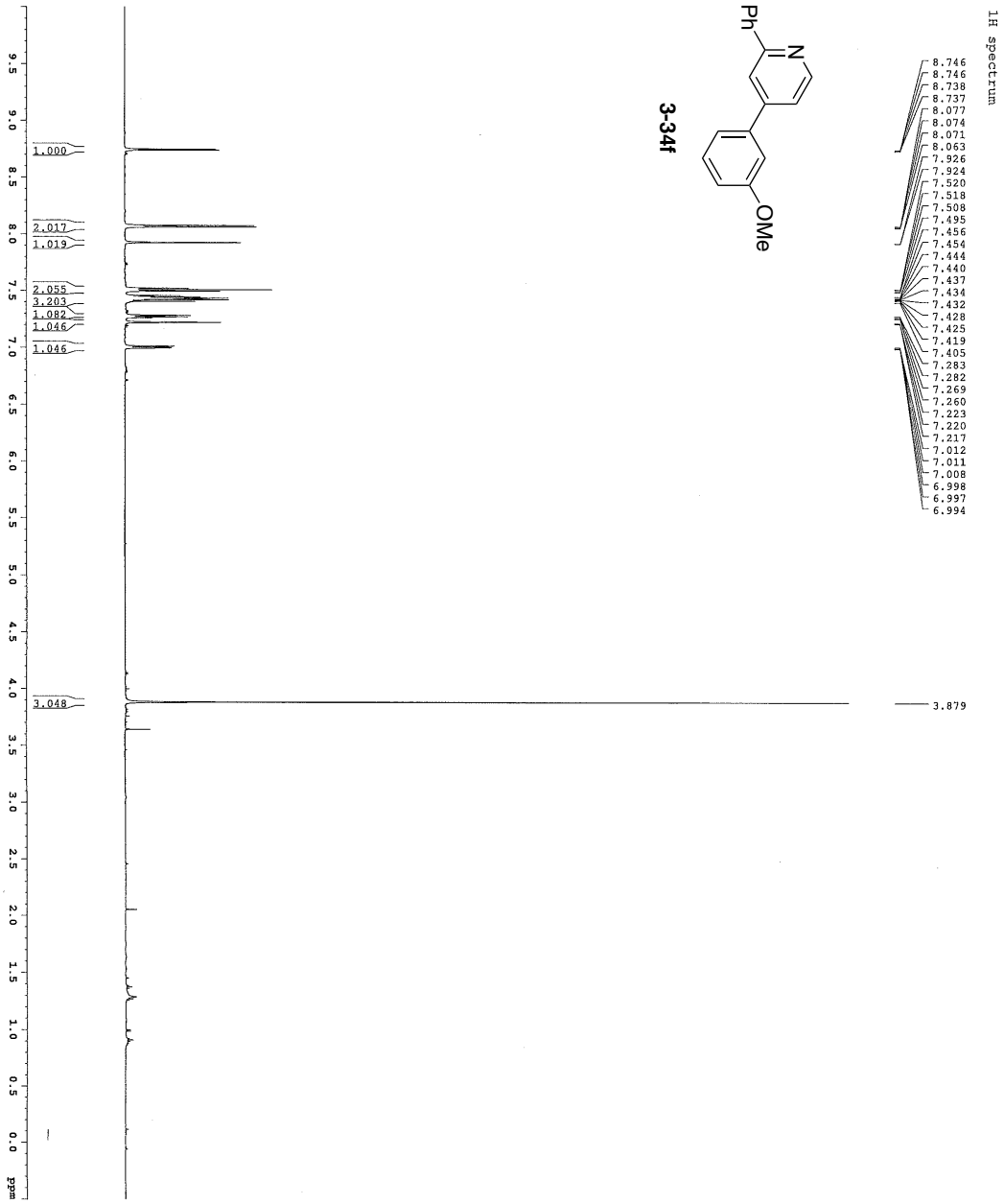
1H spectrum
8.746
8.746
8.738
8.737
8.077
8.074
8.071
8.063
7.926
7.924
7.520
7.518
7.508
7.495
7.456
7.454
7.444
7.440
7.437
7.434
7.432
7.428
7.425
7.419
7.405
7.283
7.282
7.269
7.260
7.223
7.220
7.217
7.012
7.011
7.008
6.998
6.997
6.994
3.879
1.000
2.017
1.019
2.055
3.203
1.082
1.046
1.046
3.048
Ph
N
OMe
3-34f
ppm

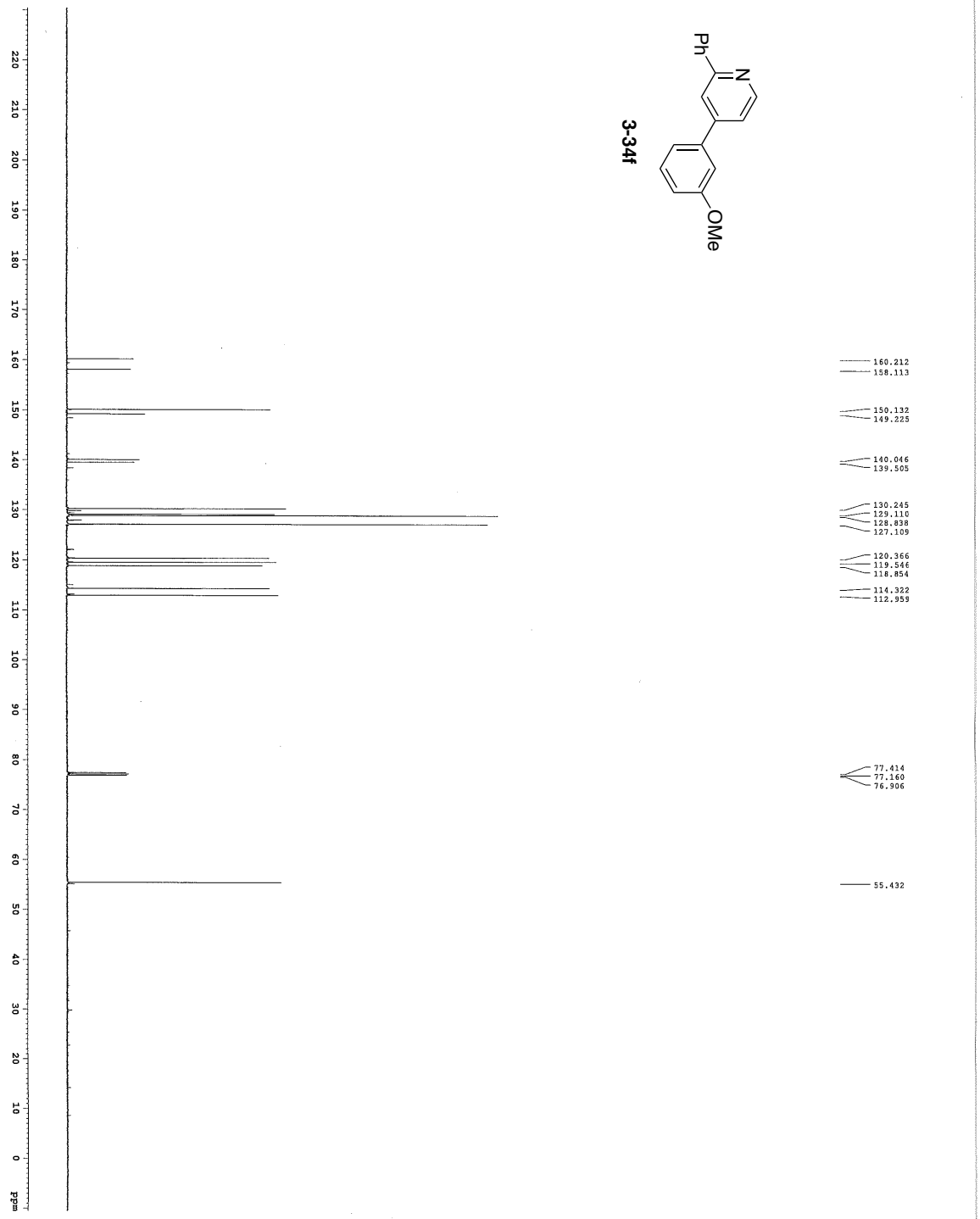
Ph
N
OMe
3-34f
160.212
158.113
150.132
149.225
140.046
139.505
130.245
129.110
128.838
127.109
120.366
119.546
118.854
114.322
112.959
77.414
77.160
76.906
55.432
220
210
200
190
180
170
160
150
140
130
120
110
100
90
80
70
60
50
40
30
20
10
0
ppm

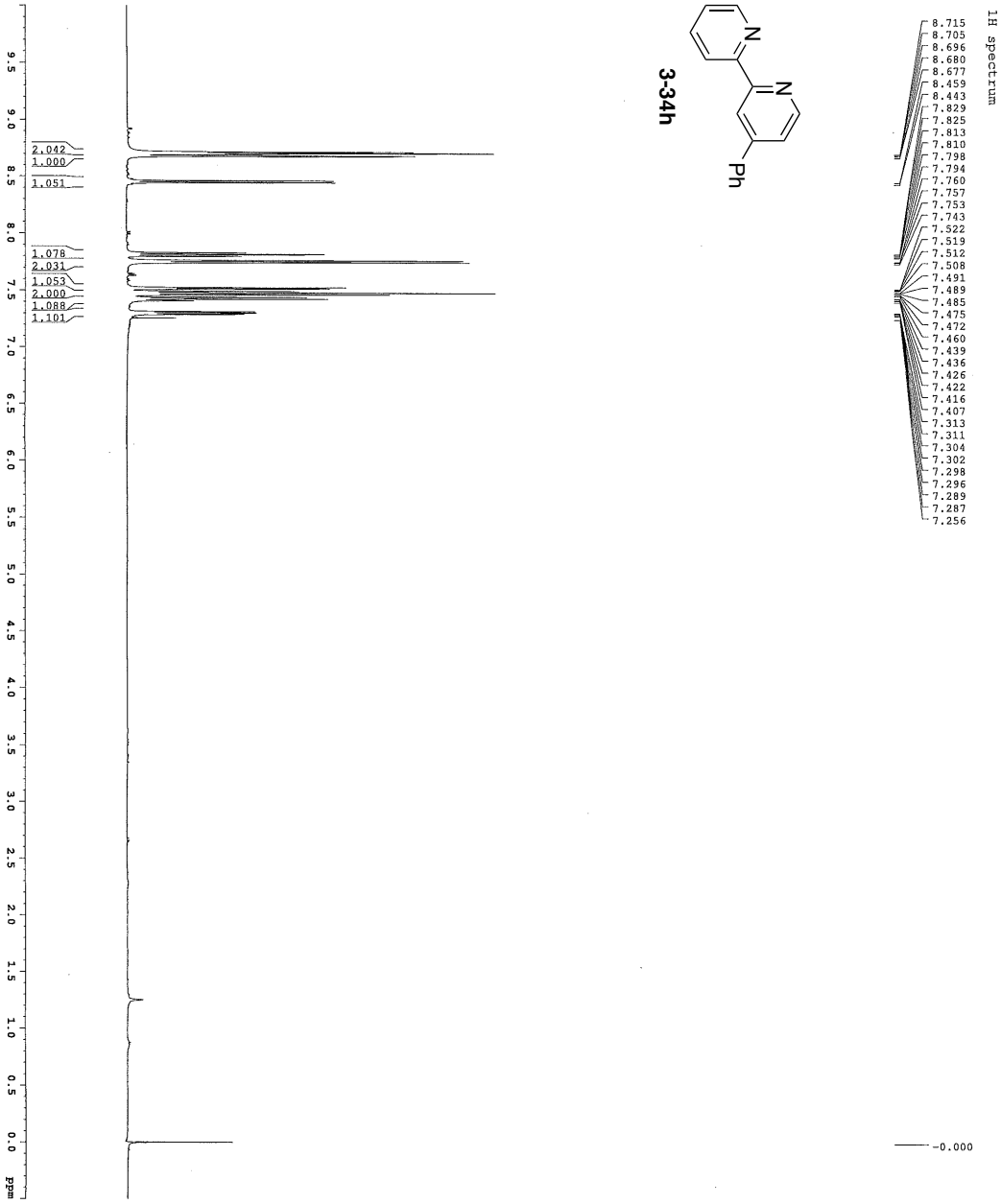
1H spectrum
8.715
8.705
8.696
8.680
8.677
8.459
8.443
7.829
7.825
7.813
7.810
7.798
7.794
7.760
7.757
7.753
7.743
7.522
7.519
7.512
7.508
7.491
7.489
7.485
7.475
7.472
7.460
7.439
7.436
7.426
7.422
7.416
7.407
7.313
7.311
7.304
7.302
7.298
7.296
7.289
7.287
7.256
-0.000
3-34h
N
N
Ph
2.042
1.000
1.051
1.078
2.031
1.053
2.000
1.088
1.101
ppm

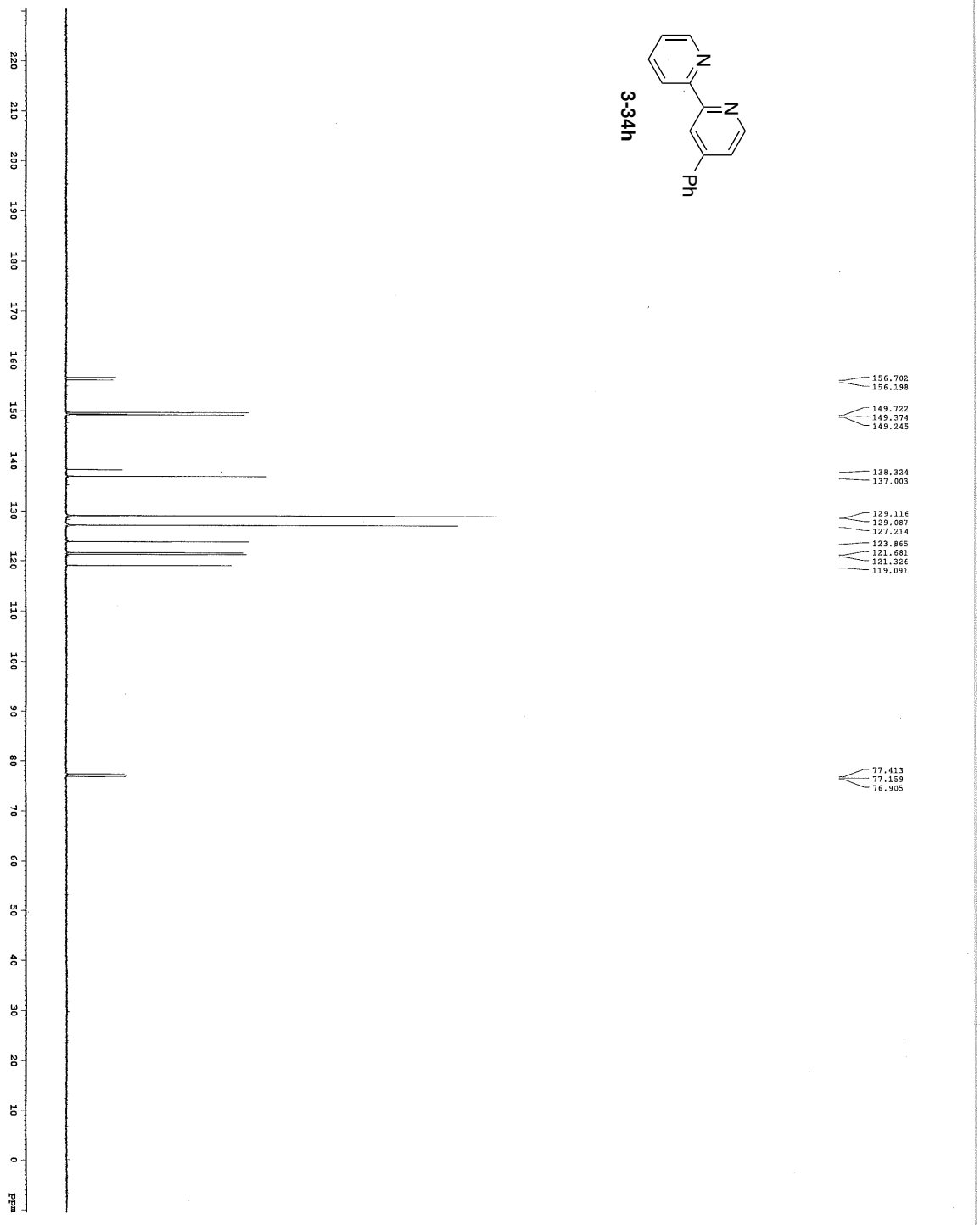
3-34h
N
N
Ph
156.702
156.198
149.722
149.374
149.245
138.324
137.003
129.116
129.087
127.214
123.865
121.681
121.326
119.091
77.413
77.159
76.905
220
210
200
190
180
170
160
150
140
130
120
110
100
90
80
70
60
50
40
30
20
10
0
ppm

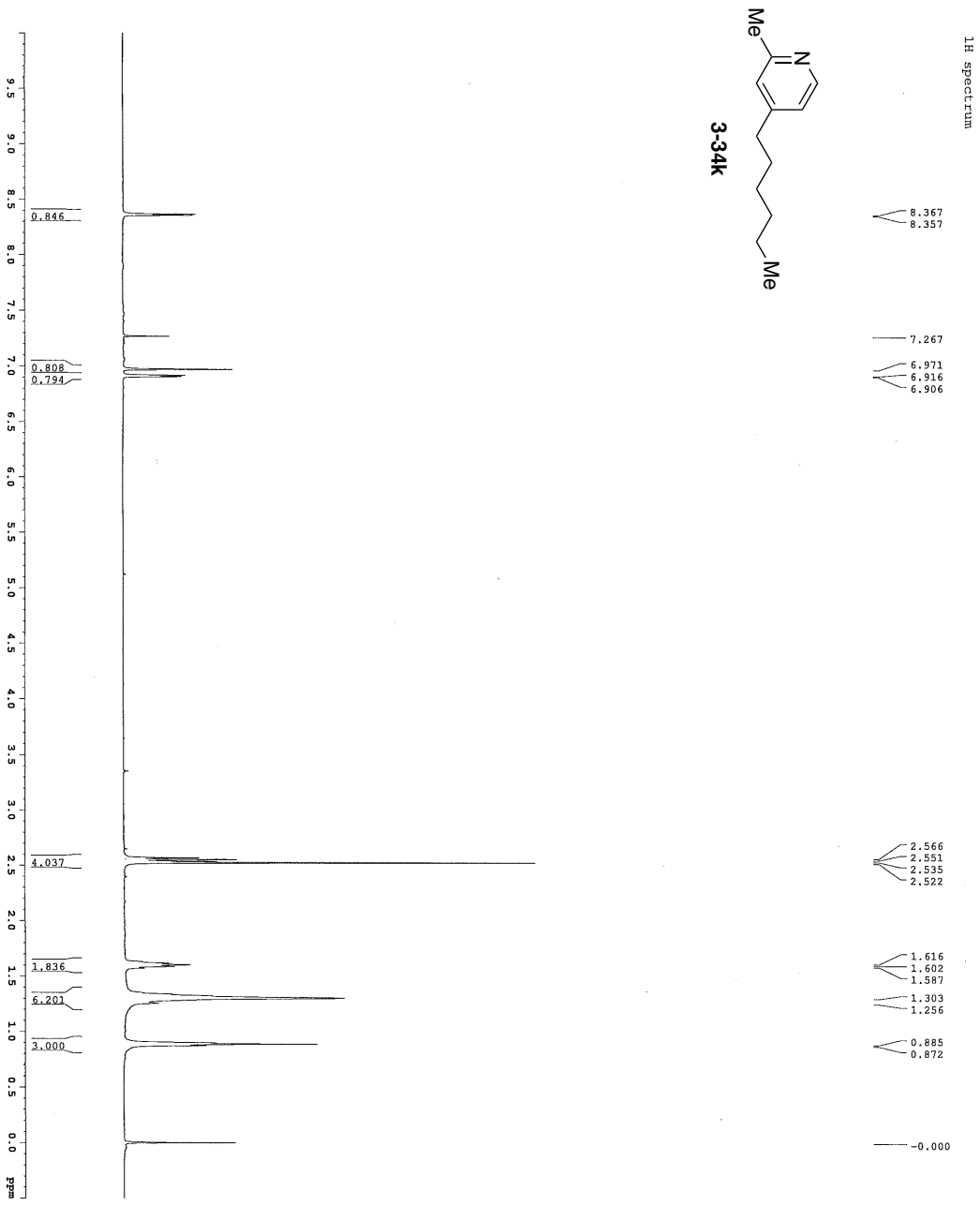
1H spectrum
Me
N
Me
3-34k
8.367
8.357
7.267
6.971
6.916
6.906
2.566
2.551
2.535
2.522
1.616
1.602
1.587
1.303
1.256
0.885
0.872
-0.000
0.846
0.808
0.794
4.037
1.836
6.201
3.000
ppm

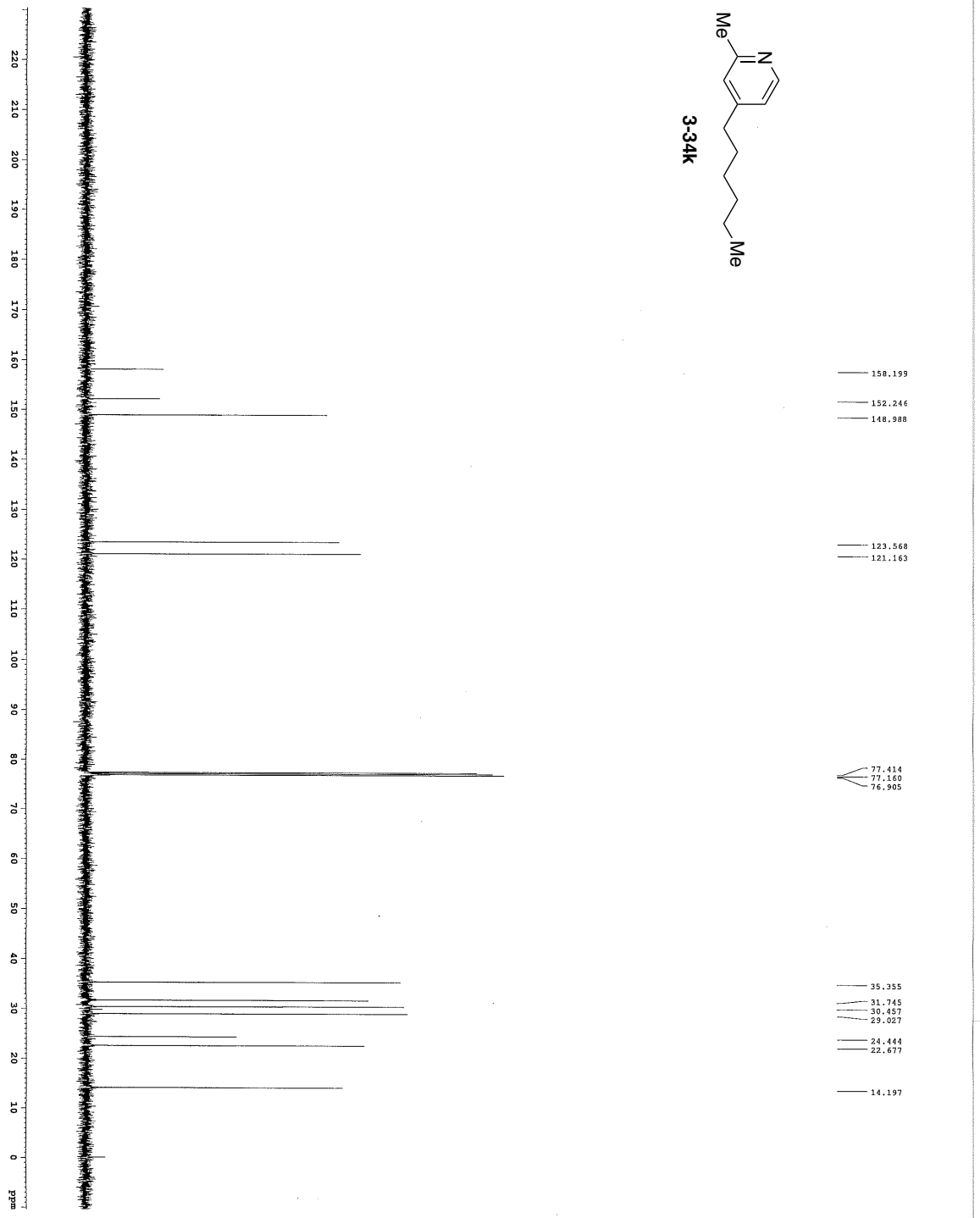
Me
N
Me
3-34k
158.199
152.246
148.988
123.568
121.163
77.414
77.160
76.905
35.355
31.745
30.457
29.027
24.444
22.677
14.197
ppm

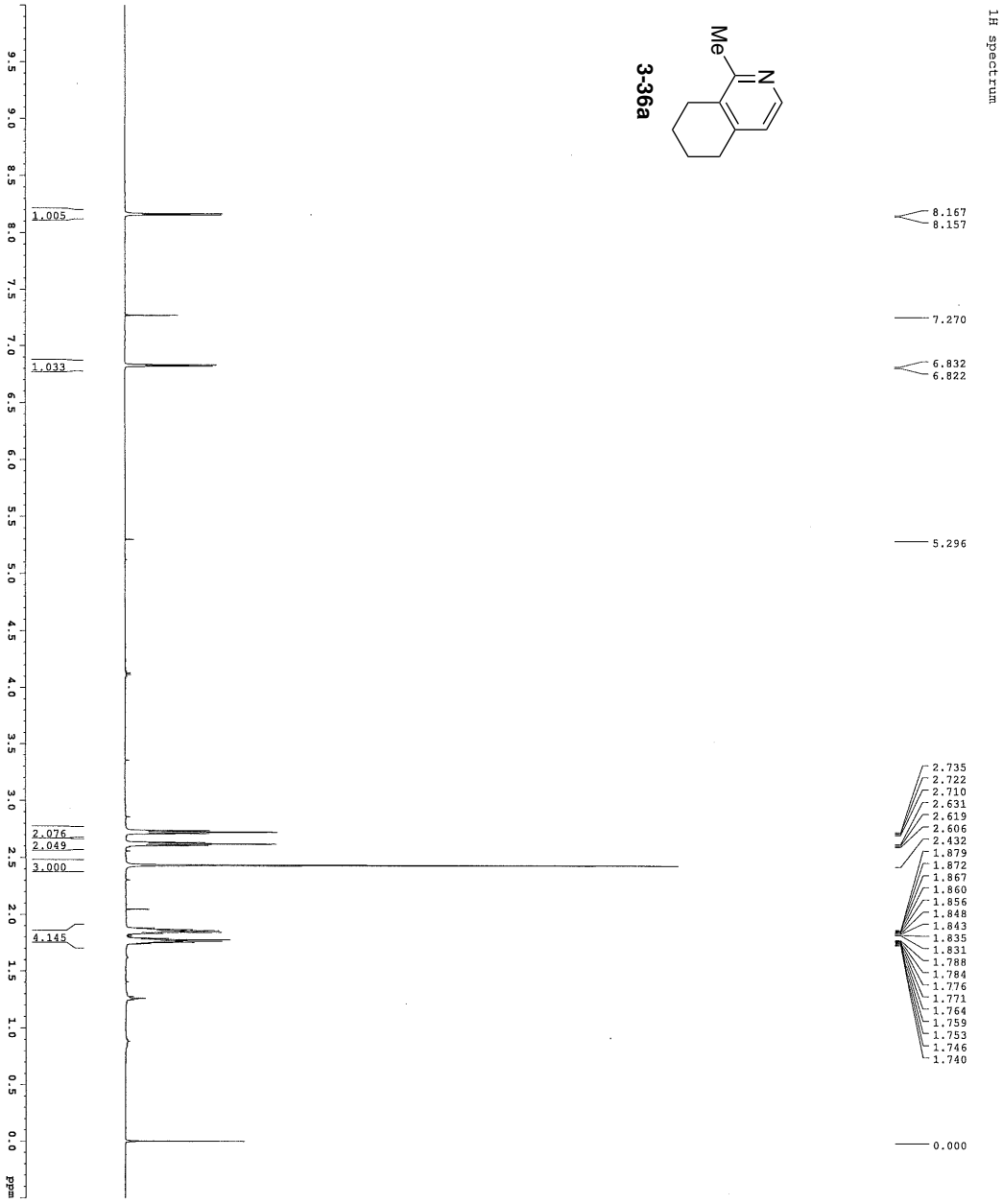
1H spectrum
Me
N
3-36a
1.005
1.033
2.076
2.049
3.000
4.145
8.167
8.157
7.270
6.832
6.822
5.296
2.735
2.722
2.710
2.631
2.619
2.606
2.432
1.879
1.872
1.867
1.860
1.856
1.848
1.843
1.835
1.831
1.788
1.784
1.776
1.771
1.764
1.759
1.753
1.746
1.740
0.000
ppm

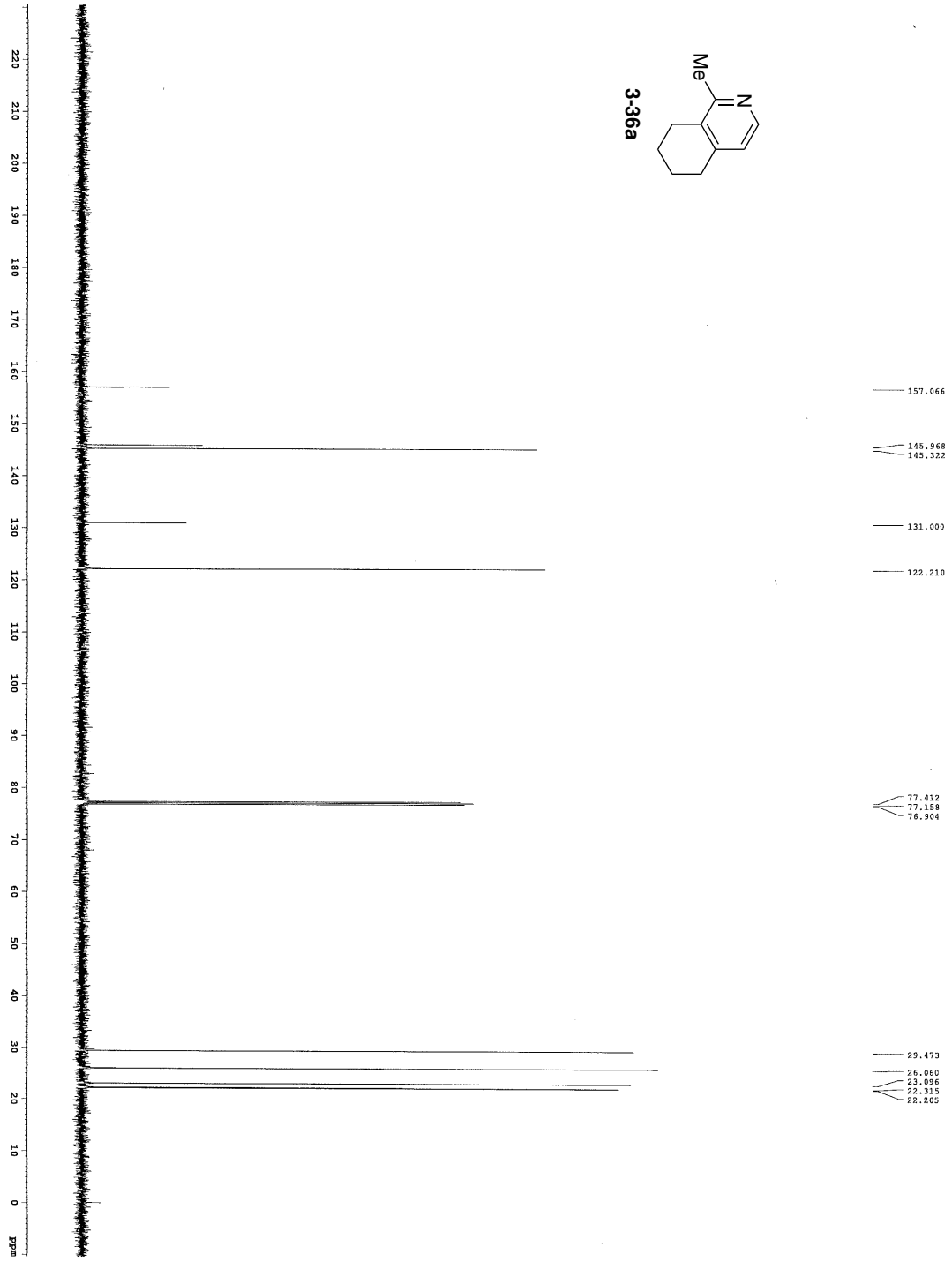
3-36a
Me
N
157.066
145.968
145.322
131.000
122.210
77.412
77.158
76.904
29.473
26.060
23.096
22.315
22.205
220
210
200
190
180
170
160
150
140
130
120
110
100
90
80
70
60
50
40
30
20
10
0
ppm

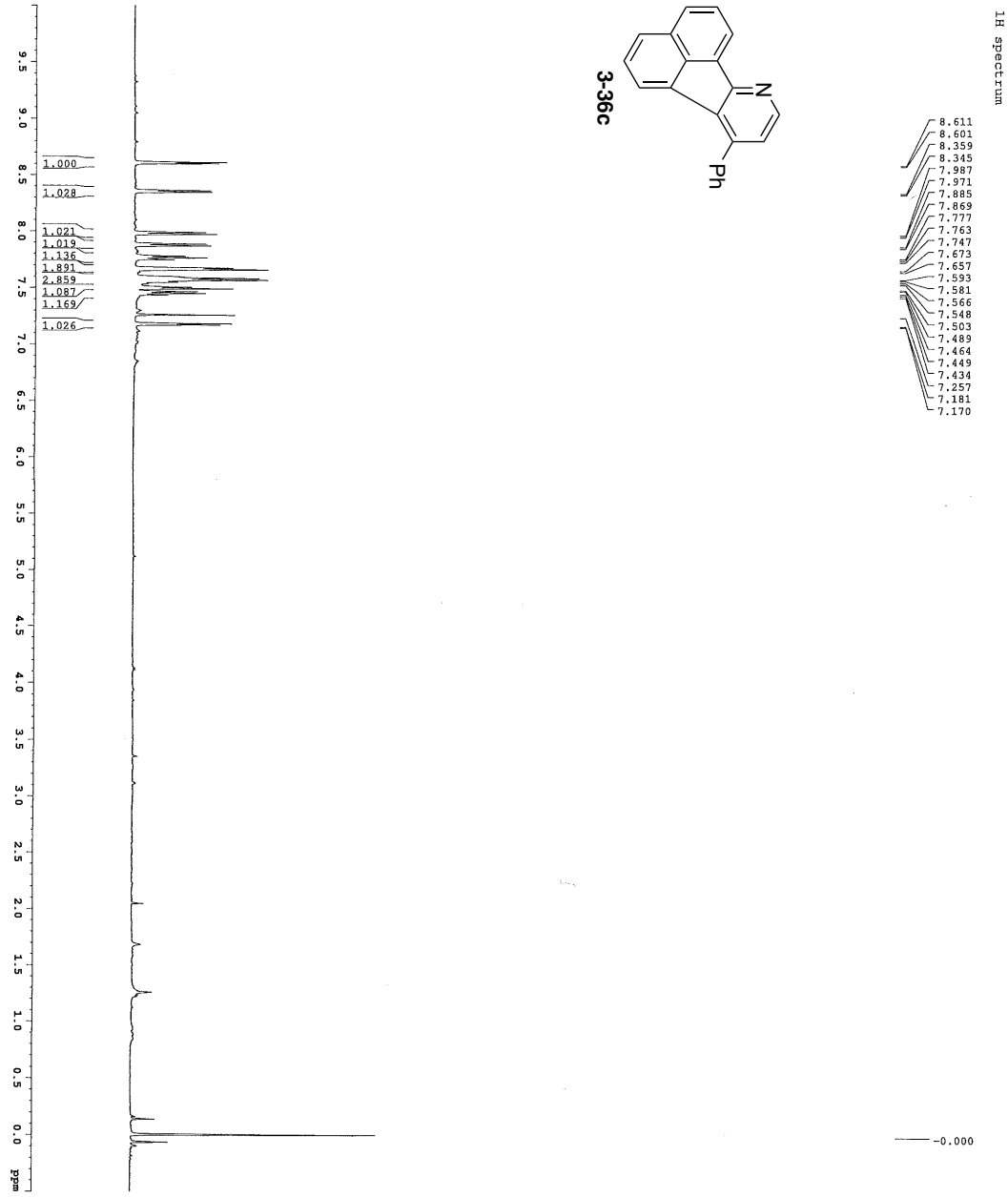
1H spectrum
3-36c
Ph
N
8.611
8.601
8.359
8.345
7.987
7.971
7.885
7.869
7.777
7.763
7.747
7.673
7.657
7.593
7.581
7.566
7.548
7.503
7.489
7.464
7.449
7.434
7.257
7.181
7.170
-0.000
1.000
1.028
1.021
1.019
1.136
1.891
2.859
1.087
1.169
1.026
ppm

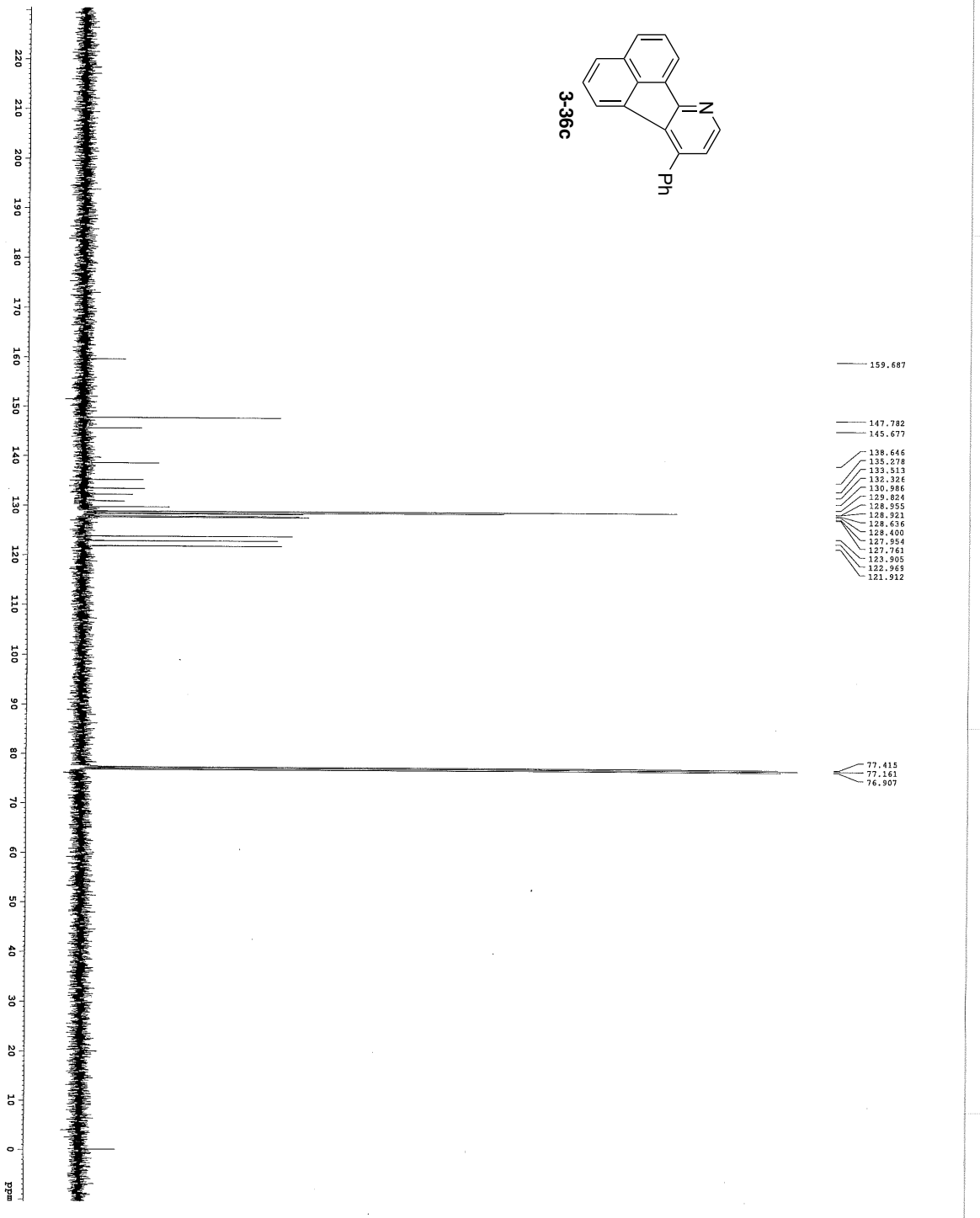
3-36c
N
Ph
159.687
147.782
145.677
138.646
135.278
133.513
132.326
130.986
129.824
128.955
128.921
128.636
128.400
127.954
127.761
123.905
122.969
121.912
77.415
77.161
76.907
220
210
200
190
180
170
160
150
140
130
120
110
100
90
80
70
60
50
40
30
20
10
0
ppm

1H spectrum

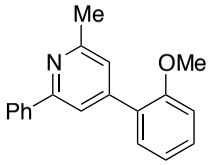

3-39b

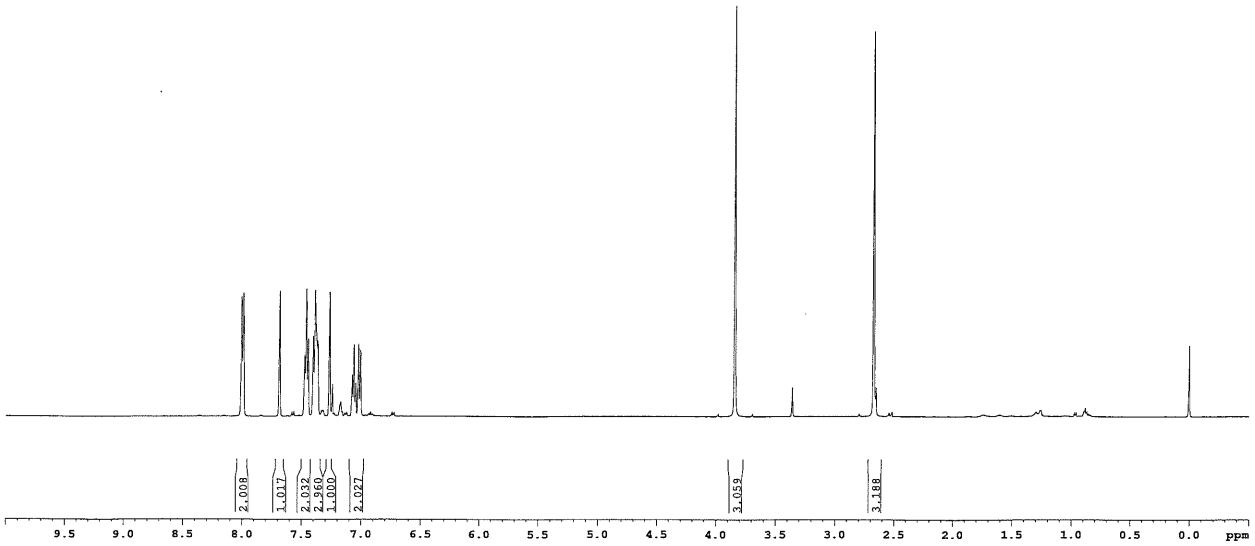

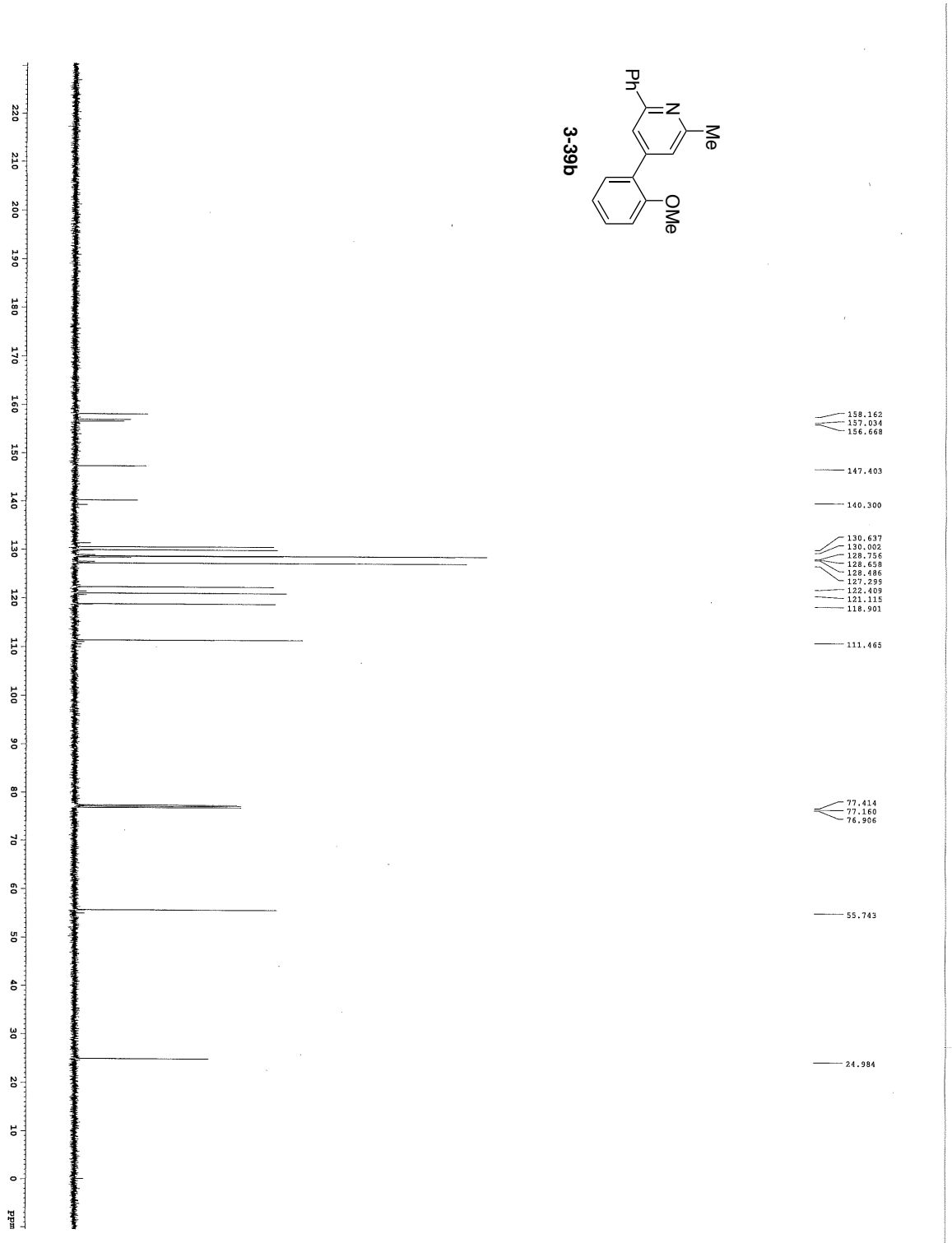
Ph
N
Me
OMe
3-39b
158.162
157.034
156.668
147.403
140.300
130.637
130.002
128.756
128.658
128.486
127.299
122.409
121.115
118.901
111.465
77.414
77.160
76.906
55.743
24.984
ppm

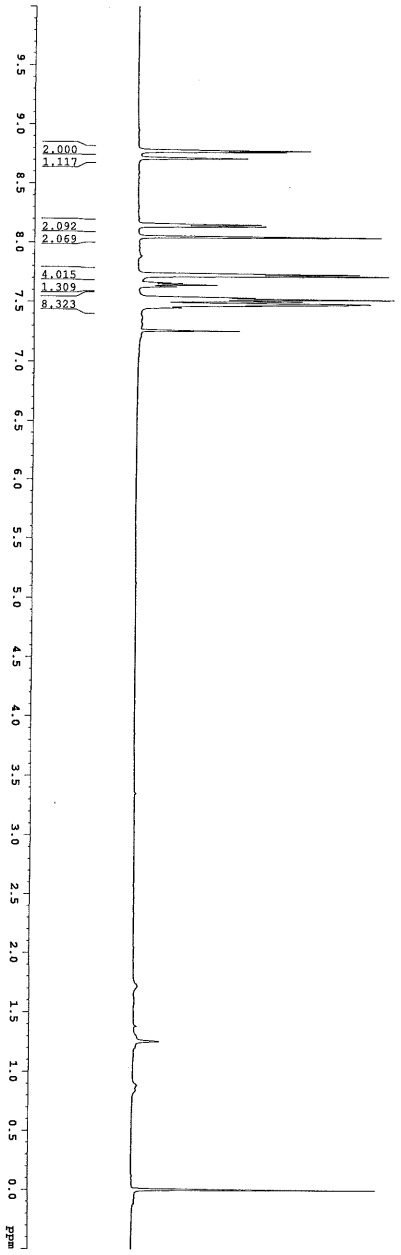
9.5
9.0
8.5
8.0
7.5
7.0
6.5
6.0
5.5
5.0
4.5
4.0
3.5
3.0
2.5
2.0
1.5
1.0
0.5
0.0
ppm
2.000
1.117
2.092
2.069
4.015
1.309
8.323

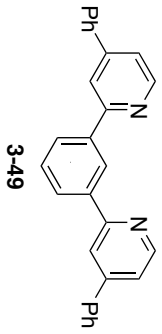
Ph
N
N
Ph

3-49

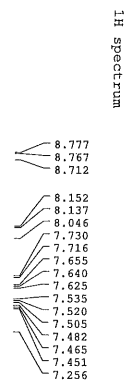
1H spectrum
8.777
8.767
8.712
8.152
8.137
8.046
7.730
7.716
7.655
7.640
7.625
7.535
7.520
7.505
7.482
7.465
7.451
7.256
-0.000

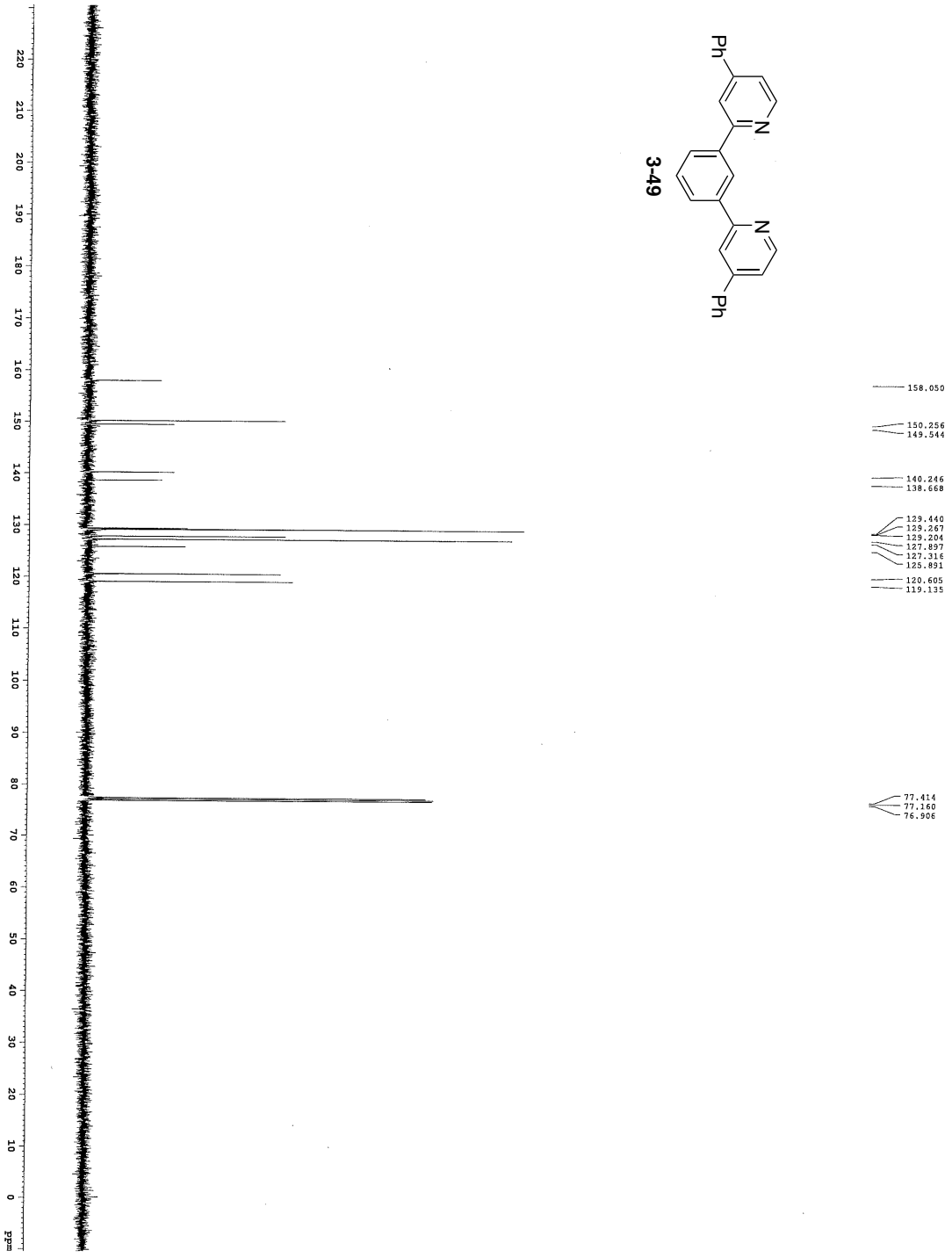
Ph
N
N
Ph
3-49
158.050
150.256
149.544
140.246
138.668
129.440
129.267
129.204
127.897
127.316
125.891
120.605
119.135
77.414
77.160
76.906
220
210
200
190
180
170
160
150
140
130
120
110
100
90
80
70
60
50
40
30
20
10
0
ppm

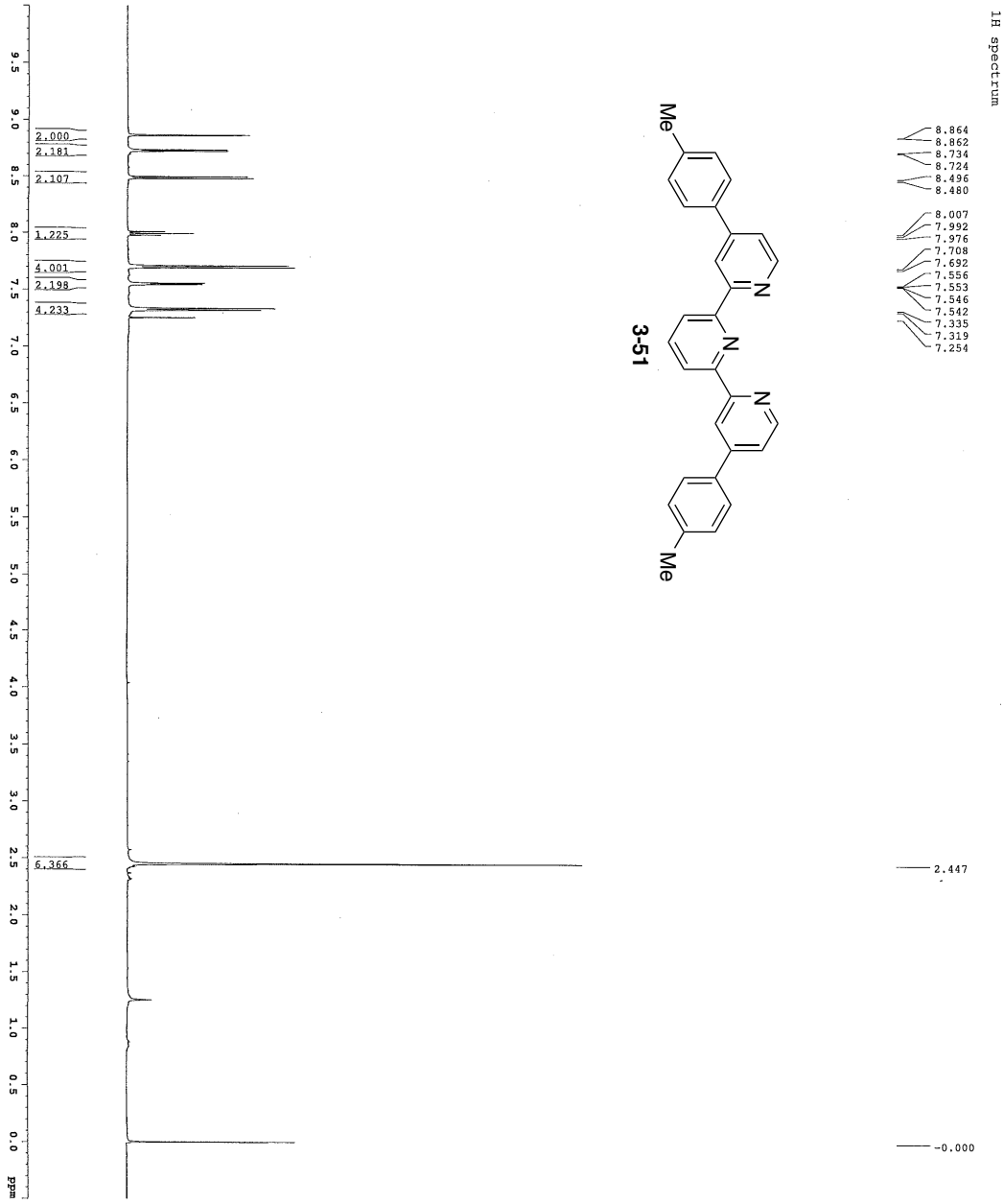
1H spectrum
8.864
8.862
8.734
8.724
8.496
8.480
8.007
7.992
7.976
7.708
7.692
7.556
7.553
7.546
7.542
7.335
7.319
7.254
2.447
-0.000
2.000
2.181
2.107
1.225
4.001
2.198
4.233
6.366
ppm
Me
Me
N
N
N
3-51

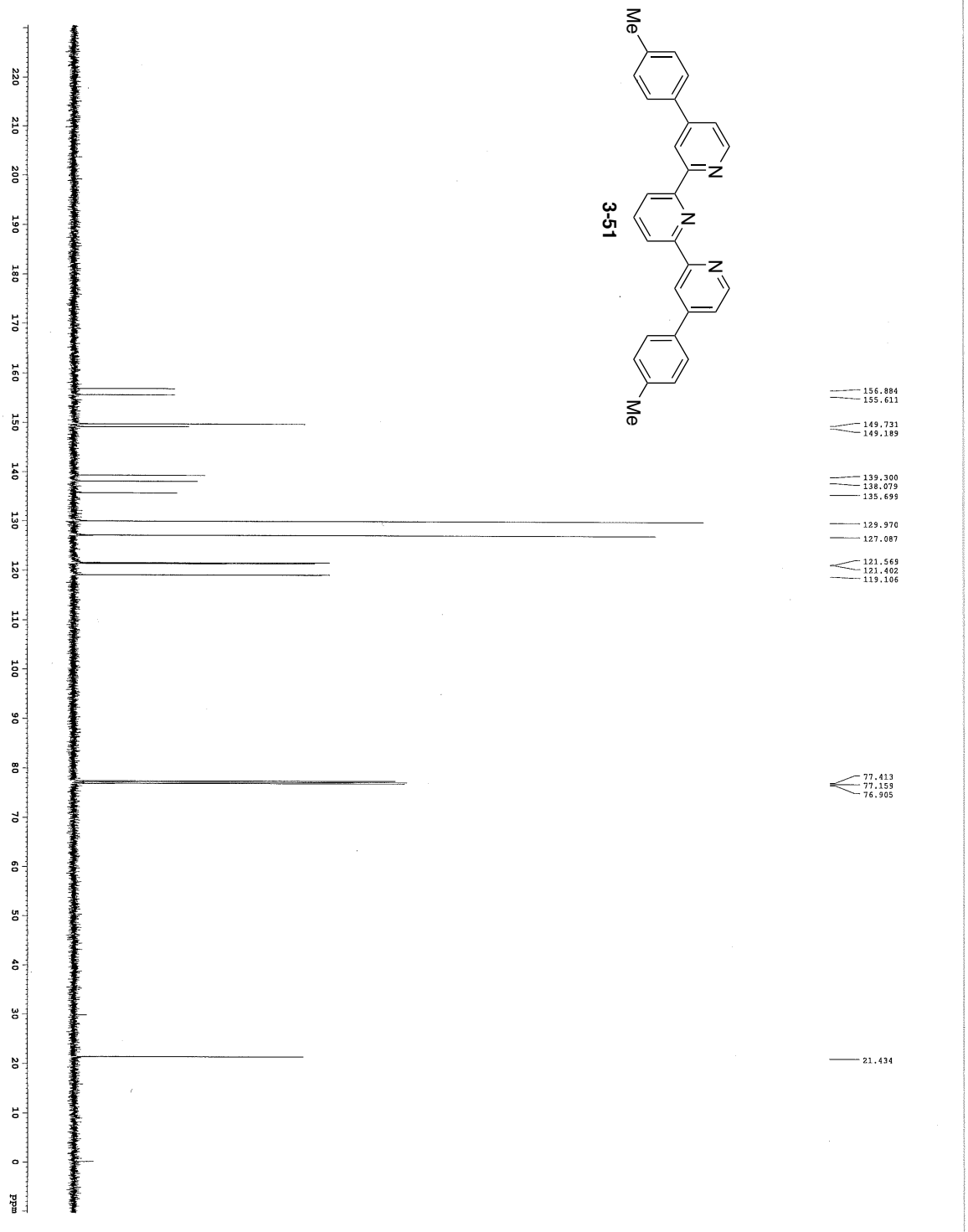
Me
N
N
N
Me
3-51
156.884
155.611
149.731
149.189
139.300
138.079
135.699
129.970
127.087
121.569
121.402
119.106
77.413
77.159
76.905
21.434
220
210
200
190
180
170
160
150
140
130
120
110
100
90
80
70
60
50
40
30
20
10
0
ppm